

AD-A193 865

HIGHER DISTRIBUTION FUNCTION: RELATION TO SHORT-TERM  
SPECTRAL ESTIMATION. (U) NAVAL UNDERWATER SYSTEMS  
CENTER NEW LONDON CT NEW LONDON LAB. A H MUTTALL

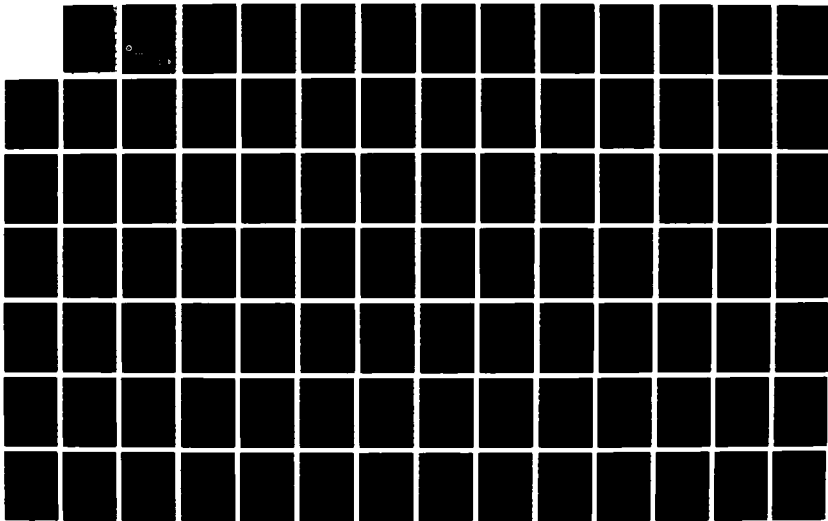
1/2

UNCLASSIFIED

16 FEB 88 MUSC-TR-8225

F/G 12/3

NL





MICROCOPY RESOLUTION TEST CHART  
- FBI AL - STANDARDS - 1963 -

AD-A193 865

NUSC Technical Report 8225  
16 February 1988

DTIC FILE COPY

①

# Wigner Distribution Function: Relation to Short-Term Spectral Estimation, Smoothing, and Performance in Noise

Albert H. Nuttall  
Surface ASW Directorate



**Naval Underwater Systems Center**  
Newport, Rhode Island/New London, Connecticut

Approved for public release; distribution is unlimited.

DTIC  
ELECTE  
MAY 05 1988  
S a D  
H

88 5 05 019

## Preface

This research was conducted under NUSC Project Nos. A60080 and G20021, "CUARP3," Principal Investigator Dr. Kent Scarbrough (Code 3331), Program Manager Mr. Ronald Tompkins (Code 33A). The sponsoring activities are the Office Of Naval Technology (Code 231), Program Manager Dr. Tom Warfield, and the Naval Sea Systems Command (Code 630), Program Manager CDR L. Schneider. Also, this research was conducted under NUSC Project No. A75205, Subproject No. ZR0000101, "Applications of Statistical Communication Theory to Acoustic Signal Processing," Principal Investigator Dr. Albert H. Nuttall (Code 304). This technical report was prepared with funds provided by the NUSC In-House Independent Research and Independent Exploratory Development Program, sponsored by the Chief of Naval Research.

The Technical Reviewer for this report was Dr. John W. Fay (Code 3331).

Reviewed and Approved:



W. A. Von Winkle  
Associate Technical Director for Research and Technology

**REPORT DOCUMENTATION PAGE**

1a. REPORT SECURITY CLASSIFICATION UNCLASSIFIED		1b. RESTRICTIVE MARKINGS	
2a. SECURITY CLASSIFICATION AUTHORITY		3. DISTRIBUTION/AVAILABILITY OF REPORT Approved for public release; distribution is unlimited.	
2b. DECLASSIFICATION/DOWNGRADING SCHEDULE			
4. PERFORMING ORGANIZATION REPORT NUMBER(S) TR 8225		5. MONITORING ORGANIZATION REPORT NUMBER(S)	
6a. NAME OF PERFORMING ORGANIZATION Naval Underwater Systems Center	6b. OFFICE SYMBOL (If applicable)	7a. NAME OF MONITORING ORGANIZATION	
6c. ADDRESS (City, State, and ZIP Code). New London Laboratory New London, CT 06320		7b. ADDRESS (City, State, and ZIP Code)	
8a. NAME OF FUNDING/SPONSORING ORGANIZATION	8b. OFFICE SYMBOL (If applicable)	9. PROCUREMENT INSTRUMENT IDENTIFICATION NUMBER	
8c. ADDRESS (City, State, and ZIP Code)		10. SOURCE OF FUNDING NUMBERS	
		PROGRAM ELEMENT NO.	PROJECT NO.
		TASK NO.	WORK UNIT ACCESSION NO.
11. TITLE (Include Security Classification) WIGNER DISTRIBUTION FUNCTION: RELATION TO SHORT-TERM SPECTRAL ESTIMATION, SMOOTHING, AND PERFORMANCE IN NOISE			
12. PERSONAL AUTHOR(S) Albert H. Nuttall			
13a. TYPE OF REPORT	13b. TIME COVERED FROM TO	14. DATE OF REPORT (Year, Month, Day) 1988 February 16	15. PAGE COUNT
16. SUPPLEMENTARY NOTATION			
17. COSATI CODES			18. SUBJECT TERMS (Continue on reverse if necessary and identify by block number) Wigner Distribution Function; Noise Performance; Short-Term Spectral Estimation; Linear Frequency Smoothing; Modulation; next page
FIELD	GROUP	SUB-GROUP	
19. ABSTRACT (Continue on reverse if necessary and identify by block number) <p>→ The properties and behavior of the Wigner Distribution Function (WDF) are investigated both analytically and by means of a number of simple informative examples. The lack of local temporal averaging when obtaining the instantaneous correlation function, and the lack of weighting the longer delay values when transforming to the instantaneous spectrum, are shown to be the causes of the deleterious interference effects that are inherent to the WDF. The equivalence of short-term spectral estimation to the smoothed WDF offers an attractive alternative with guaranteed positive distribution values and no interference effects.</p> <p>The performance of a processor which estimates the WDF of a signal waveform in the presence of additive noise is investigated in terms of the output mean, bias, and variance. Dependence on filtering the input and time-weighting is allowed and included in the analysis. Numerical application to a particular example is carried out.</p>			
20. DISTRIBUTION/AVAILABILITY OF ABSTRACT <input checked="" type="checkbox"/> UNCLASSIFIED/UNLIMITED <input type="checkbox"/> SAME AS RPT. <input type="checkbox"/> DTIC USERS		21. ABSTRACT SECURITY CLASSIFICATION UNCLASSIFIED	
22a. NAME OF RESPONSIBLE INDIVIDUAL Albert H. Nuttall		22b. TELEPHONE (Include Area Code) (203) 440-4618	22c. OFFICE SYMBOL Code 304

18. SUBJECT TERMS (Cont'd.)

Interference Effects,  
 Gaussian Amplitude Modulation  
 Marginals  
 Moments  
 Spread of Distribution  
 Positive Distributions  
 Ambiguity Function



<b>Accession For</b>	
NTIS GRA&I	<input checked="" type="checkbox"/>
DTIC TAB	<input type="checkbox"/>
Unannounced	<input type="checkbox"/>
Justification	
By _____	
Distribution/	
<b>Availability Codes</b>	
<b>Dist</b>	<b>Avail and/or Special</b>
A-1	

## TABLE OF CONTENTS

	Page
LIST OF ILLUSTRATIONS . . . . .	iii
LIST OF SYMBOLS . . . . .	iv
INTRODUCTION . . . . .	1
BASIC PROPERTIES OF THE WDF . . . . .	3
Definitions . . . . .	3
Properties of WDF . . . . .	6
Product and Convolution . . . . .	8
Ambiguity Function . . . . .	9
First Moments of $W$ . . . . .	12
Second Moments of $W$ . . . . .	15
Moments of $W^2$ . . . . .	16
Cross Wigner Distribution Function . . . . .	19
Narrowband Real Waveform . . . . .	22
Sampling Properties . . . . .	23
EXAMPLES OF WDF . . . . .	28
Gaussian Waveform . . . . .	29
Gaussian-Modulated Tone . . . . .	31
Multiple Modulated Tones . . . . .	32
Linear Frequency Modulation . . . . .	35
Gated Linear Frequency Modulation . . . . .	40
SHORT-TERM SPECTRAL ESTIMATION . . . . .	43
Weighted Spectral Estimate . . . . .	43
Relation to WDFs . . . . .	44
Marginals of Spectral Estimate . . . . .	46
Moments of Spectral Estimate . . . . .	47
Conditional Moment . . . . .	49
EXAMPLES OF SHORT-TERM SPECTRAL ESTIMATION . . . . .	51
Gaussian Waveform . . . . .	51
Multiple Modulated Tones . . . . .	53
Linear Frequency Modulation . . . . .	55
More-General Weighting . . . . .	57
SMOOTHING THE WDF . . . . .	60
Philosophy and Approach . . . . .	60
Alternative Averaging Procedures . . . . .	63
Efficient Calculation of Short-Term Spectral Estimate . . . . .	66
WDF With Minimum Spread . . . . .	69

## TABLE OF CONTENTS (Cont'd)

PERFORMANCE IN NOISE . . . . .	70
Waveform Weighting . . . . .	70
Mean Values . . . . .	72
Variance of WDF Estimate . . . . .	73
WDF Processor . . . . .	77
SUMMARY . . . . .	80
APPENDIX A. SLICES IN TIME OF THE WDF . . . . .	A-1
APPENDIX B. OSCILLATING WDF FOR SEPARATED PULSES . . . . .	B-1
APPENDIX C. AMBIGUITY FUNCTION OF (79) . . . . .	C-1
APPENDIX D. ROTATION OF AXES . . . . .	D-1
APPENDIX E. DISCRETE APPROXIMATION TO SHORT-TERM SPECTRAL ESTIMATE . . . . .	E-1
APPENDIX F. SOME SMOOTHING CONSIDERATIONS . . . . .	F-1
APPENDIX G. DERIVATION OF MINIMUM-SPREAD WDF . . . . .	G-1
APPENDIX H. EXAMPLE OF WDF PROCESSOR . . . . .	H-1
APPENDIX I. SMOOTHED WDF FOR $s(t) = t \exp(-t^2/2)$ . . . . .	I-1
APPENDIX J. DOUBLE CONVOLUTION OF TWO GAUSSIAN FUNCTIONS . . . . .	J-1
REFERENCES . . . . .	R-1



## LIST OF ILLUSTRATIONS

Figure		Page
1	WDF for Narrowband Real Waveform . . . . .	23
2	WDF for Sampled Version $\tilde{W}(t,f)$ . . . . .	25
3	$\tilde{W}(t,f)$ for Real Waveform $s(t)$ . . . . .	25
4	Contour of WDF (72) at $1/e$ Relative Level . . . . .	30
5	Contour of (91) for $\theta_0 = 1.5$ . . . . .	39
6	Contours of WDF for Gated Linear Frequency Modulation . . . . .	41
7	WDF Processor . . . . .	77
8	Time and Frequency Characteristics of Figure 7 . . . . .	79
A-1	Low-Pass Spectrum $S(f)$ . . . . .	A-2
B-1	Waveform $s(t)$ . . . . .	B-1
D-1	Rotated Coordinate Axes . . . . .	D-1
D-2	Triangle Interpretation of (D-5) . . . . .	D-3
D-3	Ellipse in Rotated Coordinates . . . . .	D-5
H-1	Plot of (H-40) or (H-41) for Fixed $\theta_0$ . . . . .	H-12
H-2	Plot for $\theta_0 = 0$ . . . . .	H-12
H-3	Plot for $\theta_0 = 1$ . . . . .	H-13
H-4	Plot for $\theta_0 = 5$ . . . . .	H-13
H-5	Minimum MD Product . . . . .	H-14
H-6	Quality Ratio for $\theta_0 = 0, E_0/N_d = 20$ . . . . .	H-21
H-7	Quality Ratio for $\theta_0 = 1, E_0/N_d = 20$ . . . . .	H-22
H-8	Quality Ratio for $\theta_0 = 5, E_0/N_d = 20$ . . . . .	H-23

## LIST OF SYMBOLS

WDF	Wigner Distribution Function
$t$	Time, (1)
$s(t)$	Waveform, function of time, (1)
$\tau$	Time separation or lag variable, (1)
$R(t, \tau)$	Instantaneous correlation, (1)
$f$	Frequency, (3)
$W(t, f)$	WDF at time $t$ and frequency $f$ , (3), (10)
$E$	Waveform energy, (5), (14)
$S(f)$	Voltage density spectrum of $s(t)$ , (9)
$\delta$	Delta function, (13)
$\otimes$	Convolution, (19), (20)
$\nu$	Frequency shift variable, (22)
$\chi(\nu, \tau)$	Ambiguity function, (22)
$A(\nu, f)$	Spectral function, (24)
$\text{Im}$	Imaginary part, (28)
$\delta'$	Derivative of delta function, (29)
$\mu_f(t)$	Frequency center at time $t$ , (30)
$M(t)$	Magnitude of $s(t)$ , (31)
$\theta(t)$	Phase of $s(t)$ , (31)
$\mu_t(f)$	Time center at frequency $f$ , (33)
$A(f)$	Magnitude of $S(f)$ , (34)
$\phi(f)$	Phase of $S(f)$ , (34)
$\bar{f}$	Frequency center, (36)
$\bar{t}$	Time center, (37)

## LIST OF SYMBOLS (Cont'd)

$\sigma_f^2(t)$	Instantaneous mean-square frequency spread, (42)
$W_{ab}(t,f)$	Cross WDF, (51)
$a(t), A(f)$	Fourier transform pair, (51)
$\chi_{ab}(v,\tau)$	Cross ambiguity function, (53)
$c(t)$	Complex envelope, (55)
$f_0$	Carrier frequency, (55)
Re	Real part, (55)
$\Delta_t$	Sampling increment in time, (57)
$\tilde{W}$	Approximation to W, (57), (59)
$m,n,N_f$	Integers, (60)
T	Time spread, figure 2
B	Frequency spread, figure 3
$f_H$	Highest frequency in $s(t)$ , (65)
$t_0, f_0$	Time and frequency shifts, (66)
$\theta_0$	Time-bandwidth product, (88)-(90)
$u(t)$	Weighting in time, (102)
$S_u(t,f)$	Voltage spectrum of $s$ , relative to $u$ , (102)
STSE	Short-term spectral estimate, (103)
$E_s$	Energy of waveform $s(t)$ , (111)
$E_u$	Energy of weighting $u(t)$ , (111)
$\alpha_c$	Effective duration of weighting, (146)
$\alpha_c$	Linear frequency modulation parameter, (146)
$\theta_c$	Time-bandwidth product, (146)
$v_1(t)$	Time weighting, (148)
$\hat{R}$	Locally averaged correlation, (148), (150)

## LIST OF SYMBOLS (Cont'd)

$\hat{W}$	Locally averaged WDF, (149)
$v_2(t, \tau)$	Time and lag weighting, (150)
$V_2(t, f)$	Transform (on $\tau$ ) of $v_2$ , smoothing function, (151)
$I$	Spread measure, (163)
$\beta_c$	Specified slope in $t, f$ plane, (163)
$\alpha_c$	$2\pi\beta_c$ , (163)
$s(t)$	Signal, (165)
$n(t)$	Additive noise, (165)
$x(t)$	Observed waveform, (165)
$C_n(\tau)$	Noise correlation, (166)
$G_n(f)$	Noise spectrum, (166)
$v(t)$	Weighting of $x$ , (167)
$y(t)$	Weighted waveform, (167)
$a, b, c, d$	Components of $W_{yy}$ , (168), (169)
overbar	Ensemble average, (172), (173)
$G_n^{(2)}(f)$	Modified noise spectral quantity, (178)
$B(t, f)$	Auxiliary function, (183)
Var	Variance of WDF estimate, (188)
$s_0(t)$	Input signal, figure 7
$n_0(t)$	Input noise, figure 7
$H(f)$	Filter, figure 7
$N_d$	Noise spectral level, (189)
$B$	Passband of filter $H$ , figure 8
$L$	Duration of weighting $v$ , figure 8
LFM	Linear Frequency Modulation
$\text{sgn}(x)$	1 for $x > 0$ , -1 for $x < 0$

WIGNER DISTRIBUTION FUNCTION: RELATION TO SHORT-TERM  
SPECTRAL ESTIMATION, SMOOTHING, AND PERFORMANCE IN NOISE

INTRODUCTION

The potential of the Wigner Distribution Function (WDF) for characterizing the short-term local time and frequency content of a transient waveform has been amply demonstrated in a series of papers; for example, see the recent publications [1,2,3] and the extensive references listed therein. In particular, [1] contains numerical examples of the WDF for rectangularly gated linear frequency modulation and a version which has been smoothed with a square window in the time-frequency plane, in order to yield positive distribution values. Here, we will be concerned with smoothing so as to minimally spread the WDF, but will not presume all the information that is required for implementation via [2], nor do we limit consideration to a constant-magnitude function. We will then use the close connection between short-term spectral estimation and smoothed WDFs to suggest a possible analysis procedure and philosophy to extract information about a given waveform without an extensive search in waveform parameters. Finally, the performance of a particular WDF estimator in the presence of additive noise will be analyzed, both in terms of bias and variance.

This report summarizes and compiles many of the results in the publications noted above in a unified framework and notation. Also, numerous examples are presented in the various sections of this report to

illustrate and bring out some of the fundamental concepts and limitations of the WDF; these examples can be evaluated analytically in closed form, allowing for close investigation of the behavior of the WDF, and as control cases on any computer-written program for numerical evaluation of the WDF.

## BASIC PROPERTIES OF THE WDF

## DEFINITIONS

A natural definition of the time-varying correlation of a nonstationary complex stochastic process  $s(t)$  is

$$R(t, \tau) = \overline{s(t + \frac{\tau}{2}) s^*(t - \frac{\tau}{2})} . \quad (1)$$

where the overbar denotes an ensemble average. The "center" time in (1) is  $t$ , while the "separation" time is  $\tau$ . However, if an ensemble is not available, or if  $s(t)$  is a deterministic waveform, the obvious extension of (1) is simply

$$R(t, \tau) = s(t + \frac{\tau}{2}) s^*(t - \frac{\tau}{2}) . \quad (2)$$

This quantity is interpreted as the instantaneous correlation of waveform  $s(t)$  at time  $t$ , for separation (or lag)  $\tau$ .

The associated "spectrum" at time  $t$  is then available, as usual, by Fourier transforming (2) on separation variable  $\tau$ , to get at frequency  $f$ ,

$$\begin{aligned} W(t, f) &= \int d\tau \exp(-i2\pi f\tau) R(t, \tau) = \\ &= \int d\tau \exp(-i2\pi f\tau) s(t + \frac{\tau}{2}) s^*(t - \frac{\tau}{2}) . \end{aligned} \quad (3)$$

(Integrals without limits are over the range of nonzero integrand. Also, it is presumed that  $s(t)$  and its derivatives decay fast enough to zero at  $t = \pm\infty$  for all the integrals to converge.) This time-frequency function  $W(t,f)$  is called the Wigner Distribution Function (WDF). It is a real function, even when  $s(t)$  is complex, since

$$\begin{aligned} W^*(t,f) &= \int d\tau \exp(i2\pi f\tau) s^*(t + \frac{\tau}{2}) s(t - \frac{\tau}{2}) = \\ &= \int du \exp(-i2\pi fu) s^*(t - \frac{u}{2}) s(t + \frac{u}{2}) = W(t,f) . \end{aligned} \quad (4)$$

However, it is not necessarily positive, as the simple example of a rectangularly gated pulse quickly shows: for

$$s(t) = \begin{cases} a & \text{for } |t| < T/2 \\ 0 & \text{otherwise} \end{cases} .$$

then

$$W(t,f) = 2E \frac{\sin[2\pi f(T - 2|t|)]}{2\pi fT} \quad \text{for } |t| < \frac{T}{2} , \quad \text{all } f ,$$

and zero otherwise, where  $E$  is the waveform energy:

$$E = \int dt |s(t)|^2 = |a|^2 T . \quad (5)$$

An even simpler example is furnished by waveforms with odd symmetry,  $s(-t) = -s(t)$ . Substitution in (3) immediately yields  $W(0,0) = -\int d\tau |s(\tau/2)|^2 = -2E$ . Thus the origin value of the WDF is always negative for an odd waveform.



More generally, when waveform  $s(t)$  is expressed in terms of its even and odd parts according to

$$s(t) = e(t) + o(t) , \quad (6)$$

then the origin value of the WDF is

$$\begin{aligned} W(0,0) &= \int d\tau s(\tau/2) s^*(-\tau/2) = 2 \int dt s(t) s^*(-t) = \\ &= 2 \int dt [e(t) + o(t)] [e^*(t) - o^*(t)] = 2E_e - 2E_o , \end{aligned} \quad (7A)$$

where

$$E_e = \int dt |e(t)|^2 , \quad E_o = \int dt |o(t)|^2 \quad (7B)$$

are the energies of the even and odd parts respectively. For nonzero  $t, f$ , it can readily be shown that the magnitude of the WDF is upper bounded by  $2E = 2(E_e + E_o)$ .

## PROPERTIES OF WDF

For  $s(t)$  real, it readily follows from the definition of the WDF in (3) that

$$W(t, -f) = W(t, f) \quad \text{for } s(t) \text{ real .} \quad (8)$$

In this special case, it is only necessary to evaluate  $W(t, f)$  for  $f \geq 0$ .

Define the voltage density spectrum of waveform  $s(t)$  as

$$S(f) = \int dt \exp(-i2\pi ft) s(t) . \quad (9)$$

Then an alternative form for the WDF in (3) is

$$\begin{aligned} W(t, f) &= \int d\tau \exp(-i2\pi f\tau) s(t + \frac{\tau}{2}) s^*(t - \frac{\tau}{2}) = \\ &= \int dv \exp(i2\pi vt) S(f + \frac{v}{2}) S^*(f - \frac{v}{2}) , \end{aligned} \quad (10)$$

in terms of  $S(f)$ .

Integration on (10) immediately yields the marginals

$$\int dt W(t, f) = |S(f)|^2 , \quad (11)$$

and

$$\int df W(t, f) = |s(t)|^2 , \quad (12)$$

where we used the result

$$\int dx \exp(i2\pi xy) = \delta(y) . \quad (13)$$

The quantity in (11) is the energy density function, while that in (12) is the instantaneous power. If we complete the integrations on the remaining variables in (11) and (12), they both yield

$$\begin{aligned} \iint dt df W(t,f) &= E = \\ &= \int dt |s(t)|^2 = \int df |S(f)|^2 , \end{aligned} \quad (14)$$

where  $E$  is the total waveform energy.

If waveform  $s(t)$  satisfies a time-limited restriction, namely

$$s(t) \neq 0 \quad \text{only for } t_1 < t < t_2 , \quad (15)$$

then (3) reduces to

$$W(t,f) = \int_{-T_m}^{T_m} d\tau \exp(-i2\pi f\tau) s(t + \frac{\tau}{2}) s^*(t - \frac{\tau}{2}) \quad \text{for } t_1 < t < t_2 , \quad (16)$$

and zero otherwise, where

$$T_m = 2 \min(t_2 - t, t - t_1) \quad \text{for } t_1 < t < t_2 . \quad (17)$$

Thus the WDF is time-limited if waveform  $s(t)$  is time-limited; however, if there are gaps in  $s(t)$ , the behavior of the WDF is more complicated, as will be demonstrated later.

## PRODUCT AND CONVOLUTION

If waveform  $s(t)$  is the product of two other waveforms,

$$s(t) = a(t) b(t) , \quad (18)$$

then the WDF of  $s(t)$  is (inserting subscripts as needed)

$$\begin{aligned} W_s(t, f) &= \int d\tau \exp(-i2\pi f\tau) R_s(t, \tau) = \\ &= \int d\tau \exp(-i2\pi f\tau) R_a(t, \tau) R_b(t, \tau) = \\ &= \int dv W_a(t, v) W_b(t, f - v) = \\ &= W_a(t, f) \otimes W_b(t, f) , \end{aligned} \quad (19)$$

which is a convolution on frequency  $f$ , for fixed  $t$ .

In a similar fashion, if  $s(t)$  is the convolution in time, of two other waveforms,

$$s(t) = a(t) \otimes^t b(t) = \int d\tau a(\tau) b(t - \tau) , \quad (20)$$

then the WDF of  $s(t)$  is

$$W_s(t, f) = W_a(t, f) \overset{t}{\otimes} W_b(t, f) = \int d\tau W_a(\tau, f) W_b(t - \tau, f) , \quad (21)$$

which is a convolution on time  $t$ , for fixed  $f$ .

#### AMBIGUITY FUNCTION

The WDF is closely related to the complex ambiguity function of  $s(t)$ , which is defined here as [4; section 7.2]

$$\begin{aligned} \chi(\nu, \tau) &= \int dt \exp(-i2\pi\nu t) s(t + \frac{\tau}{2}) s^*(t - \frac{\tau}{2}) = \\ &= \int dt \exp(-i2\pi\nu t) R(t, \tau) = \\ &= \int df \exp(i2\pi f \tau) S(f + \frac{\nu}{2}) S^*(f - \frac{\nu}{2}) . \end{aligned} \quad (22)$$

In fact, the two are double Fourier transforms of each other:

$$\begin{aligned} &\iint dt df \exp(i2\pi\tau f - i2\pi\nu t) W(t, f) = \\ &= \iint dt df \exp(i2\pi\tau f - i2\pi\nu t) \int d\tau_1 \exp(-i2\pi f \tau_1) s(t + \frac{\tau_1}{2}) s^*(t - \frac{\tau_1}{2}) = \\ &= \iint dt d\tau_1 \exp(-i2\pi\nu t) s(t + \frac{\tau_1}{2}) s^*(t - \frac{\tau_1}{2}) \delta(\tau - \tau_1) = \\ &= \int dt \exp(-i2\pi\nu t) s(t + \frac{\tau}{2}) s^*(t - \frac{\tau}{2}) = \chi(\nu, \tau) . \end{aligned} \quad (23)$$

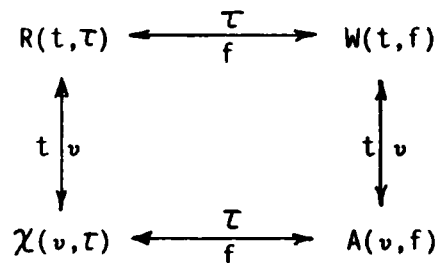
Here we used (3), (13), and (22).

In a similar fashion, the following (single) Fourier transform relationships on the WDF hold:

$$\int df \exp(i2\pi f\tau) W(t, f) = s(t + \frac{\tau}{2}) s^*(t - \frac{\tau}{2}) = R(t, \tau) ,$$

$$\int dt \exp(-i2\pi vt) W(t, f) = S(f + \frac{v}{2}) S^*(f - \frac{v}{2}) = A(v, f) . \quad (24)$$

These properties are summarized in the following diagram, where an arrow denotes a Fourier transform:



Not every function of  $t, f$  is a (legal) WDF; in fact, from (24) there follows

$$\int df \exp(i2\pi f(t_1 - t_2)) W\left(\frac{t_1 + t_2}{2}, f\right) = s(t_1) s^*(t_2) = R\left(\frac{t_1 + t_2}{2}, t_1 - t_2\right) . \quad (25)$$

Thus, in order for a candidate function  $W(t,f)$  to be a WDF, the function resulting on the right-hand side of (25) must be separable in the variables  $t_1$  and  $t_2$ . When and only when that separability occurs, the waveform  $s(t)$  can be recovered from correlation  $R$  or  $W$  (within a constant unknown phasor) as follows: let

$$s(t_0) = |s(t_0)| \exp(i\theta(t_0)), \quad R(t_0, 0) = |s(t_0)|^2, \quad (26)$$

where  $t_0$  is arbitrary, except that  $s(t_0) \neq 0$ . Then, from the right-hand side of (25),

$$s(t) = \frac{R\left(\frac{t+t_0}{2}, t-t_0\right)}{s^*(t_0)} = \frac{R\left(\frac{t+t_0}{2}, t-t_0\right)}{\sqrt{R(t_0, 0)}} \exp(i\theta(t_0)) \quad \text{for all } t. \quad (27)$$

The special case of  $t_0 = 0$  was given in [3; (17)]. The fact that the constant phase  $\theta(t_0)$  is irretrievably lost in  $R$  and  $W$  can easily be seen by considering  $s(t) = c g(t)$ , for which  $W_s(t,f) = |c|^2 W_g(t,f)$ .

The box-like function  $\text{rect}(t/T) \text{rect}(f/F) = 1$  for  $|t| < T/2$  and  $|f| < F/2$ , zero otherwise, which was employed for smoothing in [1], is not a WDF, since the transform on the left-hand side of (25) yields  $F \text{sinc}(Ft_1 - Ft_2)$  for  $|t_1 + t_2| < T$ , which is not separable in  $t_1$  and  $t_2$ . Also, the Gaussian function  $\exp(-t^2/\sigma^2 - b^2 4\pi^2 f^2)$  is a legal WDF if and only if  $b = \sigma$ , in which case  $s(t) = (4\pi\sigma^2)^{-1/4} \exp(-t^2/(2\sigma^2))$ , with  $\sigma$  arbitrary.

## FIRST MOMENTS OF W

The marginal integrals of W were given in (11) and (12). The (conditional) first moment of W, with respect to frequency, is

$$\begin{aligned} \int df f W(t, f) &= \int df f \int d\tau \exp(-i2\pi f\tau) s(t + \frac{\tau}{2}) s^*(t - \frac{\tau}{2}) = \\ &= \int d\tau s(t + \frac{\tau}{2}) s^*(t - \frac{\tau}{2}) \int df f \exp(-i2\pi f\tau) = \\ &= \frac{i}{2\pi} \int d\tau s(t + \frac{\tau}{2}) s^*(t - \frac{\tau}{2}) \delta'(\tau) = \frac{1}{2\pi} \text{Im}\{s'(t) s^*(t)\} . \end{aligned} \quad (28)$$

Here we used the result

$$i2\pi \int dx x \exp(i2\pi xy) = \delta'(y) , \quad (29)$$

obtainable directly from (13) by taking a derivative with respect to y.

Therefore the "frequency center at time t" of waveform s(t) is defined as

$$\nu_f(t) = \frac{\int df f W(t, f)}{\int df W(t, f)} = \frac{1}{2\pi} \frac{\text{Im}\{s'(t) s^*(t)\}}{|s(t)|^2} , \quad (30)$$

upon use of (28) and (12). If we let complex waveform s(t) be represented in terms of its amplitude and phase modulations according to

$$s(t) = M(t) \exp[i\theta(t)] , \quad (31)$$



then (30) yields simply

$$\nu_f(t) = \frac{1}{2\pi} \theta'(t) , \quad (32)$$

which is independent of amplitude modulation  $M(t)$ . (32) can also be interpreted as the instantaneous frequency at time  $t$  of waveform  $s(t)$ .

The "time center at frequency  $f$ " follows in an analogous fashion as

$$\nu_t(f) = \frac{\int dt t W(t, f)}{\int dt W(t, f)} = - \frac{1}{2\pi} \frac{\text{Im}\{S'(f) S^*(f)\}}{|S(f)|^2} . \quad (33)$$

If we represent the voltage density spectrum  $S(f)$  in terms of its magnitude and phase,

$$S(f) = A(f) \exp[-i\theta(f)] , \quad (34)$$

then (33) reduces to

$$\nu_t(f) = \frac{1}{2\pi} \theta'(f) , \quad (35)$$

which is independent of  $A(f)$ . (35) can also be interpreted as the group delay at frequency  $f$  of waveform  $s(t)$ .

The unconditional first moments of  $W$  are frequency center

$$\bar{f} = \frac{\iint dt df f W(t, f)}{\iint dt df W(t, f)} = \frac{\int df f |S(f)|^2}{\int df |S(f)|^2} = \frac{\int df f A^2(f)}{\int df A^2(f)} \quad (36)$$

and time center

$$\bar{t} \equiv \frac{\iint dt df t W(t, f)}{\iint dt df W(t, f)} = \frac{\int dt t |s(t)|^2}{\int dt |s(t)|^2} = \frac{\int dt t M^2(t)}{\int dt M^2(t)} \quad (37)$$

(36) follows directly from (11) and (34), while (37) follows directly from (12) and (31). Thus,  $\bar{f}$  is independent of  $\theta(f)$ , and  $\bar{t}$  is independent of  $\theta(t)$ .

Alternative forms to (36) and (37), in the complementary domains, are available:

$$\bar{f} = \frac{1}{2\pi} \frac{\int dt \operatorname{Im}\{s'(t) s^*(t)\}}{\int dt |s(t)|^2} = \frac{1}{2\pi} \frac{\int dt M^2(t) \theta'(t)}{\int dt M^2(t)}, \quad (38)$$

and

$$\bar{t} = -\frac{1}{2\pi} \frac{\int df \operatorname{Im}\{S'(f) S^*(f)\}}{\int df |S(f)|^2} = \frac{1}{2\pi} \frac{\int df A^2(f) \theta'(f)}{\int df A^2(f)}. \quad (39)$$

The result in (38) follows from the use of (28) and (12) in definition (36); a similar procedure yields (39). The frequency center  $\bar{f}$  in (38) is an average of the instantaneous frequency  $\nu_f(t)$  in (32), weighted according to the magnitude-squared waveform,  $M^2(t)$ ; similarly, time center  $\bar{t}$  in (39) is a weighted average of  $\nu_t(f)$  in (35).

## SECOND MOMENTS OF W

By taking two partial derivatives with respect to  $\tau$  in (24), there follows

$$\int df f^2 W(t, f) = \frac{1}{8\pi^2} \left[ |s'(t)|^2 - \operatorname{Re} \{ s''(t) s^*(t) \} \right]. \quad (40)$$

When we then employ (12) and (31), the (conditional) second moment with respect to  $f$  develops into the form

$$\frac{\int df f^2 W(t, f)}{\int df W(t, f)} = \frac{1}{8\pi^2} \left[ \frac{M'^2(t)}{M^2(t)} - \frac{M''(t)}{M(t)} \right] + \left[ \frac{\Theta'(t)}{2\pi} \right]^2. \quad (41)$$

Therefore the instantaneous "mean-square frequency spread" is

$$\begin{aligned} \sigma_f^2(t) &\equiv \frac{\int df [f - \nu_f(t)]^2 W(t, f)}{\int df W(t, f)} = \\ &= \frac{1}{8\pi^2} \left[ \frac{M'^2(t)}{M^2(t)} - \frac{M''(t)}{M(t)} \right] = -\frac{1}{8\pi^2} \frac{d}{dt} \left\{ \frac{M'(t)}{M(t)} \right\}, \end{aligned} \quad (42)$$

where we employed (32) and (12). This result does not depend on phase modulation  $\Theta(t)$ . However, it should be observed that this quantity can be negative; consider the example  $M(t) = \exp(-t^\nu)$  for  $t > 0$ , with  $0 < \nu < 1$ . Thus (42) can not be interpreted as a true variance. This unfortunate feature of the WDF is due to the fact that  $W(t, f)$  can go negative for some values of  $t, f$ .

The unconditional second moment with respect to  $f$  follows from (40) and (11), respectively, as

$$\iint dt df f^2 W(t, f) = \frac{1}{4\pi^2} \int dt |s'(t)|^2 = \int df f^2 |S(f)|^2. \quad (43)$$

Analogous relations for the second moments with respect to  $t$  can also be derived via a similar approach.

#### MOMENTS OF $W^2$

The marginal integral of the square of the WDF with respect to  $f$  is, via (3), (13), and (2),

$$\begin{aligned} \int df W^2(t, f) &= \int df \iint d\tau du \exp(-i2\pi f(\tau - u)) R(t, \tau) R^*(t, u) = \\ &= \int d\tau |R(t, \tau)|^2 = \int d\tau \left| s\left(t + \frac{\tau}{2}\right) \right|^2 \left| s\left(t - \frac{\tau}{2}\right) \right|^2 = \\ &= 2 \left\{ |s(\tau)|^2 \otimes_{\tau=2t} |s(\tau)|^2 \right\}, \end{aligned} \quad (44)$$

which is the convolution of  $|s|^2$  with itself, at argument  $2t$ . The complementary result, integrating with respect to  $t$ , is

$$\begin{aligned} \int dt W^2(t, f) &= \int dv \left| s\left(f + \frac{v}{2}\right) \right|^2 \left| s\left(f - \frac{v}{2}\right) \right|^2 = \\ &= 2 \left\{ |s(v)|^2 \otimes_{v=2f} |s(v)|^2 \right\}. \end{aligned} \quad (45)$$

If we complete the integrations in (44) and (45) on the remaining variables, both yield the result

$$\iint dt df W^2(t,f) = E^2 ; \quad (46)$$

see (14). Also note, for comparison, that the double integral on  $W$  yielded  $E$ .

Although the results in (44) and (45) are not overly simple, continued integration does yield a surprisingly simple result; multiplying (44) by  $t$ , there follows

$$\begin{aligned} \iint dt df t W^2(t,f) &= \int dt t^2 \int dx |s(x)|^2 |s(2t-x)|^2 = \\ &= \int dx |s(x)|^2 \int dt t |s(2t-x)|^2 = \int dx |s(x)|^2 \int dy |s(y)|^2 (y+x)/2 = \\ &= \frac{1}{2} \int dx |s(x)|^2 [\bar{t}E + xE] = \frac{1}{2}[\bar{t}E^2 + \bar{t}E^2] = E^2 \bar{t} . \end{aligned} \quad (47)$$

Here we used (44), (37), and (14). Thus

$$\frac{\iint dt df t W^2(t,f)}{\iint dt df W^2(t,f)} = \bar{t} = \frac{\int dt t |s(t)|^2}{\int dt |s(t)|^2} \quad (48)$$

from (47), (46), and (37). This result in (48) is the same as (37), but now for  $W^2$  rather than  $W$ .

Conditional first moments of  $W^2$  with respect to  $f$  and  $t$  are also deriveable; for example,

$$\begin{aligned}
 \int df f W^2(t, f) &= \frac{1}{i2\pi} \int d\tau R^*(t, \tau) \frac{\partial}{\partial \tau} R(t, \tau) = \\
 &= \frac{1}{2\pi} \int d\tau \left| s\left(t + \frac{\tau}{2}\right) \right|^2 \operatorname{Im} \left\{ s'\left(t - \frac{\tau}{2}\right) s^*\left(t - \frac{\tau}{2}\right) \right\} = \\
 &= \frac{1}{\pi} \int dx \left| s(2t - x) \right|^2 \operatorname{Im} \left\{ s'(x) s^*(x) \right\} = \\
 &= \frac{1}{\pi} \int dx M^2(2t - x) M^2(x) \Theta'(x) . \tag{49}
 \end{aligned}$$

Here we used (3), (29), (2), and (31). When normalized by the quantity in (44), the result is considerably more complicated than the corresponding result for  $W$  in (30) and (32); nevertheless, continued integrations simplify tremendously. In particular, there follows, from (49), (14), (38), (46), and (36),

$$\frac{\iint dt df f W^2(t, f)}{\iint dt df W^2(t, f)} = \bar{f} = \frac{\int df f |S(f)|^2}{\int df |S(f)|^2} . \tag{50}$$

This is the dual relation to (48), but derived by means of a different approach. Comparison of (50) with (36) reveals the same result for  $W$  as for  $W^2$ .

## CROSS WIGNER DISTRIBUTION FUNCTION

The cross WDF of two complex waveforms  $a(t)$  and  $b(t)$  is a generalization of (3) and (10) according to

$$\begin{aligned}
 W_{ab}(t,f) &= \int d\tau \exp(-i2\pi f\tau) R_{ab}(t,\tau) = \\
 &= \int d\tau \exp(-i2\pi f\tau) a\left(t + \frac{\tau}{2}\right) b^*\left(t - \frac{\tau}{2}\right) = \\
 &= \int dv \exp(i2\pi vt) A\left(f + \frac{v}{2}\right) B^*\left(f - \frac{v}{2}\right), \quad (51)
 \end{aligned}$$

which is generally complex. If  $a(t)$  and  $b(t)$  are nonzero only for  $a_1 < t < a_2$  and  $b_1 < t < b_2$ , respectively, then the integral limits on  $\tau$  in (51) are explicitly  $\tau_1, \tau_2$ , where

$$\tau_1 = 2 \max(a_1 - t, t - b_2), \quad \tau_2 = 2 \min(a_2 - t, t - b_1).$$

If  $\tau_1 \geq \tau_2$ , then  $W_{ab}$  is zero.

The following properties of the cross WDF result immediately:

$$W_{a^*b^*}(t,f) = W_{ab}^*(t,-f),$$

$$W_{ba}(t,f) = W_{ab}^*(t,f),$$

$$\int df W_{ab}(t,f) = a(t) b^*(t),$$

$$\int dt W_{ab}(t, f) = A(f) B^*(f) ,$$

$$\iint dt df W_{ab}(t, f) = \int dt a(t) b^*(t) = \int df A(f) B^*(f) ,$$

$$\iint dt df |W_{ab}(t, f)|^2 = E_a E_b ,$$

$$\iint dt df W_{aa}(t, f) W_{bb}(t, f) = \left| \int dt a(t) b^*(t) \right|^2 = \left| \iint dt df W_{ab}(t, f) \right|^2 ,$$

$$\iint dt df W_{ab}(t, f) W_{cd}^*(t, f) = \int dt a(t) c^*(t) * \int dt b^*(t) d(t) . \quad (52)$$

The last three relations follow upon substitution of (51), interchanging integrals, and the use of (13). Again, the double Fourier transform of the cross WDF yields the cross ambiguity function:

$$\begin{aligned} \iint dt df \exp(-i2\pi vt + i2\pi f\tau) W_{ab}(t, f) &= \\ &= \int dt \exp(-i2\pi vt) a(t + \frac{\tau}{2}) b^*(t - \frac{\tau}{2}) = \\ &= \int df \exp(i2\pi f\tau) A(f + \frac{v}{2}) B^*(f - \frac{v}{2}) = \\ &= \chi_{ab}(v, \tau) = \int dt \exp(-i2\pi vt) R_{ab}(t, \tau) . \end{aligned} \quad (53)$$



The magnitude-squared cross-WDF of waveforms a and b is also related to the auto-WDFs by means of a double convolution:

$$\begin{aligned}
 |W_{ab}(t, f)|^2 &= \iint d\tau_1 d\tau_2 \exp(-i2\pi f(\tau_1 - \tau_2)) * \\
 &* R_{aa}\left(t + \frac{\tau_1 + \tau_2}{4}, \frac{\tau_1 - \tau_2}{2}\right) R_{bb}\left(t - \frac{\tau_1 + \tau_2}{4}, \frac{\tau_1 - \tau_2}{2}\right) = \\
 &= \iint d\tau' d\tau \exp(-i2\pi f\tau') R_{aa}\left(t + \frac{\tau}{2}, \frac{\tau'}{2}\right) R_{bb}\left(t - \frac{\tau}{2}, \frac{\tau'}{2}\right) = \\
 &= \iint d\tau' d\tau \exp(-i2\pi f\tau') R_{aa}\left(t + \frac{\tau}{2}, \frac{\tau'}{2}\right) \int df' \exp\left(i2\pi f' \frac{\tau'}{2}\right) W_{bb}\left(t - \frac{\tau}{2}, f'\right) = \\
 &= \iint d\tau df' W_{bb}\left(t - \frac{\tau}{2}, f'\right) \int d\tau' \exp\left(-i2\pi(2f - f') \frac{\tau'}{2}\right) R_{aa}\left(t + \frac{\tau}{2}, \frac{\tau'}{2}\right) = \\
 &= 2 \iint d\tau df' W_{bb}\left(t - \frac{\tau}{2}, f'\right) W_{aa}\left(t + \frac{\tau}{2}, 2f - f'\right) = \\
 &= \iint d\tau d\nu W_{aa}\left(t + \frac{\tau}{2}, f + \frac{\nu}{2}\right) W_{bb}\left(t - \frac{\tau}{2}, f - \frac{\nu}{2}\right), \tag{54}
 \end{aligned}$$

where we let  $\tau = (\tau_1 + \tau_2)/2$ ,  $\tau' = \tau_1 - \tau_2$  in the third line.

## NARROWBAND REAL WAVEFORM

When waveform  $s(t)$  is narrowband and real, it can be expressed in terms of its low-pass complex envelope  $c(t)$  according to

$$\begin{aligned} s(t) &= 2 \operatorname{Re}\{c(t) \exp(i2\pi f_0 t)\} = \\ &= c(t) \exp(i2\pi f_0 t) + c^*(t) \exp(-i2\pi f_0 t) . \end{aligned}$$

where  $f_0$  is the carrier or center frequency of  $s(t)$ . The WDF of  $s(t)$  is then expressible as

$$\begin{aligned} W_{SS}(t, f) &= \int d\tau \exp(-i2\pi f\tau) s(t + \frac{\tau}{2}) s^*(t - \frac{\tau}{2}) = \\ &= W_{CC}(t, f - f_0) + W_{CC}(t, -f - f_0) + \\ &+ 2 \operatorname{Re}\{W_{CC^*}(t, f) \exp(i4\pi f_0 t)\} . \end{aligned} \quad (55)$$

Here, we substituted for  $s(t)$ , and used (51) and (52). Since complex envelope  $c(t)$  is low-pass, a representative contour plot of (55) appears as shown in figure 1. The wiggly lobe centered at  $f = 0$  is subject to rapid oscillations in  $t$ , whereas those lobes centered at  $\pm f_0$  are slowly varying with  $f$  and  $t$ . A small amount of averaging in time would wipe out the undesired oscillating lobe, but maintain the desired components at  $f = \pm f_0$ .

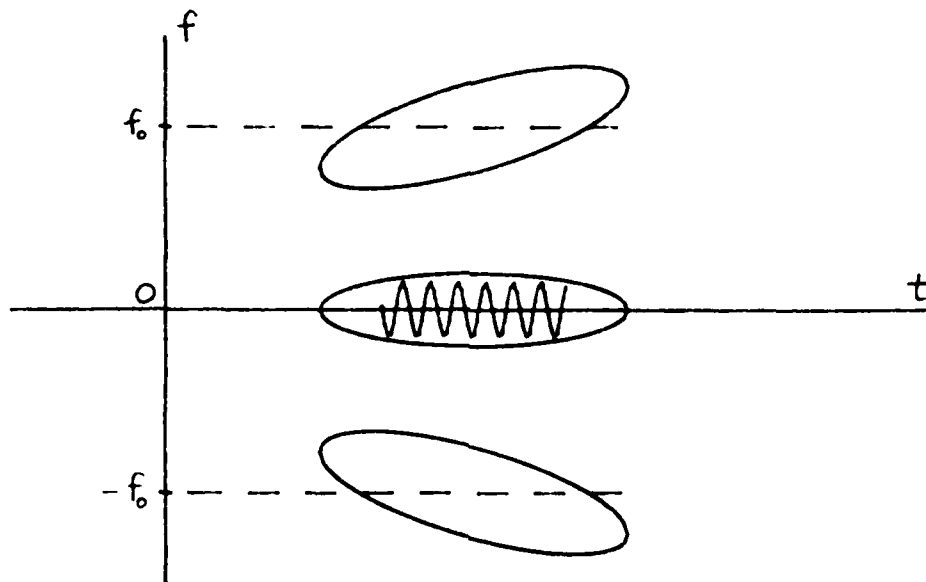


Figure 1. WDF for Narrowband Real Waveform

## SAMPLING PROPERTIES

By letting  $u = \tau/2$  in (3), the WDF becomes

$$W(t, f) = 2 \int du \exp(-i4\pi fu) s(t + u) s^*(t - u), \quad (56)$$

where we again now allow general complex  $s(t)$ . If this integral is to be evaluated numerically on a computer, we will need to sample the integrand at some increment  $\Delta_t$ , and apply some integration rule. In particular, if we use the Trapezoidal rule and carry out the summation over  $-\infty, +\infty$ , we have approximation

$$\bar{W}(t, f) \cong 2\Delta_t \sum_k \exp(-i4\pi fk\Delta_t) s(t + k\Delta_t) s^*(t - k\Delta_t) \quad (57)$$

for all  $t, f$ . Since it is immediately seen from (57) that

$$\tilde{W}\left(t, f + \frac{1}{2\Delta_t}\right) = \tilde{W}(t, f) , \quad (58)$$

it follows that  $\tilde{W}(t, f)$  has period  $(2\Delta_t)^{-1}$  in  $f$ , when waveform  $s(t)$  is sampled at increment  $\Delta_t$ . In fact, it can be shown that  $\tilde{W}$  is the aliased version of  $W$ :

$$\tilde{W}(t, f) = \sum_n W\left(t, f - \frac{n}{2\Delta_t}\right) . \quad (59)$$

Thus,  $\tilde{W}(t, f)$  need be evaluated only over one period, say  $(0, .5/\Delta_t)$ .

Since (57) cannot be evaluated for all continuous values of  $t$  and  $f$ , we will limit its evaluation to

$$t = m\Delta_t , \quad f = \frac{n}{2N_f\Delta_t} , \quad (60)$$

where  $m, n, N_f$  are integers. Then (57) becomes (exactly)

$$\tilde{W}\left(m\Delta_t, \frac{n}{2N_f\Delta_t}\right) = 2\Delta_t \sum_k \exp(-i2\pi nk/N_f) s\left((m+k)\Delta_t\right) s^*\left((m-k)\Delta_t\right) . \quad (61)$$

the right side of which is recognized as an  $N_f$ -point discrete Fourier transform. If the number of nonzero samples in  $k$  is greater than  $N_f$ , we simply collapse them mod  $N_f$ , without loss of accuracy; see [5; page 7]. Since the period of  $\tilde{W}(t, f)$  is  $(2\Delta_t)^{-1}$  in  $f$ , we only need consider  $0 \leq n \leq N_f - 1$ , that is,  $0 \leq f < (2\Delta_t)^{-1}$ . Values of  $m$  must be considered wherever the summand of (61) is nonzero.

A plot of two of the infinite number of lobes of  $\tilde{W}(t, f)$  in (59) is depicted in figure 2 for a representative bandpass analytic waveform  $s(t)$ .

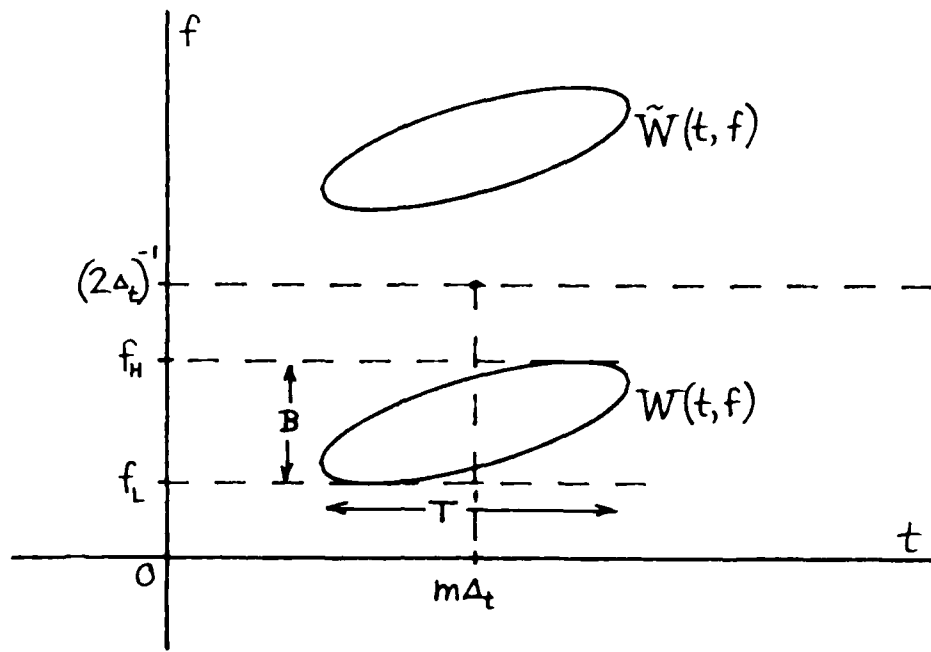


Figure 2. WDF for Sampled Version  $\tilde{W}(t, f)$

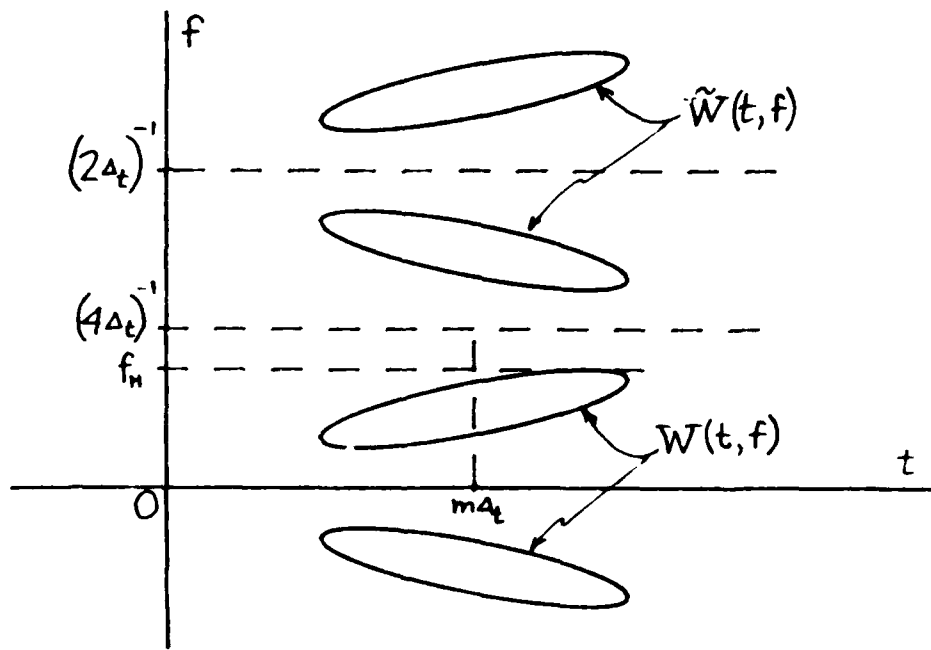


Figure 3.  $\tilde{W}(t, f)$  for Real Waveform  $s(t)$

The spreads of the desired WDF term  $W(t,f)$  are  $T$  and  $B$  in time and frequency, respectively. In order to guarantee that aliasing is insignificant in figure 2, we must choose

$$(2\Delta_t)^{-1} > B, \quad \text{that is, } \Delta_t < (2B)^{-1}. \quad (62)$$

For  $N_f$  equal to a power of 2 in (61), an FFT can be employed to evaluate  $\tilde{W}$  and will give the vertical slice in  $f$  indicated in figure 2 between  $f = 0$  and  $f = (2\Delta_t)^{-1}$ , for the particular  $m$  value under consideration. Since the spacing of frequency values in (61) is  $(2N_f\Delta_t)^{-1}$ , then in order to keep track of the wiggles in  $\tilde{W}(t,f)$  as a function of  $f$ , we must choose

$$(N_f\Delta_t)^{-1} < T^{-1}, \quad \text{that is, } N_f > T/\Delta_t > 2BT. \quad (63)$$

Thus the FFT size may have to be quite large for an extended WDF in  $t,f$  space.

If  $s(t)$  is real, then (8) applies, meaning that  $\tilde{W}$  in (61) need only be computed for

$$0 \leq n \leq N_f/2, \quad \text{that is, } 0 \leq f \leq (4\Delta_t)^{-1}. \quad (64)$$

The pertinent approximate WDF  $\tilde{W}$  is depicted in figure 3. In order to avoid aliasing now, we must have

$$(4\Delta_t)^{-1} > f_H, \quad \text{that is, } \Delta_t < (4f_H)^{-1}, \quad (65)$$

where  $f_H$  is the highest frequency contained in  $s(t)$ . This sampling rate is twice as fast as the usual Nyquist rate for waveform  $s(t)$ , and is due to the unavoidable factors of  $1/2$  in definition (3).

The procedure described above, in (61) et seq., realizes a slice in  $f$ , at fixed  $t$ , of the WDF; see figures 2 and 3. An alternative procedure for obtaining slices of the WDF in  $t$ , at fixed  $f$ , is described in appendix A; however, starting with time samples of  $s(t)$ , it requires an additional large-size FFT to start the calculations.

## EXAMPLES OF WDF

In this section, we present several examples of the WDF for waveforms that are likely to be encountered in practice, and that are amenable to simple closed form solution. A significant shortcut in the presentation is possible when it is observed from (3) that if

$$r(t) = s(t - t_0) \exp(i2\pi f_0 t + i\theta_0) , \quad (66)$$

which corresponds to a time delay and frequency shift, then

$$W_r(t, f) = W_s(t - t_0, f - f_0) . \quad (67)$$

Thus we can choose any convenient origin for the waveform  $s$  in time and frequency, without loss of generality, and then merely shift the WDF according to (67), as appropriate.

We will place heavy emphasis here on combinations of Gaussian pulses, both because of their analytic tractability and due to the fact that any waveform can be expanded into elementary waveforms consisting of Gaussian wavelets; see, for example, Gabor's original paper [6, part 1, section 5].

In the following, frequent use will be made of the following integral:

$$\int dx \exp(-\frac{1}{2} \alpha x^2 \pm Bx) = \left(\frac{2\pi}{\alpha}\right)^{1/2} \exp\left(\frac{B^2}{2\alpha}\right) \quad \text{for } \alpha_r > 0 , \quad (68)$$



where  $\alpha$  and  $\beta$  can be complex, with components

$$\alpha = \alpha_r + i\alpha_i, \quad \beta = \beta_r + i\beta_i. \quad (69)$$

Also, as a special case, there follows

$$\left| \int dx \exp\left(-\frac{1}{2} \alpha x^2 \pm \beta x\right) \right|^2 = \frac{2\pi}{(\alpha_r^2 + \alpha_i^2)^{1/2}} \exp\left[ \frac{\alpha_r(\beta_r^2 - \beta_i^2) + 2\alpha_i\beta_r\beta_i}{\alpha_r^2 + \alpha_i^2} \right], \quad (70)$$

written out in terms of purely real quantities.

#### GAUSSIAN WAVEFORM

Let waveform

$$s(t) = a_0 \exp\left(-\frac{t^2}{2\sigma_0^2}\right); \quad a_0 \text{ complex}. \quad (71)$$

(Parameters will be real unless indicated otherwise.) Use of (3) and (68) yields WDF

$$W(t, f) = 2E \exp\left[-\frac{t^2}{\sigma_0^2} - (2\pi f \sigma_0)^2\right], \quad (72)$$

where  $E$  is the waveform energy:

$$E = \sqrt{\pi} |a_0|^2 \sigma_0. \quad (73)$$

The WDF consists of a single positive lobe in  $t, f$  space, centered at the origin.

Observe that  $W(0,0)$  is equal to  $2E$  for this example; in fact, from (3),

$$W(0,0) = \int d\tau s(\tau/2) s^*(-\tau/2) = 2E \quad \text{if } s(-t) = s(t) . \quad (14)$$

Thus waveforms  $s(t)$  with this even symmetry result in peak WDF values of  $2E$  at the origin. However, if  $s$  has odd symmetry about zero,  $s(-t) = -s(t)$ , then  $W(0,0) = -2E$ .

The contours of equal height of the WDF in (72) are ellipses. The contour for the case where the levels are down to  $\exp(-1)$  of their peak value is the ellipse indicated in figure 4. The area of this particular level ellipse is  $1/2$  in the  $t, f$  plane. When this area is multiplied by the peak height of  $2E$ , the product is  $E$ , which is just the volume under the WDF; see (14). Thus the "effective extent" of the WDF in (72) is that given in figure 4, for relative level  $1/e$  of the peak.

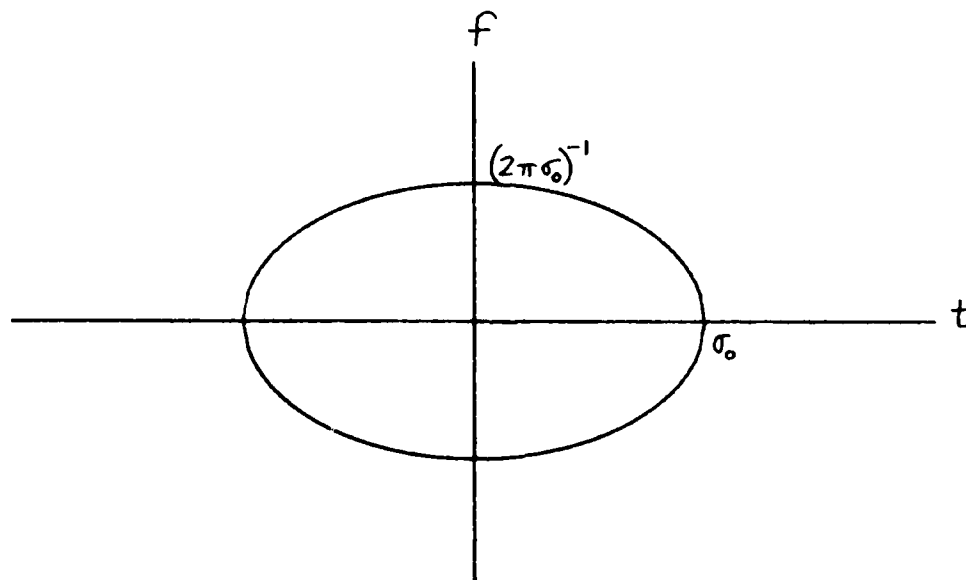


Figure 4. Contour of WDF (72) at  $1/e$  Relative Level

## GAUSSIAN-MODULATED TONE

$$s(t) = b_0 \cos(2\pi f_0 t + \theta_0) \exp\left(-\frac{t^2}{2\sigma_0^2}\right). \quad (75)$$

The energy of this waveform is

$$E = \frac{1}{2} \sqrt{\pi} b_0^2 \sigma_0 [1 + \cos(2\theta_0) \exp(-y_0^2)], \quad (76)$$

and its WDF is

$$\begin{aligned} \left(\frac{1}{2} \sqrt{\pi} b_0^2 \sigma_0\right)^{-1} W(t, f) = & \exp[-x^2 - (y - y_0)^2] + \exp[-x^2 - (y + y_0)^2] + \\ & + 2 \cos(4\pi f_0 t + 2\theta_0) \exp[-x^2 - y^2], \end{aligned} \quad (77)$$

where dimensionless variables

$$x = t/\sigma_0, \quad y = 2\pi f \sigma_0, \quad y_0 = 2\pi f_0 \sigma_0. \quad (78)$$

There are two positive lobes centered at  $(t, f) = (0, f_0)$  and  $(0, -f_0)$ , each of peak height approximately  $E$  (if  $y_0$  is large). The contours of each of these lobes are circles in the  $x, y$  plane, or ellipses in the  $t, f$  plane, as indicated in figure 4. There is also an oscillating lobe centered at the origin; this is an example of the general situation depicted in figure 1.

It should also be observed from (77) that if a slice in frequency is taken of the WDF, at fixed time  $t$ , that there is no fast oscillation in any of the three lobes. Whatever value of the  $\cos$  is encountered, that value is maintained, and the only variation with  $y$  (frequency) is the Gaussian dependence. Thus if we locally averaged the WDF with respect to frequency alone, that would not eliminate the undesired oscillating lobe centered at  $(0, 0)$ .

## MULTIPLE MODULATED TONES

Consider complex waveform

$$s(t) = \sum_k a_k \exp \left[ i2\pi f_k t - \frac{(t - t_k)^2}{2\sigma_k^2} \right]; \quad \{a_k\} \text{ complex.} \quad (79)$$

This is a collection of tone bursts centered at  $(t_k, f_k)$  in the  $t, f$  plane, with energy  $E_k = \sqrt{\pi} |a_k|^2 \sigma_k$ . The corresponding WDF follows from (3) and (68) as

$$\begin{aligned} W(t, f) = & 2 \sum_k E_k \exp \left[ -\frac{(t - t_k)^2}{\sigma_k^2} - \sigma_k^2 4\pi^2 (f - f_k)^2 \right] + \\ & + 4\sqrt{\pi} \sum_{k < l} \tilde{\sigma}_{kl} \exp \left[ -\frac{(t - t_{kl})^2}{\tilde{\sigma}_{kl}^2} - \tilde{\sigma}_{kl}^2 4\pi^2 (f - f_{kl})^2 \right] * \\ & * \operatorname{Re} \left\{ a_k a_l^* \exp \left[ i2\pi (f_k - f_l) t + i \tilde{\sigma}_{kl}^2 2\pi (f - f_{kl}) \left( \frac{t - t_k}{\sigma_k^2} - \frac{t - t_l}{\sigma_l^2} \right) \right] \right\}, \quad (80) \end{aligned}$$

where

$$\begin{aligned} t_{kl} &= \frac{1}{2} (t_k + t_l), & f_{kl} &= \frac{1}{2} (f_k + f_l), \\ \tilde{\sigma}_{kl}^2 &= \frac{1}{2} (\sigma_k^2 + \sigma_l^2), & \frac{1}{\tilde{\sigma}_{kl}^2} &= \frac{1}{2} \left( \frac{1}{\sigma_k^2} + \frac{1}{\sigma_l^2} \right). \end{aligned} \quad (81)$$

The first line of (80) represents the desired positive lobes centered at  $(t_k, f_k)$ , each scaled according to its energy. The remaining undesired lobes are centered at

$$\frac{t_k + t_l}{2}, \frac{f_k + f_l}{2} \quad \text{for all } k \neq l, \quad (82)$$

and oscillate with  $t$  and/or  $f$ . These locations in (82) are halfway between every possible pair of desired lobes; their amplitudes are proportional to the geometric means of the corresponding interacting lobes, and therefore constitute significant interference effects to interpretation of the computed WDF. Furthermore, the locations in (82) can occur in time where the waveform  $s(t)$  is zero, and/or in frequency where the spectrum  $S(f)$  is zero. This most undesirable feature of the WDF has been reported previously in [7,8]. The only saving feature, that should allow salvaging the WDF, is that the undesired lobes,  $k < l$  in (80), oscillate positive-and-negative and can be averaged out by smoothing the WDF. Of course, via this smoothing procedure, the desired lobes will also be smeared somewhat, but this trade-off appears to be required in order to make a meaningful, useful interpretation of the WDF at all points of the  $t, f$  plane.

The envelope of the  $k, l$  lobe in (80) is proportional to an exponential of an elliptical function. When this exponential has decreased to  $1/e$  of its peak value, the corresponding elliptical contour has area

$$\frac{\pi \bar{\sigma}_{kl}}{2\pi \tilde{\sigma}_{kl}} = \frac{1}{4} \left( \frac{\sigma_k}{\sigma_l} + \frac{\sigma_l}{\sigma_k} \right) \geq \frac{1}{2} \quad (83)$$

in the  $t, f$  plane, the latter value of  $1/2$  being the area of every desired lobe. Thus the undesired oscillating lobes are smeared out more than the desired positive lobes.

If we restrict (79) to two equal-duration bursts with the same time center, but different center frequencies, the undesired lobe oscillates only with  $t$ , not  $f$ . This is similar to example (75)-(77). On the other hand, if (79) is restricted to two equal-duration bursts with different time centers, but the same frequency center, the undesired lobe oscillates only with  $f$ , not  $t$ .

More generally, for two equal-duration bursts with different time and frequency centers, the undesired lobe has no fast oscillation along lines in the  $t, f$  plane which are parallel to the line joining the centers of the two positive lobes in the WDF. For two unequal-duration bursts, the situation is more complicated, and there is generally oscillation along all straight lines in the  $t, f$  plane.

What these simple examples demonstrate is that if we want to locally smooth (average) the WDF, in an effort to wipe out the undesired oscillating cross-terms, that smoothing must be applied in both  $t$  and  $f$ , not either one alone. Of course, such smoothing will also tend to smear the desired positive lobes; thus the minimum amount of smoothing to guarantee a nonnegative WDF is of interest.

Although these conclusions have been drawn from the particular example of Gaussian-modulated tone bursts in (79) (for analytic simplicity), they hold generally. Appendix B demonstrates the oscillating character of the interacting cross-terms of the WDF for a waveform with two separated energy bursts in time of general shape.

The ambiguity function of waveform  $s(t)$  in (75) is considered in appendix C. It has some similar properties to the WDF and some significant differences, which make it much less desirable as a descriptor of a signal's concentration in time-frequency space.

#### LINEAR FREQUENCY MODULATION

Here, we consider waveform

$$s(t) = a_0 \exp \left[ -\frac{t^2}{2\sigma_0^2} + i \frac{\alpha_0}{2} t^2 \right]; \quad \alpha_0 \geq 0, \quad a_0 \text{ complex.} \quad (84)$$

The instantaneous frequency, according to (31) and (32), is a linear function of time,

$$\nu_f(t) = \frac{\alpha_0}{2\pi} t, \quad (85)$$

while the envelope is Gaussian. When

$$t = t_0 = \pm \sigma_0 \sqrt{\pi/2}, \quad (86)$$

the magnitude of the waveform  $s(t)$  is

$$|s(t_0)| = |a_0| \exp(-\pi/4) = .456 |s(0)|. \quad (87)$$

If we define the duration,  $\Delta t$ , of  $s(t)$  as the time between these function values, then

$$\Delta t = \sigma_0 \sqrt{2\pi}. \quad (88)$$

During this time interval, the instantaneous frequency in (85) sweeps through a bandwidth

$$\Delta f = \frac{\alpha_0}{2\pi} \Delta t = \alpha_0 \sigma_0 \sqrt{2\pi}. \quad (89)$$

The time-bandwidth product of waveform  $s(t)$  is therefore

$$\Delta t \Delta f = \alpha_0 \sigma_0^2 \equiv \theta_0 \quad (\geq 0), \quad (90)$$

when the time duration is defined as the interval between the function values in (87). This quantity,  $\theta_0$ , is an important parameter of the linear frequency modulation waveform (84).

The WDF of (84) follows, upon use of (3) and (68), as

$$\begin{aligned} W(t, f) &= 2E \exp \left[ -\frac{t^2}{\sigma_0^2} - \sigma_0^2 (2\pi f - \alpha_0 t)^2 \right] = \\ &= 2E \exp \left[ -x^2 - (y - x\theta_0)^2 \right] = \\ &= 2E \exp \left[ -x^2 (1 + \theta_0^2) + 2xy \theta_0 - y^2 \right], \end{aligned} \quad (91)$$

where we employed (78) and (90). This is an everywhere-positive lobe centered at the origin of time-frequency space, with contours that are tilted ellipses. The peak value,  $2E$ , is independent of the amount of frequency modulation.



For a given value of time  $t$ , the frequency  $f$  that maximizes the WDF in (91) is

$$f = \frac{\alpha_0}{2\pi} t, \quad \text{that is, } y = x\theta_0, \quad (92)$$

which is just the instantaneous frequency in (85). However, this line, (92), in the  $t, f$  plane is not the major axis of the elliptical contours of the WDF. A similar observation regarding the ambiguity function  $\chi(\nu, \tau)$ , (23), of the linear frequency modulation waveform, namely

$$\chi(\nu, \tau) = E \exp \left[ -\frac{1}{4} \left\{ x'^2 (1 + \theta_0^2) - 2x'y'\theta_0 + y'^2 \right\} \right], \quad (93)$$

where

$$x' = \frac{\tau}{\sigma_0}, \quad y' = 2\pi\nu\sigma_0, \quad (94)$$

has been made in [4; page 124].

What this means is that, if the WDF of a waveform is evaluated numerically from a given data sequence (via (61) for example), then the tilt of the major axis of the contours of the computed WDF is not directly the amount of linear frequency modulation in the waveform. Rather, the major axis of the ellipse in (91) lies along the line

$$y = x \tan \psi \quad (95)$$

in the  $x, y$  plane, where

$$\tan \psi = \frac{\sqrt{\theta_0^2 + 4} + \theta_0}{2} \geq \theta_0. \quad (96)$$

(See appendix D for detailed derivations on the rotation of coordinate axes.) Thus, the major axis (95) of the ellipse is more tilted than the instantaneous frequency line (92). Equation (96) can be inverted and solved for the linear frequency modulation parameter  $\theta_0$  according to

$$\theta_0 = \tan\psi - 1/\tan\psi, \quad (97)$$

in terms of the measured or calculated major axis tilt,  $\tan\psi$ , in the x,y plane. The detailed procedure for solving for both  $\sigma_0$  and  $\alpha_0$ , in terms of a computed WDF in the t,f plane, is discussed in the example in appendix D, especially (D-28) and (D-29).

When the exponential in (91) is down to 1/e of its peak value, the ellipse at that level has area  $\pi$  in the x,y plane. This may be seen by use of (D-1) and (D-20), with  $A = 1 + \theta_0^2$ ,  $B = -2\theta_0$ ,  $C = 1$ ,  $D = E = 0$ ,  $F = -1$ , for which  $G = 1$  via (D-19). This corresponds to area 1/2 in the t,f plane, as seen by (78). Therefore, the peak height,  $2E$ , times the "effective" area is again  $E$ , as it was for the simple Gaussian pulse of (71) and figure 4. Thus, although the volume of the WDF in (91) has been redistributed in the t,f plane, by virtue of linear frequency modulation, the effective area is maintained, although now located as a tilted ellipse.

A plot of the ellipse of (91) at the 1/e level, namely

$$x^2 + (y - x\theta_0)^2 = x^2(1 + \theta_0^2) - 2xy\theta_0 + y^2 = 1, \quad (98)$$

is given in figure 5, when  $\theta_0 = 1.5$ . The instantaneous frequency line (92) as well as the major axis (95) are delineated, and are clearly seen not to overlie each other.

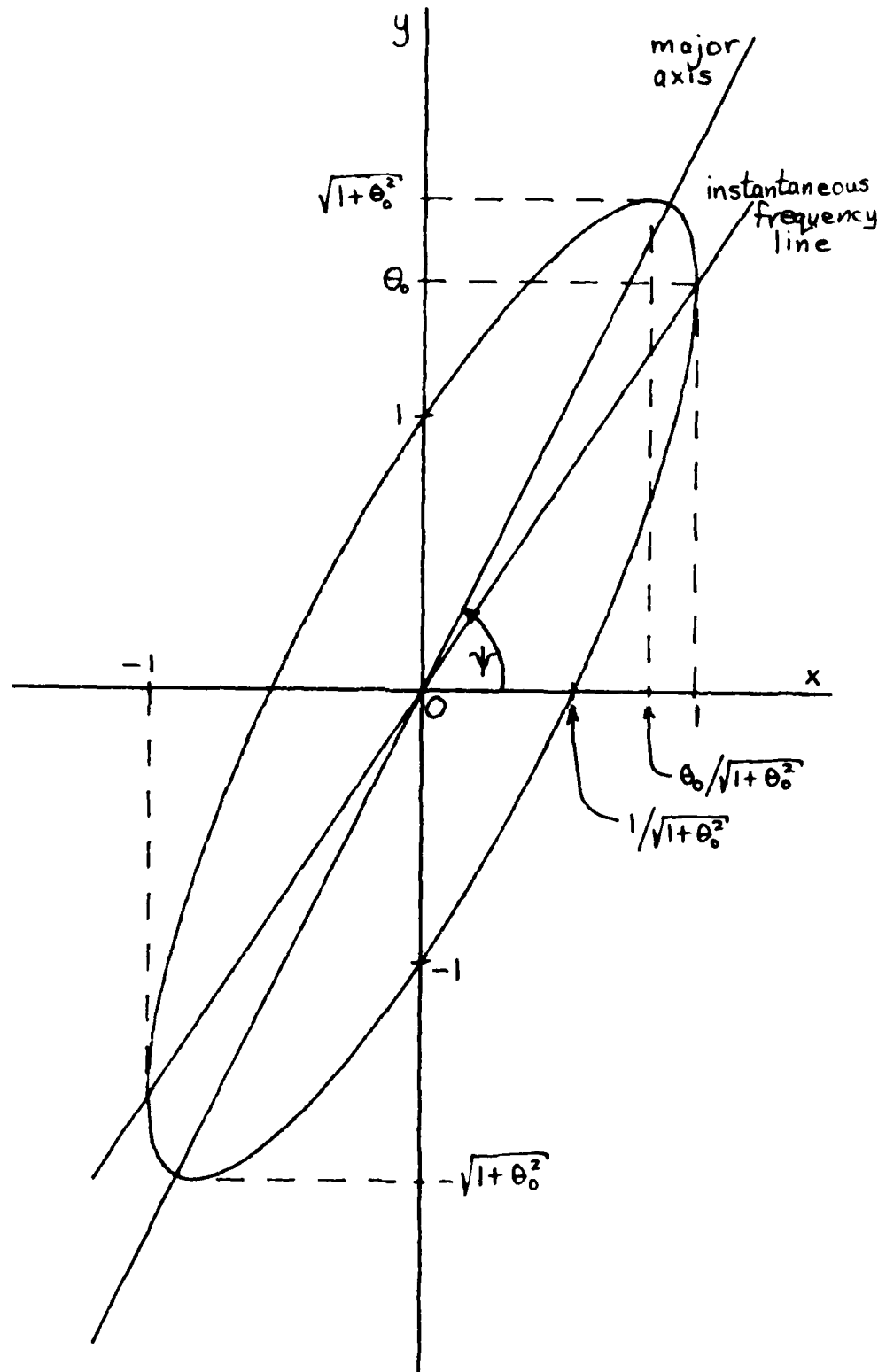


Figure 5. Contour of (91) for  $\theta_0 = 1.5$

## GATED LINEAR FREQUENCY MODULATION

All the previous examples in this section had Gaussian envelopes. We now consider a rectangularly gated waveform with linear frequency modulation:

$$s(t) = a_0 \exp\left[i \frac{\alpha_0}{2} t^2\right] \quad \text{for } |t| < \frac{T}{2}; \quad a_0 \text{ complex.} \quad (99)$$

Equation (3) yields directly WDF

$$W(t, f) = 2E \frac{\sin[(2\pi f - \alpha_0 t)(T - 2|t|)]}{(2\pi f - \alpha_0 t)T} \quad \text{for } |t| < \frac{T}{2}, \quad \text{all } f, \quad (100)$$

and zero otherwise. Along the instantaneous frequency line, (85), the WDF is  $2E (1 - 2|t|/T)$  for  $|t| < T/2$ , which is nonoscillatory and positive. However, in other portions of the  $t, f$  plane, (100) does go negative, due to the sin term.

For a given value of  $t$ , the quantity  $W$  in (100) is maximized by choosing  $f = \alpha_0 t / (2\pi)$ , but, again, this is not the major axis of the contours of the WDF. In figure 6, these contours are plotted for  $\alpha_0 T^2 = 1$  and  $\alpha_0 T^2 = 10$ . In fact, the contours are no longer ellipses, although they tend to resemble ellipses near the origin, when frequency modulation parameter  $\alpha_0 T^2$  is large; see the bottom figure, where the instantaneous frequency line and the mountain ridge (curve of slowest descent) have been sketched.

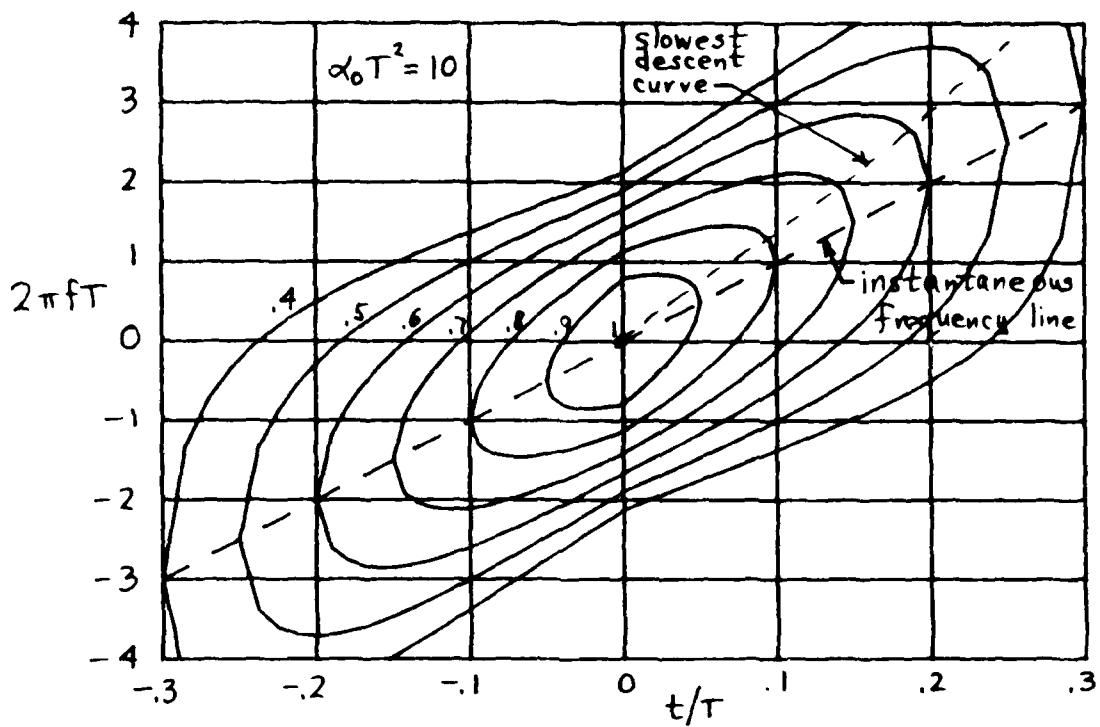
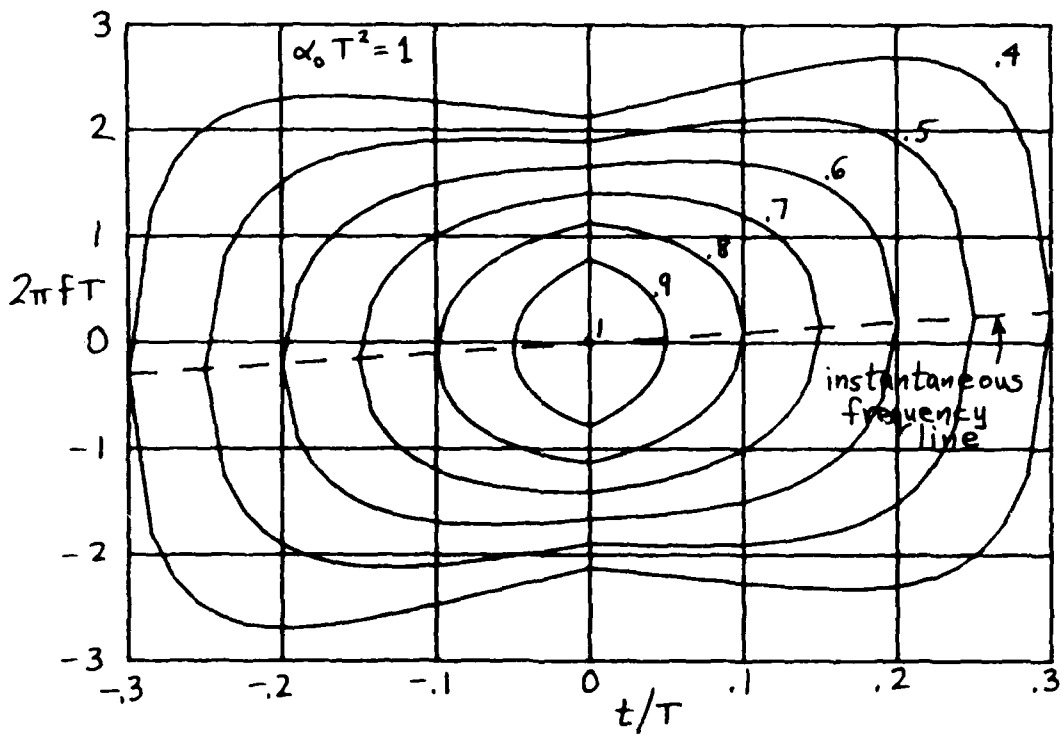


Figure 6. Contours of WDF for Gated LFM

The ambiguity function of waveform (99) is

$$\chi(\nu, \tau) = E \frac{\sin[\frac{1}{2}(2\pi\nu - \alpha_0\tau)(T - |\tau|)]}{\frac{1}{2}(2\pi\nu - \alpha_0\tau)T} \quad \text{for } |\tau| < T, \text{ all } \nu, \quad (101)$$

and zero otherwise. It is similar to the WDF in (100), but is spread out more in the  $\nu, \tau$  plane.

## SHORT-TERM SPECTRAL ESTIMATION

Some advantageous features of the WDF have been brought out by earlier examples, such as the concentrated positive lobes in the  $t, f$  plane about locations corresponding to obvious bursts of energy. However, the WDF also goes negative in surrounding regions, causing difficulty in interpretation; see figure 1, (80), appendix B, or [7,8]. What is needed is some form of smoothing of the WDF so as to eliminate or suppress the oscillating components; however, this averaging must be two-dimensional, carried out in both time and frequency, for the reasons presented in the sequel to (83). We now present one method of smoothing the WDF, which guarantees a non-negative distribution in time-frequency.

## WEIGHTED SPECTRAL ESTIMATE

The voltage density spectrum  $S(f)$ , corresponding to waveform  $s(t)$ , was defined in (9) as the Fourier transform over all time. In order to bring out properties which are local in time, a weighting must be applied before transformation. In particular, we generalize (9) to

$$\begin{aligned}
 S_U(t, f) &= \int dt_1 \exp(-i2\pi ft_1) s(t_1) u^*(t - t_1) = \\
 &= \exp(-i2\pi ft) \int df_1 \exp(i2\pi tf_1) S(f_1) U^*(f - f_1) , \quad (102)
 \end{aligned}$$

where weighting  $u$  will tend to be a narrow function centered about its origin; thus the weighting in (102) will accent the behavior of waveform  $s$  in the neighborhood of time  $t$ . The function  $U$  is the Fourier transform of  $u$ . The short-term power spectral estimate (at time  $t$  and frequency  $f$ ) of waveform  $s$ , relative to weighting  $u$ , is then defined as

$$|S_u(t, f)|^2. \quad (103)$$

See also [2, p. 768].

The following symmetry properties of definition (102) follow:

$$S_u(t, f) = U_s^*(t, f) \exp(-i2\pi ft),$$

$$|S_u(t, f)|^2 = |U_s(t, f)|^2, \quad (104)$$

where  $U_s$  is the spectrum of waveform  $u$  relative to weighting  $s$ . That is,  $U_s$  is the dual of  $S_u$ . Also, by use of (53), we can express

$$S_u(t, f) = \chi_{s\bar{u}}(f, t) \exp(-i\pi ft), \quad (105)$$

in terms of the complex cross-ambiguity function of  $s$  and  $\bar{u}$ , where  $\bar{u}$  is the mirror image of  $u$ :  $\bar{u}(t) = u(-t)$ . Also, the same shifting property, given in (66) and (67) for the WDF, holds as well for quantity (103).

#### RELATION TO WDFs

There is a very important relation between the short-term spectral estimate (STSE), (103), and the WDFs of  $s$  and  $u$ ; namely, by use of (102), (2), and (3), we have



$$\begin{aligned}
|S_u(t, f)|^2 &= \iint dt_1 dt_2 \exp(-i2\pi f(t_1 - t_2)) s(t_1) s^*(t_2) u^*(t - t_1) u(t - t_2) = \\
&= \iint d\tau dt' \exp(-i2\pi f\tau) s\left(t' + \frac{\tau}{2}\right) s^*\left(t' - \frac{\tau}{2}\right) u\left(t - t' + \frac{\tau}{2}\right) u^*\left(t - t' - \frac{\tau}{2}\right) = \\
&= \iint d\tau dt' \exp(-i2\pi f\tau) R_s(t', \tau) R_u(t - t', \tau) = \\
&= \iint dt' df' W_s(t', f') W_u(t - t', f - f') = \\
&= W_s(t, f) \overset{tf}{\otimes} W_u(t, f) . \tag{106}
\end{aligned}$$

This relation states that the STSE is a double convolution, in both  $t$  and  $f$ , of the WDFs of waveform  $s$  and weighting  $u$ . That is, the STSE  $|S_u(t, f)|^2$  of waveform  $s$ , relative to weighting  $u$ , is a smoothed version of the WDF of waveform  $s$ , where the smoothing function is the WDF of weighting  $u$ . Furthermore, since the left-hand side of (106) can never be negative, and since  $s$  and  $u$  are arbitrary, (106) shows that the double convolution of any two WDFs is never negative for any values of  $t, f$ . This furnishes a possibility of accomplishing smoothing of a computed WDF of waveform  $s$ , with a guarantee of a nonnegative distribution resulting; of course,  $W_u$  must be a legal WDF, as discussed in (25) et seq., in order to guarantee this nonnegative property.

Since  $|S_u|^2$  is a double convolution of WDFs  $W_s$  and  $W_u$ , it follows that the double Fourier transform of the STSE is given by

$$\iint dt df \exp(i2\pi f\tau - i2\pi t\nu) |S_u(t, f)|^2 = \chi_u(\nu, \tau) \chi_s(\nu, \tau), \quad (107)$$

where  $\chi_u$  and  $\chi_s$  are the complex ambiguity functions of  $u$  and  $s$ , respectively; see (23). This leads to an alternative expression for the STSE as

$$|S_u(t, f)|^2 = \iint d\tau d\nu \exp(-i2\pi f\tau + i2\pi t\nu) \chi_u(\nu, \tau) \chi_s(\nu, \tau). \quad (108)$$

Therefore, if the complex ambiguity function of  $s$  is computed, it can be multiplied by the ambiguity function of an arbitrary weighting function  $u$ , and followed by a two-dimensional Fourier transform. There is no need to calculate the WDF  $W_s$  via this route; also several different weighting functions could be utilized, each at the expense of a two-dimensional Fourier transform. The end result for the STSE is always nonnegative. Of course, the same result is obtainable directly by taking the magnitude-square of definition (102).

#### MARGINALS OF SPECTRAL ESTIMATE

There follows, from (106) and (12), the marginal relation

$$\int df |S_u(t, f)|^2 = \int dt' |s(t')|^2 |u(t - t')|^2 = |s(t)|^2 \otimes |u(t)|^2. \quad (109)$$

Thus, the time marginal of  $|S_u|^2$  is not directly  $|s(t)|^2$ , but is smeared by the weighting, according to  $|u(t)|^2$ . In a similar fashion, from (106) and (11), the frequency marginal is

$$\int dt |S_u(t, f)|^2 = |S(f)|^2 \otimes |U(f)|^2 . \quad (110)$$

Again,  $|S(f)|^2$  is smeared by window  $|U(f)|^2$ .

Finally, completing either of the integrations in (109) or (110), over the remaining variable, yields

$$\iint dt df |S_u(t, f)|^2 = E_s E_u , \quad (111)$$

where  $E_s$  and  $E_u$  are the energies of  $s$  and  $u$ , respectively; see (14).

Since weighting  $u$  is arbitrary and under our control, we can easily choose  $E_u$  to be 1, without loss of generality; then the volume under the STSE will be equal to the energy in waveform  $s$  being analyzed, just as for the WDF in (14).

#### MOMENTS OF SPECTRAL ESTIMATE

If we use (110) and (14), we find the following development:

$$\begin{aligned} \iint dt df f |S_u(t, f)|^2 &= \int df f \int dv |S(v)|^2 |U(f - v)|^2 = \\ &= \int dv |S(v)|^2 \int df (f - v + v) |U(f - v)|^2 = \\ &= \int dv |S(v)|^2 \left[ \int df_1 f_1 |U(f_1)|^2 + v E_u \right] = \\ &= E_s \int df_1 f_1 |U(f_1)|^2 + E_u \int dv v |S(v)|^2 . \end{aligned} \quad (112)$$

Combined with (111), there results

$$\frac{\iint dt df f |S_u(t, f)|^2}{\iint dt df |S_u(t, f)|^2} = \frac{\int df f |U(f)|^2}{\int df |U(f)|^2} + \frac{\int df f |S(f)|^2}{\int df |S(f)|^2} \quad (113)$$

That is, the first moment in  $f$  of the STSE is the sum of the frequency centers of  $|U|^2$  and  $|S|^2$ . This should be compared with the corresponding result in (36) for the WDF, where only the last term in (113) is present. The presence of weighting  $u$  in definition (102) adds an additional term to the frequency center unless  $|U(f)|$  is even about  $f = 0$ ; in this latter case, (113) reduces to (36).

In a similar fashion, the first moment in  $t$  of the STSE is found to be

$$\frac{\iint dt df t |S_u(t, f)|^2}{\iint dt df |S_u(t, f)|^2} = \frac{\int dt t |u(t)|^2}{\int dt |u(t)|^2} + \frac{\int dt t |s(t)|^2}{\int dt |s(t)|^2} \quad (114)$$

Again, a sum of time centers results; but if weighting  $|u(t)|$  is even about  $t = 0$ , then (114) reduces to the same result, (37), as for the WDF.

## CONDITIONAL MOMENT

Just as in (28)-(35) for the WDF, conditional moments of the SISE can be defined. For example, directly from (105), we have

$$\int df f |S_u(t, f)|^2 = \int df f |\chi_{s\bar{u}}(f, t)|^2, \quad (115)$$

in terms of the cross-ambiguity function of  $s$  and  $\bar{u}$ , where  $\bar{u}(t) = u(-t)$ .

An alternative time-domain expression is possible for the frequency moment in (115): define

$$g(t, t_1) = s(t_1) u^*(t - t_1). \quad (116)$$

Then from (102) and (29),

$$\begin{aligned} \int df f |S_u(t, f)|^2 &= \int df f \iint dt_1 dt_2 \exp(-i2\pi f(t_1 - t_2)) g(t, t_1) g^*(t, t_2) = \\ &= \iint dt_1 dt_2 g(t, t_1) g^*(t, t_2) \frac{i}{2\pi} \delta'(t_1 - t_2) = \\ &= \frac{-i}{2\pi} \int dt_1 g'(t, t_1) g^*(t, t_1), \end{aligned} \quad (117)$$

where

$$g'(t, t_1) \equiv \frac{\partial}{\partial t_1} g(t, t_1) = \frac{\partial}{\partial t_1} \{s(t_1) u^*(t - t_1)\}. \quad (118)$$

If we represent waveform  $s$  in terms of its magnitude and phase according to (31), and do likewise for weighting  $u$  as

$$u(t) = E(t) \exp[iP(t)] , \quad (119)$$

then substitution in (117) results in the simplified form

$$\int df f |S_u(t, f)|^2 = \frac{1}{2\pi} \int dt_1 [\Theta'(t_1) - P'(t - t_1)] M^2(t_1) E^2(t - t_1) . \quad (120)$$

When this result is combined with (109), the normalized conditional first moment is

$$\frac{\int df f |S_u(t, f)|^2}{\int df |S_u(t, f)|^2} = \frac{1}{2\pi} \frac{\int dt_1 [\Theta'(t_1) - P'(t - t_1)] M^2(t_1) E^2(t - t_1)}{\int dt_1 M^2(t_1) E^2(t - t_1)} . \quad (121)$$

(This reduces to (38) when  $E(t) = 1$ ,  $P(t) = 0$ , that is,  $u(t) = 1$ , in which case  $S_u(t, f) = S(f)$ .) Generally, (121) is an average of  $\Theta'(t_1) - P'(t - t_1)$ , weighted according to the instantaneous powers of  $s$  and  $u$ .

## EXAMPLES OF SHORT-TERM SPECTRAL ESTIMATION

Here we will reconsider many of the examples presented earlier for the WDF investigation. The particular example of weighting  $u$  adopted here in spectral definition (102) will be, for the time being,

$$u(t) = (\pi \sigma^2)^{-1/4} \exp\left(-\frac{t^2}{2\sigma^2}\right), \quad (122)$$

where duration measure  $\sigma$  is under our control. The energy  $E_u$  of this waveform is unity, in keeping with the discussion in (111) et seq., which guarantees that the volume under the SISE will be the energy  $E_s = E$  of the waveform  $s$  being analyzed.

## GAUSSIAN WAVEFORM

The waveform  $s$  was given in (71); its transform  $S_u(t, f)$  is obtained by substituting (71) and (122) in (102) and using (68):

$$S_u(t, f) = \left(E \frac{\sigma_h}{\sigma_a}\right)^{1/2} \exp\left[-\frac{t^2}{4\sigma_a^2} - \pi^2 f^2 \sigma_h^2 - i\pi f t \frac{\sigma_0^2}{\sigma_a^2} + i \arg(a_0)\right], \quad (123)$$

where  $E$  is the energy of  $s$  and

$$\sigma_a^2 = \frac{1}{2}(\sigma^2 + \sigma_0^2), \quad \frac{1}{\sigma_h^2} = \frac{1}{2}\left(\frac{1}{\sigma^2} + \frac{1}{\sigma_0^2}\right), \quad \frac{\sigma_a}{\sigma_h} = \frac{1}{2}\left(\frac{\sigma}{\sigma_0} + \frac{\sigma_0}{\sigma}\right). \quad (124)$$

The quantity  $\sigma_a^2$  is the arithmetic average of  $\sigma^2$  and  $\sigma_0^2$ , while  $\sigma_h^2$  is the harmonic average. The STSE then follows immediately (or by use of (70) directly) as

$$|S_u(t,f)|^2 = E \frac{\sigma_h}{\sigma_a} \exp \left[ -\frac{1}{2} \left( \frac{t^2}{\sigma_a^2} + 4\pi^2 f^2 \sigma_h^2 \right) \right]. \quad (125)$$

The volume under STSE (125) is readily verified to be  $E$ , as it *must* be. The half widths of the ellipse at the  $1/e$  relative level are  $\sqrt{2} \sigma_a$ ,  $\sqrt{2} (2\pi\sigma_h)^{-1}$ , respectively, in the  $t,f$  plane. The area of this ellipse in the  $t,f$  plane is

$$\frac{\sigma_a}{\sigma_h} = \frac{1}{2} \left( \frac{\sigma}{\sigma_0} + \frac{\sigma_0}{\sigma} \right) \geq 1. \quad (126)$$

This area is at least twice as great as that for the corresponding WDF in figure 4, and even then, only when the proper guess is used for the weighting  $u$ , namely  $\sigma = \sigma_0$ . Since waveform duration  $\sigma_0$  will likely be unknown in practice, the mismatch factor in (126) will smear the concentration of the STSE somewhat. For example, if  $\sigma$  is off by a factor of 2 from  $\sigma_0$  (either double or half), (126) is 1.25 instead of its minimum value of 1.

The area enlargement factor  $\sigma_a/\sigma_h$  in (126) is also the same factor by which the peak of the STSE in (125) is down from its best value of  $E$ . Thus, the STSE has a decreased peak and enlarged effective area relative to the WDF, the relative factor being at least 2, and being  $\sigma/\sigma_0 + \sigma_0/\sigma$  in general. Both distributions contain volume  $E$ , independent of  $\sigma$ .



This example demonstrates the presence of "window effects" in the STSE that are not seen in the WDF. That is, whereas the effective ellipse in figure 4 depended only on waveform parameter  $\sigma_0$ , the ellipse here depends additionally on weighting parameter  $\sigma$ , in such a fashion as to always smear the concentration of energy in the  $t, f$  plane by at least a factor of 2. In trade, we always have the guarantee that the STSE (103) will be nonnegative, and that it will not contain the large interference phenomena inherent in the WDF; see (80)-(81).

#### MULTIPLE MODULATED TONES

The waveform of interest is given in (79). The transform  $S_u(t, f)$  is found by use of (122), (102), and (68):

$$S_u(t, f) = \sum_k \left( E_k \frac{\sigma_{hk}}{\sigma_{ak}} \right)^{1/2} \exp \left[ - \frac{(t - t_k)^2}{4 \sigma_{ak}^2} - \pi^2 (f - f_k)^2 \sigma_{hk}^2 - i\pi (f - f_k) \frac{\sigma_k^2 t + \sigma^2 t_k}{\sigma_{ak}^2} + i \arg(a_k) \right], \quad (127)$$

where energy  $E_k = \sqrt{\pi} |a_k|^2 \sigma_k$ , and averages

$$\sigma_{ak}^2 = \frac{1}{2} (\sigma^2 + \sigma_k^2), \quad \frac{1}{\sigma_{hk}^2} = \frac{1}{2} \left( \frac{1}{\sigma^2} + \frac{1}{\sigma_k^2} \right). \quad (128)$$

The STSE is the magnitude squared value of (127); the resulting double sum has diagonal terms

$$\sum_k E_k \frac{\sigma_{hk}}{\sigma_{ak}} \exp \left[ -\frac{1}{2} \left\{ \frac{(t - t_k)^2}{\sigma_{ak}^2} + 4\pi^2 (f - f_k)^2 \sigma_{hk}^2 \right\} \right], \quad (129)$$

which are identical to (125), except for the indexing by  $k$  and the shift to center  $t_k, f_k$  in the  $t, f$  plane, as expected. If one value of weighting parameter  $\sigma$  is used to evaluate the STSE for all  $t$  of interest, it cannot simultaneously match all the different possible values of  $\{\sigma_k\}$  for the various pulses. This will cause some of the components in (129) to be more severely degraded than others, in terms of decreased peaks and spread effective areas; the pertinent factor is again

$$\frac{\sigma_{ak}}{\sigma_{hk}} = \frac{1}{2} \left( \frac{\sigma}{\sigma_k} + \frac{\sigma_k}{\sigma} \right) \quad (130)$$

for the  $k$ -th component lobe. If some a priori knowledge of the values of  $\{\sigma_k\}$  is available, this suggests using different values of  $\sigma$  for those values of  $t$  near the corresponding values of  $\{t_k\}$ , in an effort to minimize the factors (130) for different  $k$ .

As for the off-diagonal terms of  $|S_U(t, f)|^2$  in (127), the  $k, l$  term is proportional to

$$\exp \left[ -\frac{(t - t_k)^2}{4 \sigma_{ak}^2} - \frac{(t - t_l)^2}{4 \sigma_{al}^2} - \pi^2 (f - f_k)^2 \sigma_{hk}^2 - \pi^2 (f - f_l)^2 \sigma_{hl}^2 \right]. \quad (131)$$

If  $t$  is not near one of the time centers  $\{t_k\}$ , or if  $f$  is not near one of the  $\{f_k\}$ , this term will be very small, due to the exponential decay. In particular, halfway between the dominant desired peaks of (129) at  $\{t_k, f_k\}$ , the quantity (131) will be essentially zero. This is in distinction to the WDF result in (80) et seq.

#### LINEAR FREQUENCY MODULATION

This waveform is specified in (84). Its STSE is, upon use of (70),

$$|S_u(t, f)|^2 = \frac{2E}{\sqrt{H_2}} \exp \left[ -\frac{1}{H_2} \left\{ x^2(1+r+r\theta_0^2) + y^2(1+r)/r - 2xy\theta_0 \right\} \right], \quad (132)$$

where

$$\theta_0 = \alpha_0 \sigma_0^2, \quad r = \frac{\sigma^2}{\sigma_0^2}, \quad H_2 = \frac{1}{r} + 2 + r + r\theta_0^2, \quad (133)$$

and where we define, here,

$$x = \frac{t}{\sigma}, \quad y = 2\pi f \sigma. \quad (134)$$

By means of the results in appendix D, the area of the contour ellipse in (132), at the  $1/e$  relative level, is found to be

$$\text{area} = \frac{1}{2} \sqrt{H_2} \quad \text{in the } t, f \text{ plane.} \quad (135)$$

Thus, the product of the peak height of the STSE in (132) and the effective area is again  $E$ , the volume under the STSE, regardless of the values of  $\sigma$ ,  $\sigma_0$ ,  $\theta_0$ . (For  $\theta_0 = 0$ , (135) reduces to (126), as it must.)

To minimize the effective area and to maximize the peak value of the STSE, the common quantity  $H_2$  in (133) should be minimized. This is accomplished by choosing the weighting parameter  $\sigma$  in (122) as

$$\sigma_{\text{opt}} = \frac{\sigma_0}{(1 + \theta_0^2)^{1/4}}, \quad r_{\text{opt}} = \frac{1}{(1 + \theta_0^2)^{1/2}}, \quad (136)$$

which would require knowledge of both the duration  $\sigma_0$  and the amount of frequency modulation  $\theta_0$  in waveform  $s$ . Even if that information were available, the minimum area in (135) becomes

$$\text{minimum area} = \left( \frac{1 + \sqrt{1 + \theta_0^2}}{2} \right)^{1/2} \quad \text{in the } t, f \text{ plane,} \quad (137)$$

which still increases as  $\sqrt{\theta_0/2}$  for large  $\theta_0$ . Thus, even the best choice of  $\sigma$  for the weighting results in considerable spreading of the concentration ellipse and in peak reduction of the STSE; searching in  $\sigma$  is not overly helpful because the simple weighting pulse (122) is a poor facsimile to the linear frequency modulation waveform (84), especially for large amounts of frequency modulation, as measured by parameter  $\theta_0$ .

## MORE GENERAL WEIGHTING

There is no need to restrict the weighting  $u$  in SISE (102) and (103) to be the simple Gaussian pulse in (122). In this section, we generalize it to allow for some linear frequency modulation:

$$u(t) = (\pi \sigma^2)^{-1/4} \exp \left[ -\frac{t^2}{2\sigma^2} + i \frac{\alpha}{2} t^2 \right]; \quad E_u = 1. \quad (138)$$

The waveform of interest here is again the linear frequency modulation example

$$s(t) = a_0 \exp \left[ -\frac{t^2}{2\sigma_0^2} + i \frac{\alpha_0}{2} t^2 \right], \quad \alpha_0 \geq 0, \quad (139)$$

as in (84).

The SISE follows from (102), (103), and (70), after a considerable amount of manipulations, as

$$\begin{aligned} |S_u(t, f)|^2 = & \frac{2E}{\sqrt{H_3}} \exp \left[ -\frac{1}{H_3} \left\{ x^2(1+r+r\theta_0^2+r^2q^2\theta_0^2) + \right. \right. \\ & \left. \left. + y^2(1+r)/r - 2xy(1+rq)\theta_0 \right\} \right], \end{aligned} \quad (140)$$

where

$$r = \frac{\sigma^2}{\sigma_0^2}, \quad q = \frac{\alpha}{\alpha_0}, \quad H_3 = \frac{1}{r} + 2 + r + r(q-1)^2 \theta_0^2, \quad (141)$$

in addition to (134). The quantities  $r$  and  $q$  are mismatch factors, reflecting the lack of knowledge of weighting (138) about the waveform (139).

The area of the contour ellipse of (140) at the  $1/e$  relative level is (by means of appendix D)

$$\text{area} = \frac{1}{2} \sqrt{H_3} \quad \text{in the } t, f \text{ plane.} \quad (142)$$

This is also the same factor by which the peak of (140) is down from  $E$ . Thus, a minimum value for  $H_3$  is desired. This can be achieved by choosing  $r = 1$ ,  $q = 1$  in (141), for which the minimum  $H_3 = 4$  and the minimum area = 1; however, this requires that we choose  $\sigma = \sigma_0$  and  $\alpha = \alpha_0$ , which is not a likely situation in practice, without some apriori knowledge about the waveform  $s$ . If this fortuitous situation of perfect match of the parameters does occur, the STSE in (140) reduces to

$$|S_u(t, f)|^2 = E \exp \left[ -\frac{1}{2} \left\{ x^2 (1 + \theta_0^2) - 2xy \theta_0 + y^2 \right\} \right], \quad (143)$$

which is identical to the corresponding WDF in (91), except for a factor of 2 outside and inside the exponential. Thus, the effective area is doubled and the peak is halved.

As special cases of weighting (138), if  $\alpha = 0$  (no frequency modulation in the weighting), then  $H_3$  in (141) reduces to  $H_2$  in (133). Alternatively, if  $\alpha_0 \rightarrow 0$  (no frequency modulation in the waveform  $s$ ), then  $\theta_0(q - 1) = \alpha_0 \sigma_0^2 (\alpha/\alpha_0 - 1) \sim \alpha \sigma_0^2$  and

$$H_3 \sim \frac{1}{r} + 2 + r + r \alpha^2 \sigma_0^4 = \left( \frac{\sigma}{\sigma_0} + \frac{\sigma_0}{\sigma} \right)^2 + (\alpha \sigma \sigma_0)^2 . \quad (144)$$

This is minimized by choosing  $\alpha = 0$  and  $\sigma = \sigma_0$ , giving value 4 as usual. Finally, for given  $q$ ,  $H_3$  in (141) is minimized by choosing  $r = (1 + (q - 1)^2 \theta_0^2)^{-1/2}$ , for which the minimum  $H_3 = 2 + 2(1 + (q - 1)^2 \theta_0^2)^{1/2}$ ; however, again, this increases as  $2|q - 1|\theta_0$  as  $\theta_0$  increases.

## SMOOTHING THE WDF

It was demonstrated in (106) that the double convolution of any two WDFs is always nonnegative, and is in fact equal to the STSE of one waveform relative to the other:

$$W_s(t,f) \otimes_{t,f} W_u(t,f) = |S_u(t,f)|^2 . \quad (145)$$

This suggests that one should choose a (legal) WDF for weighting  $u$  which is as narrow as possible (least area or spread) in the  $t,f$  plane, in order to minimize the inherent spreading that (145) implies. The simple examples in the previous section demonstrated that, for the best choices of duration and linear frequency modulation parameters in the Gaussian weighting, an increase of .5 in the effective area in the  $t,f$  plane of the STSE, relative to the WDF, resulted.

## PHILOSOPHY AND APPROACH

Since fine detail of the WDF  $W_s(t,f)$  will likely vary in different portions of the  $t,f$  plane, this suggests the following possible procedure for analysis: For a given waveform  $s(t)$ , compute and plot the WDF  $W_s(t,f)$  according to (3) or (61). Locate a  $t,f$  region of interest in the plane, where large (perhaps oscillatory) values of  $W_s$  occur; denote the center of the region as  $t_c, f_c$ . Estimate the duration,  $\sigma_c$ , and linear frequency



modulation index,  $\alpha_c$ , of this particular region in the  $t, f$  plane. Perform the STSE of waveform  $s(t)$  according to (102)-(103), with weighting

$$u(t) = (\pi \sigma_c^2)^{-1/4} \exp\left[-\frac{t^2}{2\sigma_c^2} + i \frac{\alpha_c}{2} t^2\right], \quad \theta_c = \alpha_c \sigma_c^2, \quad (146)$$

(for reasons to be given below), but only for locations  $t, f$  in the plane near  $t = t_c, f = f_c$ .

The WDF of weighting (146) is (with  $\alpha_c = 2\pi\beta_c$ )

$$\begin{aligned} W_u(t, f) &= 2 \exp\left[-\frac{t^2}{\sigma_c^2} - 4\pi^2 \sigma_c^2 (f - \beta_c t)^2\right] = \\ &= 2 \exp\left[-\frac{t^2}{\sigma_c^2} (1 + \theta_c^2) + 4\pi f t \theta_c - 4\pi^2 f^2 \sigma_c^2\right], \end{aligned} \quad (147)$$

which has a contour ellipse, at the  $1/e$  relative level, of area  $1/2$  in the  $t, f$  plane, regardless of  $\sigma_c$  and  $\alpha_c$ . This STSE procedure is equivalent to smoothing the WDF  $W_s$  of waveform  $s$  with the WDF in (147), for values near  $t_c, f_c$  in the  $t, f$  plane. Thus we have two alternative procedures for conducting the smoothing of a calculated WDF  $W_s$ , the first via direct evaluation of double convolution (145) for values of  $t, f$  near regions of interest, and the second via the STSE in (102) and (103). Which one to adopt will likely depend on the number of points that must be closely investigated in the  $t, f$  plane.

For other regions of interest in the  $t, f$  plane of the original WDF  $W_s$ , different values of  $t_c$ ,  $f_c$ ,  $\sigma_c$ ,  $\alpha_c$  must be extracted and the smoothing procedure repeated. Although tedious, this procedure will minimally spread the WDF  $W_s$  (by area .5) and it will guarantee a nonnegative distribution. This procedure is similar to that given in [2]; however, the information required to implement [2] is not easily available, and the current approach is not limited to constant-magnitude waveforms. A fine-grained analysis of a given general waveform  $s$ , for various  $t, f$  values and yielding nonnegative distribution values, is not going to be achieved without the expenditure of considerable effort and interaction between a user and preliminary analysis results.

This two-stage procedure, of observing the raw WDF and then computing different smoother versions in different regions, avoids the arbitrary pre-selection of time duration and frequency modulation content of the weighting in the STSE, which would overly smear the modified WDF for improper matches of parameter values. It also guarantees nonnegative estimates. In trade, there is approximately an increase of .5 in the effective area of the distribution in the  $t, f$  plane that must be accepted, in addition to a decreased peak value. For WDFs,  $W_s$ , with lobes which already occupy portions of the  $t, f$  plane with areas significantly greater than .5, this additional spreading (by area .5) is not very damaging, provided that  $\sigma_c$  and  $\alpha_c$  are chosen correctly. Perhaps simultaneous plots of WDF  $W_s(t, f)$  and STSE  $|S_u(t, f)|^2$  would yield maximum information about waveform  $s$ .

In actual practice, where the integral definition in (102) is replaced by a numerical summation of samples taken at increment  $\Delta$ , the quantity (145) is necessarily approximated. This problem is addressed in appendix E, where it is shown that the dominant term in the numerical approach is approximately the desired quantity (145). Furthermore, since the definition in (E-1) involves a magnitude-square, the approximation is guaranteed to be nonnegative. This need not be the case if the double convolution of WDFs  $W_s$  and  $W_u$  in (145) is approximated by sampling directly in the  $t, f$  plane and performing a double summation. However, for small enough increments in both  $t$  and  $f$ , this nonnegative aspect should be small and probably negligible; this latter approach was used in [1], although the smoothing function was not a legal WDF.

#### ALTERNATIVE AVERAGING PROCEDURES

Instead of using  $R(t, \tau) = s(t + \frac{\tau}{2}) s^*(t - \frac{\tau}{2})$  in (2) as the instantaneous correlation at time  $t$  and separation  $\tau$ , one could use a local average, in hopes of improving the correlation and distribution functions. That is, consider correlation definition

$$\hat{R}(t, \tau) = v_1(t) \otimes R(t, \tau) = \int dt' v_1(t - t') s(t' + \frac{\tau}{2}) s^*(t' - \frac{\tau}{2}), \quad (148)$$

where  $v_1$  is a fairly sharp, even, real function centered at the origin.

The corresponding "locally averaged" WDF is

$$\begin{aligned}\hat{W}(t, f) &= \int d\tau \exp(-i2\pi f\tau) \hat{R}(t, \tau) = \\ &= \int dt' v_1(t - t') W(t', f) = v_1(t) \otimes W(t, f) .\end{aligned}\quad (149)$$

This is a convolution, in time only, of the WDF of  $s$  with weighting  $v_1$ . Reference to the discussion following (83) reveals that this form of averaging is inadequate, since it does not average additionally on frequency. Also, (149) need not remain positive, as would be desired of a smoothed WDF.

Furthermore, the Fourier transform in (149) (as well as (3)) is over all  $\tau$ , thereby involving argument values of waveform  $s$  in (148) which are very distant from the time point,  $t$ , of interest. If  $\hat{W}(t, f)$  or  $W(t, f)$  is to be considered as the "spectrum at time  $t$ ," it is hard to justify why arbitrarily distant time points from location  $t$  should enter into their evaluations. Therefore, in addition to the local average in (148) for stability purposes, there should be a weighting in  $\tau$  in (149) to better confine the Fourier transform to local values of waveform  $s$  about time instant  $t$  of interest.

To this aim, consider the more general form of average given by

$$\begin{aligned}\hat{R}(t, \tau) &= v_2(t, \tau) \otimes R(t, \tau) = \int dt' v_2(t - t', \tau) R(t', \tau) = \\ &= \int dt' v_2(t - t', \tau) \int df' \exp(i2\pi f'\tau) W(t', f') .\end{aligned}\quad (150)$$

where weighting  $v_2$  depends additionally on  $\tau$ . Define its transform

$$V_2(t, f) = \int d\tau \exp(-i2\pi f\tau) v_2(t, \tau) . \quad (151)$$

Then the modified WDF corresponding to  $\hat{R}$  in (150) is

$$\begin{aligned} \hat{W}(t, f) &= \iint dt' df' W(t', f') V_2(t - t', f - f') = \\ &= W(t, f) \overset{tf}{\otimes} V_2(t, f) , \end{aligned} \quad (152)$$

which is a double convolution of  $W$  with  $V_2$ , on both  $t$  and  $f$ . However, since  $V_2$  need not be a WDF,  $\hat{W}$  in (152) can become negative for some  $t, f$  values. This form of smoothing was considered previously in [9; (1.5)] and [10; (2.1)].

An additional justification of two-dimensional smoothing, from the frequency domain alternative viewpoint, is given in appendix F. Also, a generalization of the Gaussian WDF (147), with arbitrary area and linear frequency modulation content and which guarantees a positive distribution  $\hat{W}$ , is given in (F-7)-(F-19); this result generalizes that in [11] for no frequency modulation.

If we specialize weighting  $v_2$  in (150) to the form

$$v_2(t, \tau) = u(t + \frac{\tau}{2}) u^*(t - \frac{\tau}{2}) , \quad (153)$$

then (151) yields

$$V_2(t, f) = W_U(t, f) , \quad (154)$$

and the general result in (152) specializes to (106), which is guaranteed positive. Thus the special case of weighting  $v_2$  in (153) leads to the STSE of  $s$ , relative to  $u$ .

#### EFFICIENT CALCULATION OF SHORT-TERM SPECTRAL ESTIMATE

If we employ the weighting  $u$  in (146) with linear frequency modulation parameter  $\alpha_c$ , the spectrum in (102) becomes

$$\begin{aligned}
 S_u(t, f) &= \int dt_1 \exp(-i2\pi ft_1) s(t_1) u^*(t - t_1) = \\
 &= \exp(-i2\pi ft) \int dt_2 \exp(-i2\pi ft_2) s(t + t_2) u^*(-t_2) = \\
 &= (\pi \sigma_c^2)^{-1/4} \exp(-i2\pi ft) \int dt_2 \exp(-i2\pi ft_2) s(t + t_2) \exp\left(-\frac{t_2^2}{2\sigma_c^2} - i\frac{\alpha_c}{2} t_2^2\right).
 \end{aligned}
 \tag{155}$$

The  $\exp(-t_2^2/(2\sigma_c^2))$  term gates out the portion of  $s(t + t_2)$  near the origin in  $t_2$ , while the  $\exp(-i\alpha_c t_2^2/2)$  term cancels linear frequency modulation in waveform  $s$ .

An approximation to (155) is obtained by sampling at increment  $\Delta$  and using the Trapezoidal rule:

$$\begin{aligned} \tilde{S}_u(t, f) \equiv & (\pi \sigma_c^2)^{-1/4} \exp(-i2\pi ft) \Delta \sum_k \exp(-i2\pi f \Delta k) * \\ & * s(t + k\Delta) \exp\left[-\frac{1}{2} k^2 \Delta^2 \left(\frac{1}{\sigma_c^2} + i \alpha_c\right)\right], \end{aligned} \quad (156)$$

which has period  $1/\Delta$  in  $f$ . In particular, the approximation to the STSE, at selected points, is

$$\begin{aligned} \left| \tilde{S}_u\left(m\Delta, \frac{n}{N\Delta}\right) \right|^2 &= \frac{\Delta^2}{\sqrt{\pi} \sigma_c} \left| \sum_k \exp(-i2\pi nk/N) * \right. \\ & * s(m\Delta + k\Delta) \exp\left[-\frac{1}{2} k^2 \Delta^2 \left(\frac{1}{\sigma_c^2} + i \alpha_c\right)\right] \left. \right|^2, \end{aligned} \quad (157)$$

which is an  $N$ -point discrete Fourier transform;  $m, n, N$  are integers.

The procedure for analysis is as follows: for a region of interest centered at  $t_c, f_c$  in the  $t, f$  plane, choose time values  $m\Delta$  near  $t_c$ . Then for each  $m$ , sweep out  $n$  such that frequency  $n/(N\Delta)$  is near  $f_c$ ; an FFT will give all  $f$  values in  $(0, 1/\Delta)$ . Plots of (157) give a fine-tuned STSE near  $t_c, f_c$  for the particular choices of  $\sigma_c, \alpha_c$ . Additional estimates with different parameters will be required in other regions; there is no globally optimum smoothing that will yield high-quality positive spectral estimates for all  $t, f$  values.

The numerical evaluation of the exponential quantities

$$Q_2(k) \equiv \exp \left[ -\frac{1}{2} k^2 \Delta^2 \left( \frac{1}{\sigma_c^2} + i \alpha_c \right) \right] = Q_2(-k) \quad (158)$$

in (157) can be effected very efficiently by the methods given in [12].

They are given by recurrences (which need to be evaluated only once for each  $\sigma_c, \alpha_c$ )

$$\left. \begin{aligned} Q_1(k) &= Q_1(k-1) \exp(2c_2) \\ Q_2(k) &= Q_2(k-1) Q_1(k) \end{aligned} \right\} \text{for } k \geq 1, \quad (159)$$

with starting values

$$Q_1(0) = \exp(-c_2), \quad Q_2(0) = 1,$$

$$c_2 = -\frac{1}{2} \Delta^2 \left( \frac{1}{\sigma_c^2} + i \alpha_c \right). \quad (160)$$

Only two complex multiplications per stage are required in (159).

Furthermore, since

$$\exp(-c_2) = \exp \left( \frac{\Delta^2}{2\sigma_c^2} \right) \exp \left( \frac{i\alpha_c \Delta^2}{2} \right) \equiv E (C + iS), \quad (161)$$

and

$$\exp(2c_2) = \frac{C^2 - S^2 - 12SC}{E^2}, \quad (162)$$

only one exp, cos, and sin must be evaluated to accomplish (159) for all k.



## WDF WITH MINIMUM SPREAD

The virtues of smoothing WDF  $W_s$  of waveform  $s$  with the WDF  $W_u$ , (147), of weighting  $u$ , (146), were discussed earlier in this section. At that time, the selection of form (146) for the weighting was seemingly arbitrary. However, it is shown in appendix G that the weighting,  $u$ , which has a minimally spread WDF, is precisely that given in (146). The measure of spread is

$$I = \iint dt df W_u(t,f) (f - \beta_c t)^2, \quad (163)$$

where  $\beta_c$  is a specified (observed) slope of interest in the  $t, f$  plane, and  $\alpha_c = 2\pi\beta_c$ . This measure of spread concentrates the WDF about the specified slope; see (147). The actual minimum value of spread (163) is given in (G-24) as

$$\text{minimum } I = \frac{1}{8\pi^2 \sigma_c^2}, \quad (164A)$$

when weighting  $u$  is constrained to have mean square duration

$$\int dt t^2 |u(t)|^2 = \frac{\sigma_c^2}{2}, \quad (164B)$$

in addition to unit energy. Without these two constraints, the minimization of spread (163) is ill-posed; see appendix G.

## PERFORMANCE IN NOISE

In this section, we investigate the bias and stability of a WDF estimate obtained from a noisy waveform. In particular, the given waveform  $x$  is

$$x(t) = s(t) + n(t) , \quad (165)$$

where  $s$  is a deterministic signal of interest, and  $n$  is an additive zero-mean stationary noise. In fact, we have

$$\overline{n(t)} = 0 , \quad \overline{n(t_1)n^*(t_2)} = C_n(t_1 - t_2) ,$$

$$G_n(f) = \int d\tau \exp(-i2\pi f\tau) C_n(\tau) , \quad (166)$$

where  $C_n$  and  $G_n$  are the noise covariance and power density spectrum, respectively.

## WAVEFORM WEIGHTING

If the WDF of given waveform  $x$  in (165) were directly evaluated via definition (3), the result would be infinite, since the  $N \times N$  (noise-cross-noise) terms do not decay for large arguments. Also, since the signal  $s$  will be assumed to be transient and decay to zero for large arguments, some gating or weighting of given waveform  $x$  is appropriate, in order to

concentrate on the time regions where signal  $s$  is largest. Accordingly, we consider the weighted waveform

$$y(t) = v(t) \quad x(t) = v(t) [s(t) + n(t)] , \quad (167)$$

where  $v(t)$  is a deterministic function under our control.

The WDF that will be calculated is therefore

$$\begin{aligned} W_{yy}(t, f) &= \int d\tau \exp(-i2\pi f\tau) y(t + \frac{\tau}{2}) y^*(t - \frac{\tau}{2}) = \\ &= a + b + c + d , \end{aligned} \quad (168)$$

where

$$\begin{aligned} a &= \int d\tau \exp(-i2\pi f\tau) R_{VV}(t, \tau) s(t + \frac{\tau}{2}) s^*(t - \frac{\tau}{2}) , \\ b &= \int d\tau \exp(-i2\pi f\tau) R_{VV}(t, \tau) n(t + \frac{\tau}{2}) n^*(t - \frac{\tau}{2}) , \\ c &= \int d\tau \exp(-i2\pi f\tau) R_{VV}(t, \tau) s(t + \frac{\tau}{2}) n^*(t - \frac{\tau}{2}) , \\ d &= \int d\tau \exp(-i2\pi f\tau) R_{VV}(t, \tau) n(t + \frac{\tau}{2}) s^*(t - \frac{\tau}{2}) , \end{aligned} \quad (169)$$

and

$$R_{VV}(t, \tau) = v(t + \frac{\tau}{2}) v^*(t - \frac{\tau}{2}) . \quad (170)$$

The first two quantities in (168) are, respectively,  $SxS$  and  $NxN$  terms, while the last two are  $SxN$  terms; here,  $S$  denotes signal, while  $N$  denotes noise. The  $SxS$  term,  $a$ , in (169) is real and non-random, while  $NxN$  term,  $b$ , is real and random. On the other hand, the  $SxN$  terms,  $c$  and  $d$ , are complex random, with  $d^* = c$ .

## MEAN VALUES

An alternative expression for the SxS term in (169) is

$$\begin{aligned} a &= \int d\tau \exp(-i2\pi f\tau) R_{VV}(t, \tau) R_{SS}(t, \tau) = \\ &= W_{VV}(t, f) \overset{f}{\otimes} W_{SS}(t, f) , \end{aligned} \quad (171)$$

in terms of the WDFs of weighting  $v$  and signal  $s$ .

The mean of the NxN term is

$$\begin{aligned} \bar{b} &= \int d\tau \exp(-i2\pi f\tau) R_{VV}(t, \tau) C_n(\tau) = \\ &= W_{VV}(t, f) \overset{f}{\otimes} G_n(f) , \end{aligned} \quad (172)$$

where we made use of (166). And since noise  $n$  has zero mean, there follows, for the SxN terms,  $\bar{c} = \bar{d} = 0$ . Collecting these results together, the mean of WDF estimate (168) is

$$\overline{W_{yy}(t, f)} = W_{VV}(t, f) \overset{f}{\otimes} [W_{SS}(t, f) + G_n(f)] . \quad (173)$$

No additional statistical properties on the noise  $n$ , such as a Gaussian process, are needed for result (173); this holds for an arbitrary stationary noise process. The difference in mean outputs, for signal present versus signal absent, is just  $a$ , as given by (171).

## VARIANCE OF WDF ESTIMATE

In order to determine the variance of estimate (168), we need to assume that noise  $n$  is Gaussian. Furthermore, in addition to properties (166), we will presume that

$$\overline{n(t_1) n(t_2)} = 0, \quad (174)$$

as is true when  $n$  is an analytic process or a complex envelope [13, ch.2]. Then (168) yields

$$\begin{aligned} \overline{w_{yy}^2(t, f)} = \overline{|w_{yy}(t, f)|^2} &= \overline{a^2 + b^2 + |c|^2 + |d|^2} + \\ &+ 2 \overline{ab} + \overline{cd^*} + \overline{c^*d}, \end{aligned} \quad (175)$$

the other terms being zero due to  $n$  being zero-mean Gaussian noise.

The second term on the right-hand side of (175) can be developed from (169) as

$$\begin{aligned} \overline{b^2} = \overline{|b|^2} &= \iint d\tau_1 d\tau_2 \exp(-i2\pi f(\tau_1 - \tau_2)) R_{VV}(t, \tau_1)^* \\ &{}^* R_{VV}^*(t, \tau_2) \left[ c_n(\tau_1) c_n^*(\tau_2) + c_n^2\left(\frac{\tau_1 - \tau_2}{2}\right) \right], \end{aligned} \quad (176)$$

where we used (166) and (174). Referring to (172), we have

$$\overline{b^2} = \overline{b}^2 + \iint d\tau_1 d\tau_2 \exp(i2\pi f(\tau_1 - \tau_2)) R_{VV}(t, \tau_1)^* \\ *R_{VV}^*(t, \tau_2) C_n^2\left(\frac{\tau_1 - \tau_2}{2}\right). \quad (177)$$

At this point, it is convenient to define

$$G_n^{(2)}(f) = \int d\tau \exp(-i4\pi f\tau) C_n^2(\tau). \quad (178)$$

Then

$$G_n^{(2)}(f/2) = \int d\tau \exp(-i2\pi f\tau) C_n^2(\tau) = G_n(f) \otimes G_n(f) \quad (179)$$

and

$$C_n^2(\tau) = \int df \exp(i2\pi f\tau) G_n^{(2)}(f/2) = \\ = 2 \int dv \exp(i4\pi v\tau) G_n^{(2)}(v). \quad (180)$$

When this result is substituted in (177), there follows

$$\overline{b^2} = \overline{b}^2 + 2 \int dv W_{VV}^2(t, f - v) G_n^{(2)}(v) = \\ = \overline{b}^2 + 2 W_{VV}^2(t, f) \otimes G_n^{(2)}(f). \quad (181)$$

The third and fourth terms in (175) are

$$\begin{aligned} \overline{|d|^2} = \overline{|c|^2} &= \iint d\tau_1 d\tau_2 \exp(-i2\pi f(\tau_1 - \tau_2)) R_{VV}(t, \tau_1)^* \\ &\quad * R_{VV}^*(t, \tau_2) s\left(t + \frac{\tau_1}{2}\right) s^*\left(t + \frac{\tau_2}{2}\right) C_n\left(\frac{\tau_1 - \tau_2}{2}\right) = \\ &= \int dv G_n(v) \left| B\left(t, f - \frac{v}{2}\right) \right|^2, \end{aligned} \quad (182)$$

where

$$\begin{aligned} B(t, f) &\equiv \int d\tau \exp(-i2\pi f\tau) R_{VV}(t, \tau) s\left(t + \frac{\tau}{2}\right) = \\ &= \int dv \exp(i2\pi vt) W_{VV}\left(t, f - \frac{v}{2}\right) S(v). \end{aligned} \quad (183)$$

(As special cases, if weighting  $v(t) = 1$  for all  $t$ , then  $R_{VV}(t, \tau) = 1$

and

$$\overline{|c|^2} = 4 \int dv G_n(v) |S(2f - v)|^2; \quad (184)$$

while, instead, if  $G_n(f) = \hat{N}_d$  for all  $f$ , then  $C_n(\tau) = \hat{N}_d \delta(\tau)$  and

$$\overline{|c|^2} = 2 \hat{N}_d \int d\tau R_{VV}^2(t, \tau) \left| s\left(t + \frac{\tau}{2}\right) \right|^2. \quad (185)$$

If both conditions above hold, then

$$\overline{|c|^2} = 4 \hat{N}_d E. \quad (186)$$

Returning to the general case again, the fifth term in (175) is given by combining (171) and (172), while the sixth term is

$$\begin{aligned} \overline{cd^*} &= \iint d\tau_1 d\tau_2 \exp(-i2\pi f(\tau_1 - \tau_2)) R_{VV}(t, \tau_1) * \\ &* R_{VV}^*(t, \tau_2) s\left(t + \frac{\tau_1}{2}\right) s^*\left(t - \frac{\tau_2}{2}\right) \overline{n^*\left(t - \frac{\tau_1}{2}\right) n\left(t + \frac{\tau_2}{2}\right)} = 0, \end{aligned} \quad (187)$$

by use of (174).

Combining the above results, we have, for the variance of the WDF estimate,

$$\begin{aligned} \text{Var}\{W_{yy}(t, f)\} &= a^2 + \overline{b^2} + 2\overline{|c|^2} + 2a\overline{b} - (a + \overline{b})^2 = \\ &= \overline{b^2} - \overline{b}^2 + 2\overline{|c|^2} = \\ &= 2 W_{VV}^2(t, f) \otimes G_n^{(2)}(f) + \quad (N \times N) \\ &+ 2 \int dv G_n(v) \left| B\left(t, f - \frac{v}{2}\right) \right|^2. \quad (S \times N) \end{aligned} \quad (188)$$

This result holds for arbitrary signal  $s$ , weighting  $v$ , and noise spectrum  $G_n$ . The quantities  $G_n^{(2)}$  and  $B$  are defined in (178) and (183), respectively.



If we do not weight waveform  $x(t)$ , that is, choose  $v(t) = 1$  for all  $t$  in (167), then  $R_{VV}(t, \tau) = 1$ ,  $W_{VV}(t, f) = \delta(f)$ , and the  $N \times N$  term in (188) becomes infinite; that is, the WDF estimate (168) has infinite variance if we do not weight in time, regardless of what the actual noise spectrum,  $G_n$ , is.

On the other hand, if the noise  $n$  is white, then  $G_n(f) = \hat{N}_d$  for all  $f$ ,  $C_n(\tau) = \hat{N}_d \delta(\tau)$ , and  $G_n^{(2)}$  in (178) is infinite, which makes the  $N \times N$  term in (188) infinite. Thus, if we do not filter out the noise which is out of the band of the signal, the WDF estimate has infinite variance, regardless of what time weighting  $v$  is employed.

#### WDF PROCESSOR

In view of the above observations, we now consider the general WDF processor depicted in figure 7. The only new element here is the

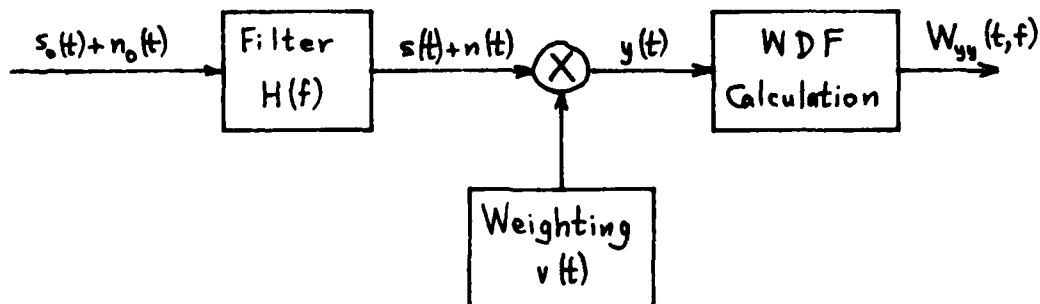


Figure 7. WDF Processor

time-invariant linear filter with transfer function  $H$ . The input noise  $n_o$  is presumed to be white over the band of the input signal  $s_o$ ; mathematically, this is handled by letting

$$G_{n_0}(f) = N_d \quad \text{for all } f, \quad (189)$$

where  $N_d$  is the double-sided noise spectral density level in watts/Hz. The linear filter  $H(f)$  approximately matches the bandwidth of the input signal and passes  $S_0(f)$  essentially unaltered, while filtering out undesired noise spectral components. The actual filter output signal  $s$  is given by

$$s(t) = h(t) \otimes s_0(t) = \int df \exp(i2\pi ft) H(f) S_0(f). \quad (190)$$

The weighting  $v(t)$  approximately matches the duration of the signal and passes  $s(t)$  essentially unaltered, while gating out undesired noise temporal components. Representative plots of the various quantities in figure 7 are given in figure 8.

A numerical example of the WDF processor in figure 7 is carried out in complete detail in appendix H, including the mean and variance results given earlier in this section. In particular, the input signal  $s_0$  is a linear frequency modulation waveform with Gaussian amplitude modulation.

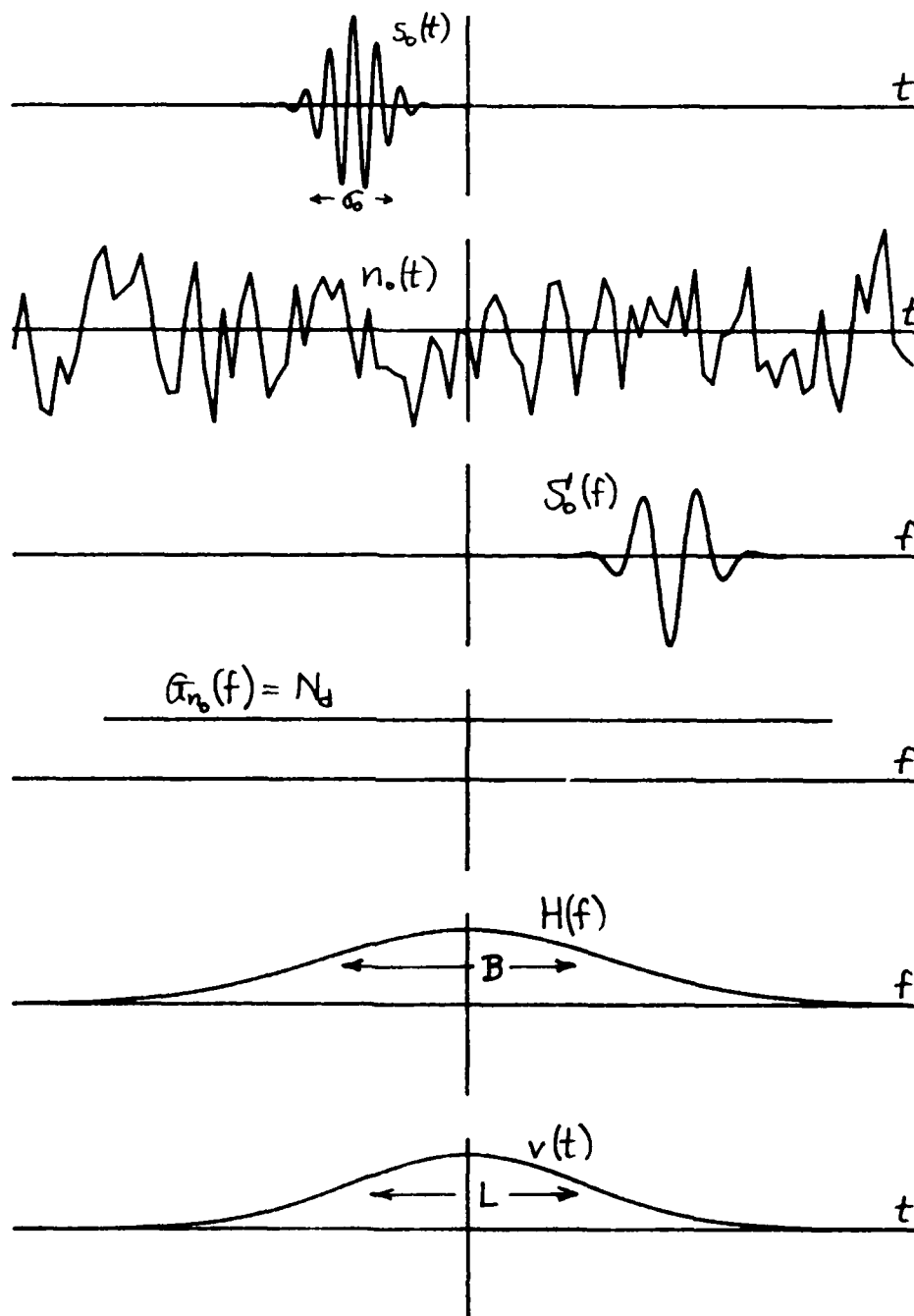


Figure 8. Time and Frequency Characteristics of Figure 7

## SUMMARY

When a segment of a stationary random process is available, the method of Blackman and Tukey [14] tells us that, to estimate the correlation function at delay  $\tau$ , we should average the product of waveform values separated in time by  $\tau$  seconds, and that we should carry out this averaging over the total available data record, in order to reduce the effect of random fluctuations. For a nonstationary process, the averaging interval is further limited to that in which a significant change in statistics does not occur.

After obtaining the estimated correlation, the Blackman-Tukey method further directs us to weight the correlation values in the neighborhood of  $\tau = 0$  more heavily than those for larger  $\tau$ , and to Fourier transform the weighted correlation estimate. The weighting should taper off to zero for larger  $\tau$ , so as to suppress these more noisy estimates, and the taper should be gradual so as not to create significant positive and negative sidelobes in the frequency domain.

These two operations, averaging in time and weighting in delay, are both totally absent in the WDF, as may be seen from (2) and (3). In fact, (2) and (3) might be viewed as the ultimate in greediness of a spectral estimate, since they include no averaging and no weighting. Viewed in this light, it is not surprising that the WDF has some very debilitating behavior in terms of negative distribution values and large interference terms.

The inclusion of averaging and weighting in the spectral estimate, as typified by (150)-(152) and (F-1), results in a modified distribution function which is a double convolution with a smoothing function in the  $t, f$  plane. Furthermore, the averaging and weighting in (F-1) takes place both in the  $f$  and  $\nu$  domain (line 4) just as well as in the  $t$  and  $\tau$  domain (line 3). Alternatively, line 2 indicates that the complex ambiguity function may be weighted in two dimensions and doubly Fourier transformed. However, the resultant modified WDF need not be positive.

The identity of this double convolution with a positive STSE, when the smoothing function is a legal WDF, allows for an alternative approach that is very attractive computationally and is easy to interpret. The preliminary calculation of the WDF serves to point out regions of interest in the  $t, f$  plane and to quantify the time and frequency extents, as well as the amount of linear frequency modulation, to utilize in weighting  $u$  in the STSE. This procedure is illustrated in appendix I for the waveform  $s(t) = t \exp(-t^2/2)$  and shown to yield a physically meaningful smoothed distribution function, whereas the WDF is very difficult to justify and interpret on any physical grounds.

It was pointed out earlier that double convolution of a given WDF with a Gaussian WDF increases the spread of the smoothed function by area .5 in the  $t, f$  plane, since the effective area of a Gaussian WDF is .5. Strictly speaking, this is only true when the Gaussian WDF contour ellipse has the same tilt and the same ratio of major-to-minor axes as the given WDF (assumed Gaussian in the region of interest in the  $t, f$  plane). More

generally, if there is a mismatch in tilt or ratio of major-to-minor axes, the effective area is increased by more than .5, thereby leading to additional spreading in the  $t, f$  plane. The detailed derivations are presented in appendix J.

The performance of an estimator of the WDF of a signal in the presence of noise depends on the amount of filtering and weighting employed to suppress noise components in frequency and time. Exact relations for the mean output, the bias, and the variance of the WDF estimate are given.

## APPENDIX A. SLICES IN TIME OF THE WDF

The voltage density spectrum of waveform  $s(t)$  was given in (9). If  $s(t)$  is sampled at increment  $\Delta_t$ , an approximation is afforded according to

$$\begin{aligned} S(f) &= \int dt \exp(-i2\pi ft) s(t) = \\ &\cong \Delta_t \sum_k \exp(-i2\pi fk\Delta_t) s(k\Delta_t) \equiv \tilde{S}(f) \quad \text{for all } f. \end{aligned} \quad (\text{A-1})$$

The summation on  $k$  runs over the range of nonzero summand. Since

$$\tilde{S}\left(f + \frac{1}{\Delta_t}\right) = \tilde{S}(f), \quad (\text{A-2})$$

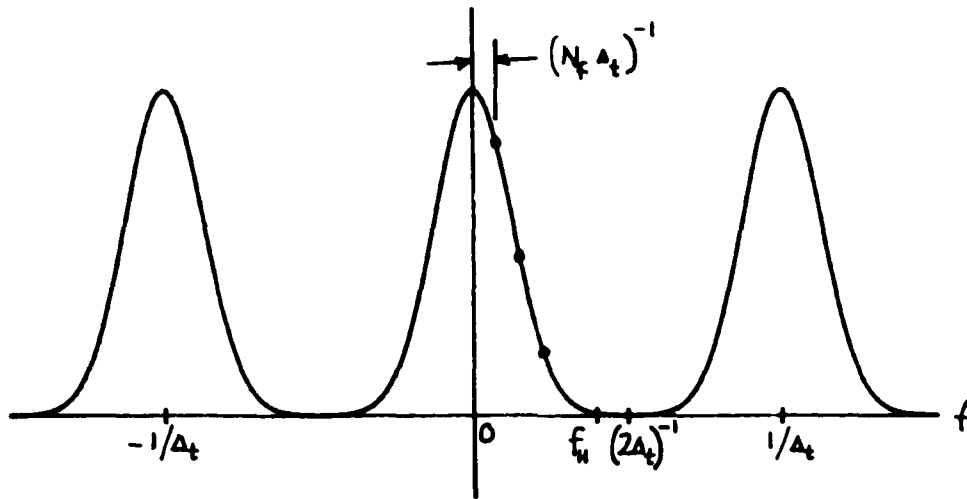
then  $\tilde{S}(f)$  has period  $1/\Delta_t$  in  $f$ . We limit the evaluation of  $\tilde{S}(f)$  to the values

$$\tilde{S}\left(\frac{n}{N_f \Delta_t}\right) = \Delta_t \sum_k \exp(-i2\pi nk/N_f) s(k\Delta_t) \quad \text{for } 0 \leq n \leq N_f - 1, \quad (\text{A-3})$$

where  $n$  and  $N_f$  are integers, and thereby cover a full period of  $\tilde{S}(f)$ . A representative plot of  $|\tilde{S}(f)|$  and its sampled values appears in figure A-1.

For the low-pass case of  $\tilde{S}(f)$  depicted in figure A-1, it is necessary to choose

$$\Delta_t < (2f_H)^{-1} \quad (\text{A-4})$$

Figure A-1. Low-Pass Spectrum  $\tilde{S}(f)$ 

in order to avoid aliasing. We will also need frequency spacing

$$(N_f \Delta_t)^{-1} < (2T)^{-1}, \quad \text{that is, } N_f > 2T/\Delta_t \quad (\text{A-5})$$

in order to track the wiggles of  $S(f)$  in frequency, where  $T$  is the effective time duration of  $s(t)$ . In fact, we may need frequency spacing  $(N_f \Delta_t)^{-1}$  to be very small if we are to do further accurate integrations on  $S(f)$ . Thus we need

$$N_f > 4 f_H T, \quad (\text{A-6})$$

and perhaps much larger for further manipulations.

The WDF can be written in terms of the spectrum  $S(f)$  according to (10):

$$\begin{aligned} W(t, f) &= \int dv \exp(i2\pi vt) S(f + \frac{v}{2}) S^*(f - \frac{v}{2}) = \\ &= 2 \int du \exp(i4\pi ut) S(f + u) S^*(f - u). \end{aligned} \quad (\text{A-7})$$



If we sample  $S(f)$  at increment  $\Delta_f$  in frequency, the Trapezoidal approximation to the WDF is

$$\hat{W}(t, f) \equiv 2\Delta_f \sum_{\ell} \exp(i4\pi t \ell \Delta_f) S(f + \ell \Delta_f) S^*(f - \ell \Delta_f) \quad (\text{A-8})$$

for all  $t, f$ . Since

$$\hat{W}\left(t + \frac{1}{2\Delta_f}, f\right) = \hat{W}(t, f), \quad (\text{A-9})$$

then  $\hat{W}(t, f)$  has period  $(2\Delta_f)^{-1}$  in  $t$ . Accordingly, we evaluate only

$$\hat{W}\left(\frac{m}{2N_t \Delta_f}, n\Delta_f\right) = 2\Delta_f \sum_{\ell} \exp(i2\pi m \ell / N_t) S((n + \ell)\Delta_f) S^*((n - \ell)\Delta_f) \quad (\text{A-10})$$

for  $0 \leq m \leq N_t - 1$ , where  $m, n, N_t$  are integers. In this manner, we get a slice of  $\hat{W}(t, f)$  in time  $t$  ( $m$ ) for fixed frequency  $f$  ( $n$ ). The operation in (A-10) can be efficiently realized as an  $N_t$ -point FFT of collapsed samples when  $N_t$  is a power of 2.

Now the only information on  $S(f)$  that we have available are the samples of  $\tilde{S}(f)$  given in (A-3). If we choose, without loss of generality,

$$\Delta_f = (N_f \Delta_t)^{-1}, \quad (\text{A-11})$$

then (A-10) becomes (exactly)

$$\hat{W}\left(\frac{m\Delta_t}{2} \frac{N_f}{N_t}, \frac{n}{N_f \Delta_t}\right) = \frac{2}{N_f \Delta_t} \sum_{\ell} \exp(i2\pi m \ell / N_t) S\left(\frac{n + \ell}{N_f \Delta_t}\right) S^*\left(\frac{n - \ell}{N_f \Delta_t}\right) \quad (\text{A-12})$$

for  $0 \leq m \leq N_t - 1$ . We then adopt as our approximation to  $\hat{W}$ , which itself is an approximation to  $W$ , the quantity

$$\tilde{W}\left(\frac{m\Delta_t}{2} \frac{N_f}{N_t}, \frac{n}{N_f\Delta_t}\right) \equiv \frac{2}{N_f\Delta_t} \sum_{\ell \in L_n} \exp(i2\pi m\ell/N_t) \tilde{S}\left(\frac{n+\ell}{N_f\Delta_t}\right) \tilde{S}^*\left(\frac{n-\ell}{N_f\Delta_t}\right) \quad (\text{A-13})$$

for  $0 \leq m \leq N_t - 1$ , where

$$\ell \in L_n \text{ denotes } |n \pm \ell| < N_f/2. \quad (\text{A-14})$$

and we presume that  $\tilde{S}(f)$  has been calculated for  $|f| < (2\Delta_t)^{-1}$ ; see figure A-1.

The quantity  $N_f\Delta_t$  may have to be large, in order to sample  $\tilde{S}(f)$  finely enough for an accurate WDF. Then since the spacing in  $t$ , applied to  $W(t,f)$ , is  $\frac{N_f\Delta_t}{2N_t}$ , it may require a large value of  $N_t$  in order to keep track of the variations versus  $t$ . Also,  $n$  may not have to run through consecutive integer values, but may take on decimated values, so that  $n/(N_f\Delta_t)$  tracks the  $f$  behavior adequately.

AD-A193 865

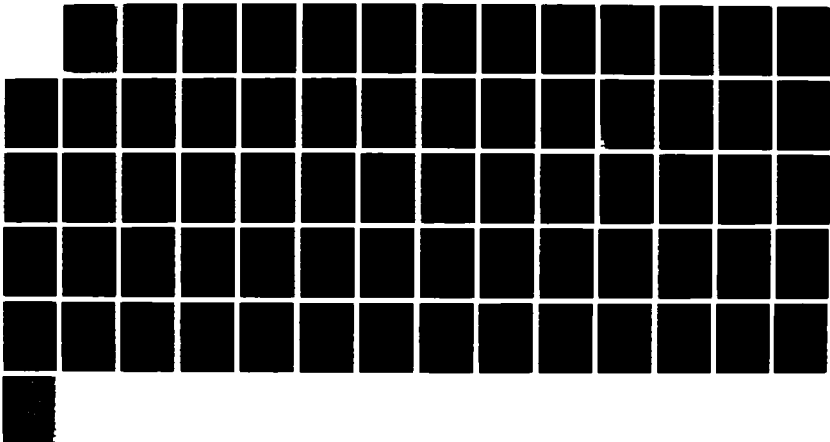
HIGHER DISTRIBUTION FUNCTION: RELATION TO SHORT-TERM  
SPECTRAL ESTIMATION. (U) NAVAL UNDERWATER SYSTEMS  
CENTER NEW LONDON CT NEW LONDON LAB. A H MUTTALL  
16 FEB 88 NUSC-TR-8225

2/2

UNCLASSIFIED

F/G 12/3

NL





MICROCOPY RESOLUTION TEST CHART  
1963 A

## APPENDIX B. OSCILLATING WDF FOR SEPARATED PULSES

Consider the waveform  $s(t)$  in figure B-1 consisting of two separated energy bursts of general shape. Let  $t_1$  and  $t_2$  represent the "center" of each pulse, and let  $T_1$  and  $T_2$  be some measure of their durations. Define

$$t_c = \frac{1}{2}(t_1 + t_2) . \quad (\text{B-1})$$

Let us investigate the WDF of  $s(t)$  for  $t$  near  $t_c$ , that is, near the center of the two pulses. In particular, let time

$$t = t_c + \Delta , \quad (\text{B-2})$$

where  $\Delta$  is small. Then from (3),

$$\begin{aligned} W(t_c + \Delta, f) &= \int d\tau \exp(-i2\pi f\tau) s(t_c + \Delta + \frac{\tau}{2}) s^*(t_c + \Delta - \frac{\tau}{2}) = \\ &= \exp(-i2\pi f(t_1 - t_2)) \int dx \exp(-i2\pi fx) s(t_2 + \Delta + \frac{x}{2}) s^*(t_1 + \Delta - \frac{x}{2}), \quad (\text{B-3}) \end{aligned}$$

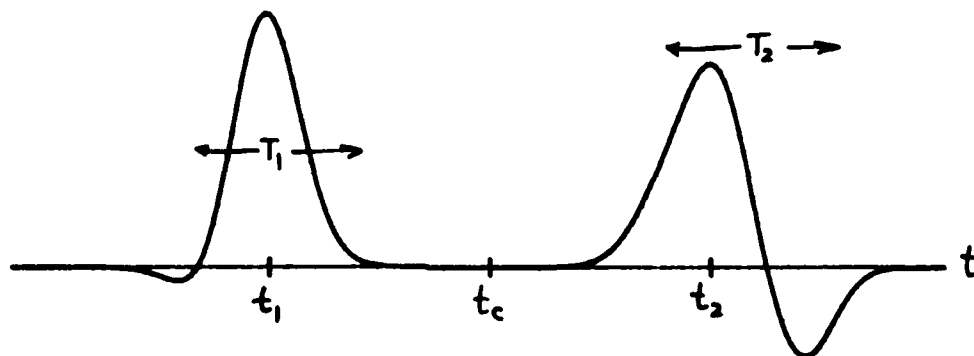


Figure B-1. Waveform  $s(t)$

where we let  $\tau = t_2 - t_1 + x$ .

It can be seen from the integral expression in (B-3) and figure B-1, that for small  $\Delta$ , only small values of  $x$  will contribute to the value of the WDF. In fact,

$$|x| < \min(T_1, T_2) \quad (B-4)$$

is the dominant range of contribution to the integral. Thus the variation with  $f$  of the integral component of (B-3) is slow. By contrast, the leading exponential term in (B-3) varies much faster with  $f$ , since

$$t_2 - t_1 > \max(T_1, T_2) > \min(T_1, T_2) . \quad (B-5)$$

Since these faster varying oscillations of the exponential term cannot be cancelled by the slower integral contribution of (B-3), the WDF will oscillate in  $f$ , for times  $t$  near  $t_c = (t_1 + t_2)/2$ . Thus separated time pulses will lead to oscillations (in  $f$ ) of the WDF, near times midway between the pulses, regardless of their detailed shapes. An analogous argument can be presented for spectral components, based upon form (10) of the WDF.

Notice that as  $t_2$  approaches  $t_1$ , and the two pulses become one, the oscillating exponential term in (B-3) disappears, allowing for the possibility of a slowly varying (hopefully positive) lobe in the WDF.

## APPENDIX C. AMBIGUITY FUNCTION OF (79)

The complex ambiguity function of waveform  $s(t)$  in (79) is obtained by substitution into (22) and use of (68):

$$\chi(\nu, \tau) = \sqrt{\pi} \sum_{k\ell} a_k a_\ell^* \tilde{\sigma}_{k\ell} \exp \left[ -\frac{1}{4} \frac{T_{k\ell}^2}{\sigma_{k\ell}^2} - \frac{1}{4} \tilde{\sigma}_{k\ell}^2 V_{k\ell}^2 + \right. \\ \left. + i \frac{1}{2} \frac{\sigma_\ell^2 - \sigma_k^2}{\sigma_\ell^2 + \sigma_k^2} T_{k\ell} V_{k\ell} + i2\pi f_{k\ell} T_{k\ell} - i t_{k\ell} V_{k\ell} + i2\pi f_{k\ell} (t_k - t_\ell) \right], \quad (C-1)$$

where

$$t_{k\ell} = \frac{1}{2}(t_k + t_\ell), \quad f_{k\ell} = \frac{1}{2}(f_k + f_\ell), \\ \tilde{\sigma}_{k\ell}^2 = \frac{1}{2}(\sigma_k^2 + \sigma_\ell^2), \quad \frac{1}{\sigma_{k\ell}^2} = \frac{1}{2} \left( \frac{1}{\sigma_k^2} + \frac{1}{\sigma_\ell^2} \right), \\ T_{k\ell} = \tau + t_\ell - t_k, \quad V_{k\ell} = 2\pi(\nu + f_\ell - f_k). \quad (C-2)$$

The diagonal terms of (C-1) are

$$\sum_k E_k \exp \left[ -\frac{1}{4} \frac{\tau^2}{\sigma_k^2} - \frac{1}{4} \sigma_k^2 4\pi^2 \nu^2 + i2\pi f_k \tau - i2\pi t_k \nu \right], \quad (C-3)$$

which are complex and oscillate with  $\tau$  and  $\nu$  due to the imaginary terms.

The contour at the  $1/e$  relative level, of the magnitude of the  $k$ -th term, is an ellipse with axes twice as large as those depicted in figure 4. In addition, the peak amplitude is decreased by a factor of 2 below that for

the WDF in (80). Thus the ambiguity function is a more smeared function of time-frequency than the WDF.

The ambiguity function has peaks of value

$$\sqrt{\pi} a_k a_l^* \tilde{\sigma}_{kl} \exp[i\pi(f_k + f_l)(t_k - t_l)] \quad (C-4)$$

centered at

$$(\tau, \nu) = (t_k - t_l, f_k - f_l) \quad (C-5)$$

for all  $k, l$ . The phases of (C-4) are virtually random relative to each other. A slice in  $\nu$ , for fixed  $\tau$ , varies (in addition to the Gaussian envelope) as

$$\exp\left[i2\pi\nu\left(\frac{1}{2}\frac{\sigma_l^2 - \sigma_k^2}{\sigma_l^2 + \sigma_k^2}\tau_{kl} - t_{kl}\right)\right], \quad (C-6)$$

which could be either a slow or fast variation, depending on the particular parameter values. All of these features make physical interpretation of the ambiguity function very difficult.



## APPENDIX D. ROTATION OF AXES

Consider the general second-order curve described by

$$Ax^2 + Bxy + Cy^2 + Dx + Ey + F = 0 . \quad (D-1)$$

If we rotate the  $x, y$  coordinate axes according to figure D-1, we have

$$x = x' \cos(\beta) - y' \sin(\beta) , \quad (D-2)$$

$$y = x' \sin(\beta) + y' \cos(\beta) .$$

Substitution in (D-1) yields

$$A'x'^2 + B'x'y' + C'y'^2 + D'x' + E'y' + F = 0 , \quad (D-3)$$

where

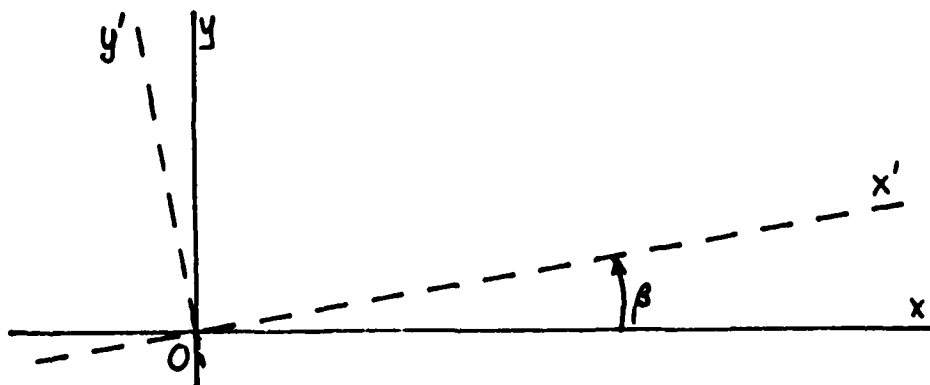


Figure D-1. Rotated Coordinate Axes

$$\begin{aligned}
 A' &= \frac{1}{2}[A + C + (A - C) \cos(2B) + B \sin(2B)] \\
 B' &= B \cos(2B) + (C - A) \sin(2B) \\
 C' &= \frac{1}{2}[A + C - (A - C) \cos(2B) - B \sin(2B)] \\
 D' &= D \cos(B) + E \sin(B) \\
 E' &= -D \sin(B) + E \cos(B) .
 \end{aligned} \tag{D-4}$$

If we want to eliminate the cross-product term in (D-3), we must make  $B' = 0$ , that is, take

$$\tan(2B) = \frac{B}{A - C} . \tag{D-5}$$

We will also choose  $2B$  in the principal value range:

$$2B = \arctan\left(\frac{B}{A - C}\right) ; \tag{D-6}$$

that is

$$-\frac{\pi}{2} \leq 2B \leq \frac{\pi}{2} , \quad -\frac{\pi}{4} \leq B \leq \frac{\pi}{4} . \tag{D-7}$$

All other solutions for  $2B$  differ by  $n\pi$ ; that is,  $B$  differs by  $n\pi/2$ . These are the major and minor axes of the curve described by (D-1).

If we now define

$$R = \sqrt{(A - C)^2 + B^2} , \quad P = \operatorname{sgn}(A - C) , \tag{D-8}$$

where  $\sqrt{\quad}$  denotes the positive square root, we find

$$\cos(2B) = \frac{|A - C|}{R} = \frac{A - C}{R} P ; \quad (D-9)$$

see figure D-2. And since  $\sin(2B)$  has the same polarity as  $\tan(2B)$  in the principal value range,

$$\sin(2B) = \frac{|B|}{R} \operatorname{sgn}\left(\frac{B}{A - C}\right) = \frac{B}{R} P . \quad (D-10)$$

Also, since

$$\cos^2(B) = \frac{1}{2}(1 + \cos(2B)) = \frac{1}{2}\left(1 + \frac{|A - C|}{R}\right), \quad (D-11)$$

then

$$\begin{aligned} \cos(B) &= \sqrt{\frac{R + |A - C|}{2R}}, \\ \sin(B) &= \sqrt{\frac{R - |A - C|}{2R}} \operatorname{sgn}\left(\frac{B}{A - C}\right). \end{aligned} \quad (D-12)$$

It then follows that the coefficients in (D-4) simplify to

$$\begin{aligned} A' &= \frac{1}{2}(A + C + RP) \\ B' &= 0 \\ C' &= \frac{1}{2}(A + C - RP), \end{aligned} \quad (D-13)$$

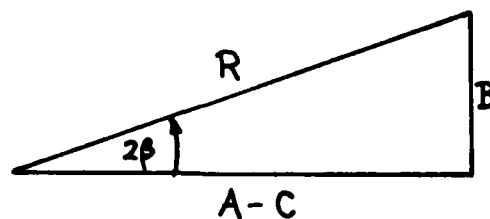


Figure D-2. Triangle Interpretation of (D-5)

from which there follows

$$A'C' = AC - \frac{1}{4} B^2 . \quad (D-14)$$

Additionally, we have

$$\begin{aligned} \tan(B) &= \frac{PR - (A - C)}{B} , \\ \cot(B) &= \frac{PR + (A - C)}{B} . \end{aligned} \quad (D-15)$$

As a result of the above, the general equation in (D-3) can be written as

$$A' \left( x' + \frac{D'}{2A'} \right)^2 + C' \left( y' + \frac{E'}{2C'} \right)^2 = \frac{D'^2}{4A'} + \frac{E'^2}{4C'} - F , \quad (D-16)$$

where

$$\frac{1}{2A'} = \frac{A + C - RP}{4AC - B^2} , \quad \frac{1}{2C'} = \frac{A + C + RP}{4AC - B^2} . \quad (D-17)$$

The simplest expressions for  $D'$  and  $E'$  appear to be those given in (D-4), in conjunction with (D-12). However,  $D'^2$  and  $E'^2$  can be simplified, resulting in expression

$$A' \left( x' + \frac{D'}{2A'} \right)^2 + C' \left( y' + \frac{E'}{2C'} \right)^2 = G , \quad (D-18)$$

where

$$G = \frac{AE^2 + CD^2 - BDE}{4AC - B^2} - F . \quad (D-19)$$

Now suppose that  $A$  and  $C$  in (D-1) are positive and that  $4AC > B^2$ . Then  $A' > 0$  and  $C' > 0$ , meaning that (D-18) is an ellipse if  $G > 0$ .

Furthermore, if  $A < C$ , then  $A' < C'$  and  $x'$  is the major axis. On the other hand, if  $A > C$ , then  $A' > C'$  and  $x'$  is the minor axis. See figure D-3. The area of this ellipse is

$$\text{Area} = \frac{\pi G}{\sqrt{A'C'}} = \frac{2\pi G}{\sqrt{4AC - B^2}}, \quad (\text{D-20})$$

by use of (D-14), where  $G$  is given by (D-19).

It follows directly from (D-18) that the curve is a circle if and only if  $A' = C'$ , that is,  $R = 0$  via (D-13), which in turn means  $A = C$  and  $B = 0$  from (D-8).

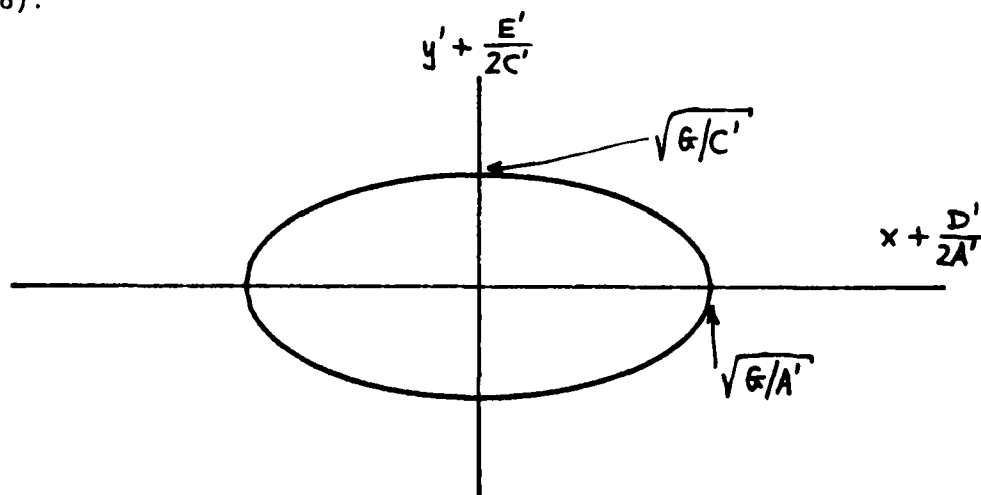


Figure D-3. Ellipse in Rotated Coordinates

## EXAMPLE

Consider the ellipse in (91), for which

$$A = 1 + \theta_0^2, \quad B = -2\theta_0, \quad C = 1; \quad \theta_0 \geq 0. \quad (D-21)$$

Then (D-5) yields

$$\tan(2\beta) = -2/\theta_0, \quad (D-22)$$

from which there follows

$$\begin{aligned} \tan\left(2\beta + \frac{\pi}{2}\right) &= -1/\tan(2\beta) = \theta_0/2, \\ \beta &= \frac{1}{2} \arctan\left(\frac{\theta_0}{2}\right) - \frac{\pi}{4}. \end{aligned} \quad (D-23)$$

As  $\theta_0$  varies from 0 to  $+\infty$ ,  $\beta$  varies from  $-\pi/4$  to 0; thus  $\beta$  always lies in the principal value range, as required by (D-7).

However, since  $A > C$  in (D-21), then  $\beta$  is the angle in the  $x,y$  plane of the minor axis of ellipse (91). The major axis angle in the  $x,y$  plane is

$$\psi = \beta + \frac{\pi}{2}, \quad (D-24)$$

which varies from  $\pi/4$  to  $\pi/2$ . There follows

$$\tan(2\psi) = \tan(2\beta + \pi) = \tan(2\beta) = -2/\theta_0 \quad (D-25)$$

from (D-22), whereupon the slope of the major axis in the  $x,y$  plane can be obtained as

$$\tan \psi = \frac{1}{2} \left( \theta_0 + \sqrt{\theta_0^2 + 4} \right). \quad (D-26)$$

This slope varies from 1 to  $+\infty$  as  $\theta_0$  varies from 0 to  $+\infty$ . Conversely, given a measured slope,  $\tan \psi$ , of the major axis of a WDF contour in the x,y plane, the corresponding amount of linear frequency modulation can be determined from (D-25) or (D-26) as

$$\theta_0 = \tan \psi - 1/\tan \psi. \quad (D-27)$$

The final determination of frequency modulation parameter  $\alpha_0$  in (84) requires the additional knowledge of  $\sigma_0$  in (90).

In practice, where both  $\sigma_0$  and  $\alpha_0$  are unknown a priori, the WDF will likely be plotted directly on the t,f plane. According to (78) and (D-24), the major axis will then lie on the line

$$f = t \frac{\tan \psi}{2\pi\sigma_0^2}, \quad (D-28)$$

which can be observed and measured. But  $\sigma_0$  can be determined separately from a slice in f (at fixed t) of the WDF, since the variation in f in (91) is proportional to

$$\exp \left[ -\sigma_0^2 (2\pi f - \alpha_0 t)^2 \right]. \quad (D-29)$$

Thus the distance, between frequency values that are down by 1/e from the peak on this frequency slice, is  $(\pi\sigma_0)^{-1}$ , and can be used for direct calculation of  $\sigma_0$ . Then (D-28) and (D-27) yield  $\tan \psi$  and  $\theta_0$ , respectively.

## APPENDIX E. DISCRETE APPROXIMATION TO SHORT-TERM SPECTRAL ESTIMATE

The STSE is given by (102) and (103). A discrete approximation, by means of the Trapezoidal rule, is furnished by

$$\begin{aligned}
 \mathcal{J}(t, f) &\equiv \left| \Delta \sum_k \exp(-i2\pi f \Delta k) s(k\Delta) u^*(t - k\Delta) \right|^2 = \\
 &= \Delta^2 \sum_{k\ell} \exp(-i2\pi f \Delta(k - \ell)) s(k\Delta) s^*(\ell\Delta) u^*(t - k\Delta) u(t - \ell\Delta) = \\
 &= \Delta^2 \sum_{k\ell} \exp(-i2\pi f \Delta(k - \ell)) R_s \left( \frac{k + \ell}{2} \Delta, k\Delta - \ell\Delta \right) R_u \left( t - \frac{k + \ell}{2} \Delta, k\Delta - \ell\Delta \right), \tag{E-1}
 \end{aligned}$$

where  $\Delta$  is the sampling increment in time. Let

$$m = k - \ell, \quad n = k + \ell, \tag{E-2}$$

to get

$$\mathcal{J}(t, f) = \Delta^2 \sum_{\substack{m+n \\ \text{even}}} \exp(-i2\pi f \Delta m) R_s \left( \frac{n\Delta}{2}, m\Delta \right) R_u \left( t - \frac{n\Delta}{2}, m\Delta \right). \tag{E-3}$$

Define, for use below, the function

$$\begin{aligned}
 C(t_1, t, f) &= W_s(t_1, f) \overset{f}{\otimes} W_u(t - t_1, f) = \\
 &= \int df_1 W_s(t_1, f_1) W_u(t - t_1, f - f_1), \tag{E-4}
 \end{aligned}$$



which is the convolution, on  $f$ , of WDFs  $W_s$  and  $W_u$ . When the integral on  $t_1$  is effected, it yields the desired double convolution:

$$\int dt_1 C(t_1, t, f) = W_s(t, f) \overset{tf}{\otimes} W_u(t, f) . \quad (E-5)$$

We now express  $R_s$  and  $R_u$  in (E-3) in terms of the inverse transforms of  $W_s$  and  $W_u$ , respectively, according to (24), interchange summations and integrations, and use the facts that [4, chapter 2]

$$\begin{aligned} \sum_{m \text{ even}} \exp(-i2\pi xm) &= \frac{1}{2} \sum_{\ell} \delta(x - \frac{1}{2}\ell) , \\ \sum_{m \text{ odd}} \exp(-i2\pi xm) &= \frac{1}{2} \sum_{\ell} (-1)^\ell \delta(x - \frac{1}{2}\ell) , \end{aligned} \quad (E-6)$$

to get approximation (E-1) in the form

$$\begin{aligned} g(t, f) &= \frac{\Delta}{2} \sum_{\ell} \sum_{n \text{ even}} C\left(\frac{n\Delta}{2}, t, f - \frac{\ell}{2\Delta}\right) + \\ &+ \frac{\Delta}{2} \sum_{\ell} (-1)^\ell \sum_{n \text{ odd}} C\left(\frac{n\Delta}{2}, t, f - \frac{\ell}{2\Delta}\right) . \end{aligned} \quad (E-7)$$

The  $\ell = 0$  terms together give, where the sum is now over all  $n$ ,

$$\frac{\Delta}{2} \sum_n C\left(\frac{n\Delta}{2}, t, f\right), \quad (\text{E-8})$$

which is a discrete approximation to desired quantity (E-5).

The  $\ell = 1$  terms in (E-7) yield

$$\frac{\Delta}{2} \sum_n (-1)^n C\left(\frac{n\Delta}{2}, t, f - \frac{1}{2\Delta}\right), \quad (\text{E-9})$$

which is approximately zero. A similar result holds for  $\ell = -1$ .

The  $\ell = 2$  terms in (E-7) are

$$\frac{\Delta}{2} \sum_n C\left(\frac{n\Delta}{2}, t, f - \frac{1}{\Delta}\right), \quad (\text{E-10})$$

which is a discrete approximation to convolution (E-5), but shifted by frequency  $1/\Delta$ . For small sampling increment  $\Delta$  in approximation (E-1), the quantity (E-10) will be small in the fundamental region centered at  $f = 0$ , and can be neglected. Thus (E-8) is the dominant term, giving

$$\begin{aligned} \mathcal{J}(t, f) &\cong \frac{\Delta}{2} \sum_n C\left(\frac{n\Delta}{2}, t, f\right) = \\ &\cong \int dt_1 C(t_1, t, f) = W_S(t, f) \odot W_U(t, f). \end{aligned} \quad (\text{E-11})$$

## APPENDIX F. SOME SMOOTHING CONSIDERATIONS

This discussion complements and extends that given in (148)-(152) regarding two-dimensional smoothing of the WDF. For easy reference, we repeat the diagram under (24) and furnish an additional one for the smoothing functions that will be employed here. An arrow denotes a Fourier transform.

## WAVEFORM FUNCTIONS

$$\begin{array}{ccc}
 s\left(t + \frac{\tau}{2}\right) s^*\left(t - \frac{\tau}{2}\right) = R(t, \tau) & \xleftrightarrow{\frac{\tau}{f}} & W(t, f) \\
 \updownarrow t \nu & & \updownarrow t \nu \\
 \chi(\nu, \tau) & \xleftrightarrow{\frac{\tau}{f}} & A(\nu, f) = S\left(f + \frac{\nu}{2}\right) S^*\left(f - \frac{\nu}{2}\right)
 \end{array}$$

## SMOOTHING FUNCTIONS

$$\begin{array}{ccc}
 v_2(t, \tau) & \xleftrightarrow{\frac{\tau}{f}} & V_2(t, f) \\
 \updownarrow t \nu & & \updownarrow t \nu \\
 q_2(\nu, \tau) & \xleftrightarrow{\frac{\tau}{f}} & Q_2(\nu, f)
 \end{array}$$

By using the basic Fourier transform relations above, we may readily show that two-dimensional smoothing of WDF  $W$  with general function  $V_2$  may be written in several alternative forms:

$$\begin{aligned}
W(t,f) \otimes_{t,f} V_2(t,f) &= \\
= \iint dv d\tau \exp[i2\pi(vt - f\tau)] \chi(v,\tau) q_2(v,\tau) &= \\
= \int d\tau \exp(-i2\pi f\tau) [R(t,\tau) \otimes_t v_2(t,\tau)] &= \\
= \int dv \exp(i2\pi vt) [A(v,f) \otimes_f Q_2(v,f)] . & \quad (F-1)
\end{aligned}$$

The second line says that the ambiguity function  $\chi$  of waveform  $s$  should be weighted by  $q_2$  and the product then double Fourier-transformed into the  $t, f$  plane. The third line indicates smoothing of  $R$  on  $t$ , followed by transformation of a weighted function of  $\tau$ . The last line performs smoothing of  $A$  on  $f$ , followed by transformation of a weighted function of  $v$ . These relations extend those given in (150)-(152). The function  $V_2$  above need not be a legal WDF. The volume under the smoothed distribution (F-1) is the product of the volumes under  $W$  and  $V_2$ ; if the latter volume is unity, the energy of waveform  $s$  results again, as is desired.

#### INADEQUACY OF TIME SMOOTHING ALONG

Consider the special case where smoothing function  $V_2$  is a delta function of  $f$ ; then

$$\begin{aligned}
V_2(t,f) &= v_1(t) \delta(f) \\
v_2(t,\tau) &= v_1(t) \\
q_2(v,\tau) &= V_1(v) \\
Q_2(v,f) &= V_1(v) \delta(f) . \quad (F-2)
\end{aligned}$$

Equation (F-1) then simplifies to an averaging of the WDF solely in time:

$$\begin{aligned}
 W(t, f) \otimes_{\tau} v_1(t) &= \\
 &= \iint dv d\tau \exp[i2\pi(vt - f\tau)] \chi(v, \tau) V_1(v) = \\
 &= \int d\tau \exp(-i2\pi f\tau) [R(t, \tau) \otimes_{\tau} v_1(t)] = \\
 &= \int dv \exp(i2\pi vt) A(v, f) V_1(v) , \tag{F-3}
 \end{aligned}$$

which is an extension of (148)-(149).

The advantageous feature of locally averaging the instantaneous correlation  $R$  in time, indicated in line 3, is equivalent to weighting the "local spectrum"

$$A(v, f) = S(f + \frac{v}{2}) S^*(f - \frac{v}{2}) \tag{F-4}$$

in line 4 by function  $V_1(v)$ , prior to Fourier transforming back into the  $t$  domain. This weighting on  $v$  is sensible, since if WDF  $W(t, f)$  or some modified version is to represent the spectrum at  $f$ , the transform on  $v$  in line 4 of (F-3) ought not to involve arbitrarily distant values of  $v$ ; otherwise, waveform spectrum  $S$  in (F-4) will then be utilized at argument values very different from the frequency  $f$  of interest and would be nonrepresentative. However, there is no weighting on  $\tau$  in line 3 of (F-3), thereby allowing arbitrarily distant argument values of signal  $s$ , from the

time instant  $t$  of interest, to be considered; this unrealistic feature of the WDF is one of the reasons for its undesirable properties.

#### INADEQUACY OF FREQUENCY SMOOTHING ALONE

Now consider the alternative special case where  $V_2$  in (F-1) is a delta function of  $t$ ; then

$$\begin{aligned} V_2(t, f) &= \delta(t) V_1(f) \\ v_2(t, \tau) &= \delta(t) v_1(\tau) \\ q_2(v, \tau) &= v_1(\tau) \\ Q_2(v, f) &= V_1(f) . \end{aligned} \tag{F-5}$$

Equation (F-1) then simplifies to an averaging of the WDF solely in frequency:

$$\begin{aligned} W(t, f) \otimes V_1(f) &= \\ &= \iint dv d\tau \exp[i2\pi(vt - f\tau)] \chi(v, \tau) v_1(\tau) = \\ &= \int d\tau \exp(-i2\pi f\tau) R(t, \tau) v_1(\tau) = \\ &= \int dv \exp(i2\pi vt) [A(v, f) \otimes V_1(f)] . \end{aligned} \tag{F-6}$$

The advantageous feature of averaging the "local spectrum"  $A$  in frequency, indicated in line 4, is equivalent to weighting the instantaneous correlation  $R(t, \tau)$  in line 3 by function  $v_1(\tau)$ , prior to Fourier transforming back into the  $f$  domain. This weighting on  $\tau$  is sensible, since if WDF  $W(t, f)$  or some modified version is to represent the time behavior at  $t$ , the transform on  $\tau$  in line 3 of (F-6) ought not to involve arbitrarily distant values of  $\tau$ ; otherwise, waveforms will then be utilized at argument values very different from the time  $t$  of interest and would be non-representative. However, there is no weighting on  $\nu$  in line 4 of (F-6), thereby allowing arbitrarily distant argument values of spectrum  $S$ , from the frequency  $f$  of interest, to be considered; this unrealistic feature of the WDF is an additional reason for its drawbacks.

#### SEPARABLE SMOOTHING

If smoothing function  $V_2$  is separable, then

$$V_2(t, f) = v_a(t) v_b(f)$$

$$v_2(t, \tau) = v_a(t) v_b(\tau)$$

$$q_2(\nu, \tau) = V_a(\nu) v_b(\tau)$$

$$Q_2(\nu, f) = V_a(\nu) V_b(f) .$$

Then (F-1) gives, for example,

$$\begin{aligned}
 W(t,f) \otimes_{t,f} v_a(t) \otimes_{t,f} v_b(f) &= \\
 &= \int d\tau \exp(-i2\pi f\tau) v_b(\tau) \int dt' R(t - t', \tau) v_a(t') .
 \end{aligned}$$

This has both the desirable features of locally averaging the correlation and suppressing large- $\tau$  contributions. However, it restricts the form of averaging in the  $t, f$  plane and specifically disallows tilted smoothing regions which are not parallel to the  $t$  or  $f$  axes.

#### GENERAL GAUSSIAN TWO-DIMENSIONAL SMOOTHING

The inadequacies of smoothing in time alone or frequency alone suggest consideration of the general two-dimensional result in (F-1):

$$\begin{aligned}
 \hat{W}(t,f) &\equiv W(t,f) \otimes_{t,f} v_2(t,f) = \\
 &= \int d\tau \exp(-i2\pi f\tau) \int dt' R(t - t', \tau) v_2(t', \tau) = \\
 &= \int d\tau \exp(-i2\pi f\tau) \int dt' s(t - t' + \frac{\tau}{2}) s^*(t - t' - \frac{\tau}{2}) v_2(t', \tau) . \quad (F-7)
 \end{aligned}$$

If we let  $t_1 = t' + \frac{\tau}{2}$ ,  $t_2 = t' - \frac{\tau}{2}$ , this becomes

$$\hat{W}(t,f) = \iint dt_1 dt_2 \exp(-i2\pi f(t_1 - t_2)) s(t - t_2) s^*(t - t_1) v_2\left(\frac{t_1 + t_2}{2}, t_1 - t_2\right) . \quad (F-8)$$



Now let two-dimensional smoothing function  $V_2$  have the general Gaussian form

$$V_2(t, f) = 2\sqrt{Q} \exp(-a^2 t^2 - 4\pi^2 b^2 f^2 - 4\pi c t f) , \quad (F-9)$$

where  $a, b, c$  are real constants and

$$Q = a^2 b^2 - c^2 . \quad (F-10)$$

The scale factor,  $2\sqrt{Q}$ , is chosen so that the volume under  $V_2$  in the  $t, f$  plane is 1; this keeps the volume under the smoothed distribution in (F-1) or (F-7) at  $E$ , the energy of waveform  $s$ . In order that  $V_2$  tend to zero at infinity in the  $t, f$  plane, we must have  $Q > 0$ . The area in the  $t, f$  plane of the contour ellipse of (F-9), at the  $1/e$  relative level, is (appendix D)

$$\text{Area} = \frac{1/2}{\sqrt{a^2 b^2 - c^2}} = \frac{1/2}{\sqrt{Q}} . \quad (F-11)$$

The transform on  $f$  of  $V_2$  in (F-9) is

$$v_2(t, \tau) = \frac{\sqrt{Q/\pi}}{b} \exp\left[-\frac{1}{b^2} \left\{ Q t^2 + \frac{\tau^2}{4} + i c t \tau \right\}\right] . \quad (F-12)$$

For completeness, the two remaining smoothing functions in (F-1) are

$$q_2(v, \tau) = \exp\left[-\frac{1}{4Q} \left( a^2 \tau^2 + 4\pi^2 b^2 v^2 + 4\pi c \tau v \right)\right] ,$$

$$Q_2(v, f) = \frac{2}{a} \sqrt{Q\pi} \exp\left[-\frac{4\pi^2}{a^2} \left( Q f^2 + \frac{v^2}{4} - i c f v \right)\right] .$$

We can now determine the quantity necessary for evaluation of (F-8), namely

$$v_2\left(\frac{t_1 + t_2}{2}, t_1 - t_2\right) = \frac{\sqrt{Q/\pi}}{b} \exp\left[-\frac{1}{4b^2} \left\{ (Q + 1 + i2c) t_1^2 + (Q + 1 - i2c) t_2^2 + 2(Q - 1) t_1 t_2 \right\}\right]. \quad (F-13)$$

By the discussion in (25) et seq., this function in (F-13) is separable in  $t_1$  and  $t_2$  if and only if

$$Q = 1, \quad \text{that is, } a^2 b^2 - c^2 = 1. \quad (F-14)$$

Then  $V_2$  in (F-9) is a legal WDF and the area in (F-11) becomes 1/2. Also, smoothing  $V_2$  in (F-9) is then exactly equivalent to the Gaussian smoothing considered previously in (147).

We are interested here, however, in the more general case of  $V_2$  where  $Q$  is not necessarily 1, and therefore  $V_2$  is not a legal WDF. If we substitute (F-13) in (F-8), the smoothed WDF becomes

$$\hat{W}(t, f) = \frac{\sqrt{Q/\pi}}{b} \iint dt_1 dt_2 x(t_1) x^*(t_2) \exp\left[-\frac{Q-1}{2b^2} t_1 t_2\right], \quad (F-15)$$

where

$$x(t_1) = s^*(t - t_1) \exp\left[-i2\pi f t_1 - (Q + 1 + i2c) \frac{t_1^2}{4b^2}\right]. \quad (F-16)$$

By expanding the exp in (F-15) in a power series, there follows

$$\hat{W}(t, f) = \frac{\sqrt{Q/\pi}}{b} \sum_{n=0}^{\infty} \frac{1}{n!} \left(\frac{1-Q}{2b^2}\right)^n \left| \int dt_1 x(t_1) t_1^n \right|^2. \quad (F-17)$$

It is obvious from (F-17) that a sufficient condition for smoothed WDF  $\hat{W}$  to be non-negative is  $Q \leq 1$ , that is

$$a^2b^2 - c^2 \leq 1 . \quad (F-18)$$

(The special case of  $c = 0$  was given in [11, (5)].) When this condition is used in (F-11), we see that the area of the concentration ellipse of (F-9) is

$$\text{Area} \geq 1/2 . \quad (F-19)$$

Thus, smoothing with the Gaussian two-dimensional function  $V_2$  in (F-9) always results in a non-negative distribution, provided that the area of the ellipse at the  $1/e$  relative level is greater than or equal to  $1/2$ . It is not necessary that  $V_2$  in (F-9) be a legal WDF; that is, the area of the ellipse need not be precisely  $1/2$ . However, the most concentrated  $V_2$  in (F-9), that guarantees nonnegative results, has area  $1/2$ . The only restrictions on parameters  $a, b, c$  are given by  $0 < Q \leq 1$ , that is,  $0 < a^2b^2 - c^2 \leq 1$ .

## APPENDIX G. DERIVATION OF MINIMUM-SPREAD WDF

The short-term spectral estimate of waveform  $s$ , relative to weighting  $u$ , is given by the double convolution (106),

$$|S_u(t,f)|^2 = W_s(t,f) \otimes W_u(t,f), \quad (G-1)$$

of the WDFs of  $s$  and  $u$ . It is therefore important to use, for weighting  $u$ , a function which has as narrow a WDF as possible, so that the smearing implied by (G-1) is minimized. In particular, since we are interested in analyzing waveforms with linear frequency modulation, we are interested in minimizing the spread of WDF  $W_u$ , as measured by the quadratic quantity

$$I = \iint dt df W_u(t,f) (f - \beta_c t)^2, \quad (G-2)$$

where  $\beta_c$  is a specified (observed) slope in the  $t, f$  plane.

By expanding the quadratic in (G-2), we obtain spread

$$I = I_0 + I_1 + I_2, \quad (G-3)$$

where

$$I_0 = \iint dt df f^2 W_u(t,f),$$

$$I_1 = -2\beta_c \iint dt df t f W_u(t,f),$$

$$I_2 = \beta_c^2 \iint dt df t^2 W_u(t,f). \quad (G-4)$$

Reference to (43), (28), and (12), respectively, allows the terms in (G-4) to be simplified and expressed solely in the time domain as

$$I_0 = \frac{1}{4\pi^2} \int dt |u'(t)|^2 ,$$

$$I_1 = -\frac{\beta_c}{\pi} \int dt t \operatorname{Im}\{u'(t) u^*(t)\} ,$$

$$I_2 = \beta_c^2 \int dt t^2 |u(t)|^2 . \quad (\text{G-5})$$

Adding these results together, the spread in (G-3) becomes

$$I = \frac{1}{4\pi^2} \int dt |u'(t) - i\alpha_c t u(t)|^2 , \quad (\text{G-6})$$

where we define

$$\alpha_c = 2\pi\beta_c . \quad (\text{G-7})$$

Observe that the spread  $I$  in (G-6) is nonnegative, for all weightings  $u$ .

The function that minimizes  $I$  in (G-6) is

$$u(t) = a_0 \exp\left(i \frac{\alpha_c}{2} t^2\right) , \quad a_0 \text{ complex}, \quad (\text{G-8})$$

for which

$$I = 0, \quad W_u(t, f) = |a_0|^2 \delta(f - \beta_c t). \quad (G-9)$$

That is, the WDF is concentrated on the  $f = \beta_c t$  line in the  $t, f$  plane.

However, the energy of (G-8) is

$$E_u = \infty, \quad (G-10)$$

which is unacceptable.

If we attempt to approximate (G-8) by unit energy weighting

$$u(t) = (\pi\sigma^2)^{-1/4} \exp\left(-\frac{t^2}{2\sigma^2} + i\frac{\alpha}{2}t^2\right), \quad (G-11)$$

the spread of  $u$ , as given by (G-6), turns out to be

$$I = \frac{1}{8\pi^2} \left[ \frac{1}{\sigma^2} + \sigma^2(\alpha - \alpha_c)^2 \right]. \quad (G-12)$$

Now if  $\alpha = \alpha_c$ , that is, the linear frequency modulation parameter  $\alpha$  in weighting  $u$  is exactly equal to given quantity  $\alpha_c$  (from (G-7) and (G-2)), the spread is

$$I = \frac{1}{8\pi^2\sigma^2} > 0. \quad (G-13)$$

However, as duration  $\sigma$  of weighting (G-11) gets larger, the spread  $I$  tends to zero, even though the weighting has finite (unit) energy. Also, then (G-11) tends to a scaled version of (G-8) at each fixed  $t$ .

In order to eliminate these undesirable features of the weighting, it will not be sufficient to minimize spread  $l$ , subject only to a constraint on the energy of  $u$ . Rather, it will also be necessary to constrict the time duration of the weighting  $u$ . Accordingly, we will minimize spread  $l$  in (G-2)-(G-6), under the two constraints that

$$\int dt |u(t)|^2 = 1 = \iint dt df W_u(t,f) ,$$

$$\int dt t^2 |u(t)|^2 = \frac{\sigma_c^2}{2} = \iint dt df t^2 W_u(t,f) ; \quad (G-14)$$

see (14) and (12).

Thus consider

$$Q = \int dt |u'(t) - i\alpha_c t u(t)|^2 + \lambda \int dt |u(t)|^2 + \mu \int dt t^2 |u(t)|^2 , \quad (G-15)$$

where  $\lambda$  and  $\mu$  are real Lagrange multipliers. Replacing  $u(t)$  by  $u(t) + \epsilon n(t)$ , where  $n(t)$  is an allowed variation, we have

$$Q + \delta Q = \int dt [u'(t) + \epsilon n'(t) - i\alpha_c t (u(t) + \epsilon n(t))] [u'^*(t) + \epsilon^* n'^*(t) + i\alpha_c t (u^*(t) + \epsilon^* n^*(t))] + \int dt [u(t) + \epsilon n(t)] [u^*(t) + \epsilon^* n^*(t)] (\lambda + \mu t^2) . \quad (G-16)$$

Since the coefficient of  $\epsilon^*$  must be zero, in order for  $u(t)$  to be the optimum [15], we require the following:

$$\int dt \eta'^*(t) [u'(t) - i\alpha_c t u(t)] + \int dt \eta^*(t) [u'(t) - i\alpha_c t u(t)] i\alpha_c t + \int dt \eta^*(t) u(t) (\lambda + \mu t^2) = 0 \quad \text{for all } \eta(t) . \quad (G-17)$$

We now integrate by parts on the first term of (G-17), and presume that  $\eta, u, u'$  all decay to zero at  $\pm\infty$ . Since  $\eta$  is arbitrary, its coefficient under the integral must be zero; namely, we find that  $u$  must satisfy the following differential equation:

$$-u''(t) + i2\alpha_c t u'(t) + (i\alpha_c + \alpha_c^2 t^2 + \lambda + \mu t^2) u(t) = 0 \quad \text{for all } t . \quad (G-18)$$

If we try solution

$$u(t) = a \exp\left(\frac{1}{2} ct^2\right) , \quad a, c \text{ complex} , \quad (G-19)$$

in (G-18), we find that

$$t^2(-c^2 + i2\alpha_c c + \alpha_c^2 + \mu) - c + i\alpha_c + \lambda = 0 \quad \text{for all } t . \quad (G-20)$$

Then a solution of the form (G-19) exists with the choices

$$c = i\alpha_c \pm \sqrt{\mu} , \quad \lambda = \pm \sqrt{\mu} . \quad (G-21)$$



To determine  $u(t)$  explicitly, we substitute (G-21) into (G-19) to get

$$u(t) = a \exp\left(i \frac{1}{2} \alpha_c t^2 \pm \frac{1}{2} \sqrt{\mu} t^2\right). \quad (G-22)$$

When the two constraints in (G-14) are satisfied, there follows, for the optimum weighting,

$$u(t) = \left(\pi \sigma_c^2\right)^{-1/4} \exp\left(-\frac{t^2}{2\sigma_c^2} + i \frac{\alpha_c}{2} t^2\right). \quad (G-23)$$

This is linear frequency modulation with a Gaussian envelope.

The minimum value of the spread  $I$  in (G-6) for the optimum weighting (G-23) is

$$\text{minimum } I = \frac{1}{8\pi^2 \sigma_c^2}, \quad (G-24)$$

and the corresponding WDF is

$$\begin{aligned} W_U(t, f) &= 2 \exp\left[-\frac{t^2}{\sigma_c^2} - 4\pi^2 \sigma_c^2 (f - \beta_c t)^2\right] = \\ &= 2 \exp\left[-\frac{t^2}{\sigma_c^2} (1 + \theta_c^2) + 4\pi f t \theta_c - 4\pi^2 f^2 \sigma_c^2\right], \end{aligned} \quad (G-25)$$

where  $\theta_c = \alpha_c \sigma_c^2$ . The area of the contour ellipse at the  $1/e$  relative level is  $1/2$  in the  $t, f$  plane.

The mean-square time extent of the optimum weighting  $u$  in (G-23) is  $\sigma_c^2/2$ , as required by constraint (G-14). The mean-square frequency extent is obtained from voltage spectrum

$$U(f) = \pi^{1/4} \left( \frac{2\sigma_c}{1 - i\theta_c} \right)^{1/2} \exp\left( \frac{-2\pi^2 f^2 \sigma_c^2}{1 - i\theta_c} \right) \quad (\text{G-26})$$

as

$$\int df f^2 |U(f)|^2 = \frac{1 + \theta_c^2}{8\pi^2 \sigma_c^2} . \quad (\text{G-27})$$

## APPENDIX H. EXAMPLE OF WDF PROCESSOR

The processor of interest here is depicted in figure 7, while representative characteristics of the waveforms and devices are sketched in figure 8. The mean output is given by (173) and the variance is given by (188). We will use the definitions and results in (165)-(189) freely in the following.

## INPUT INFORMATION

The input signal waveform to figure 7 is Gaussian-modulated linear frequency modulation:

$$s_0(t) = a_0 \exp \left[ -\frac{t^2}{2\sigma_0^2} + i \frac{\alpha_0}{2} t^2 \right], \quad E_0 = \sqrt{\pi} |a_0|^2 \sigma_0, \quad (H-1)$$

where  $a_0$  can be complex. The instantaneous input signal power,

$$|s_0(t)|^2 = |a_0|^2 \exp(-t^2/\sigma_0^2), \quad (H-2)$$

peaks at  $t = 0$  and has effective duration  $\sigma_0$ .

The corresponding signal voltage density spectrum is

$$S_0(f) = a_0 \sigma_0 \left( \frac{2\pi}{1 - i\theta_0} \right)^{1/2} \exp \left( -\frac{2\pi^2 \sigma_0^2 f^2}{1 - i\theta_0} \right), \quad \theta_0 = \alpha_0 \sigma_0^2. \quad (H-3)$$

The energy density spectrum is

$$|S_o(f)|^2 = \frac{2\pi |a_o|^2 \sigma_o^2}{\sqrt{1 + \theta_o^2}} \exp\left(-\frac{4\pi^2 \sigma_o^2 f^2}{1 + \theta_o^2}\right), \quad (\text{H-4})$$

which peaks at  $f = 0$ . When

$$f = \pm f_o = \pm \frac{\sqrt{1 + \theta_o^2}}{2\pi \sigma_o}, \quad (\text{H-5})$$

the energy density spectrum is reduced to  $1/e$  of its peak value; hence  $f_o$  is a measure of the bandwidth of the linear frequency modulation waveform.

The input noise  $n_o$  to figure 7 has a white spectrum

$$G_{n_o}(f) = N_d \quad \text{for all } f. \quad (\text{H-6})$$

The filter transfer function is

$$H(f) = \exp\left(-\frac{f^2}{2B^2}\right), \quad (\text{H-7})$$

which peaks at  $f = 0$ ; this coincides with the signal spectrum peak, which means that we are considering the most fortuitous situation. The weighting in figure 7 is taken to be

$$v(t) = \exp\left(-\frac{t^2}{2L^2}\right), \quad (\text{H-8})$$

which peaks at  $t = 0$ ; again, this coincides with the signal peak and is most favorable. The maximum values of  $H$  and  $v$ , being equal to 1, are chosen for convenience, without loss of generality; absolute level does not influence the performance of the processor in figure 7.

#### CALCULATIONS OF BASIC FUNCTIONS

We will make frequent use of (68)-(70) in evaluating the following quantities which are needed in (165)-(189); the choices for Gaussian functions for  $s_0, H, v$ , above, were made for analytic simplicity, since the various integrals can be conducted in closed form. More general cases would require numerical integrations.

The noise spectrum at the output of the filter is

$$G_n(f) = G_{n_0}(f) |H(f)|^2 = N_d \exp(-f^2/B^2) . \quad (H-9)$$

The corresponding noise correlation is

$$C_n(\tau) = \int df \exp(i2\pi f\tau) G_n(f) = \sqrt{2} N_d B \exp(-\pi^2 B^2 \tau^2) . \quad (H-10)$$

The auxiliary spectrum in (178) is

$$G_n^{(2)}(f) = \int d\tau \exp(-i4\pi f\tau) C_n^2(\tau) = \sqrt{\frac{\pi}{2}} N_d^2 B \exp(-2f^2/B^2) . \quad (H-11)$$

The instantaneous correlation of the weighting is

$$R_V(t, \tau) = v\left(t + \frac{\tau}{2}\right) v^*\left(t - \frac{\tau}{2}\right) = \exp\left(-\frac{t^2}{L^2} - \frac{\tau^2}{4L^2}\right), \quad (\text{H-12})$$

and its corresponding WDF is

$$W_V(t, f) = \int d\tau \exp(-i2\pi f\tau) R_V(t, \tau) = 2\sqrt{\pi} L \exp\left(-\frac{t^2}{L^2} - 4\pi^2 L^2 f^2\right). \quad (\text{H-13})$$

The filter impulse response is

$$h(\tau) = \int df \exp(i2\pi f\tau) H(f) = \sqrt{2\pi} B \exp(-2\pi^2 B^2 \tau^2), \quad (\text{H-14})$$

leading to filter output signal

$$\begin{aligned} s(t) &= \int d\tau h(\tau) s_0(t - \tau) = \\ &= a_0 \left(\frac{D}{1 + D - i\theta_0}\right)^{1/2} \exp\left[-2\pi^2 B^2 \frac{1 - i\theta_0}{1 + D - i\theta_0} t^2\right], \end{aligned} \quad (\text{H-15})$$

where

$$\theta_0 = \alpha_0 \sigma_0^2, \quad D = (2\pi B \sigma_0)^2. \quad (\text{H-16})$$

This filter output signal is again a Gaussian-modulated linear frequency modulation waveform.

In general, for signal

$$s(t) = c_0 \exp(-ct^2/2), \quad c_0, c \text{ complex}, \quad E = \sqrt{\pi} |c_0|^2 / \sqrt{c_r}, \quad (\text{H-17})$$

the WDF is

$$W_s(t, f) = 2\sqrt{\pi} \frac{|c_0|^2}{\sqrt{c_r}} \exp \left[ -\frac{t^2 |c|^2 + 4\pi^2 f^2 + 4\pi f t c_i}{c_r} \right]. \quad (\text{H-18})$$

When applied to example (H-15), we identify

$$c_0 = a_0 \left( \frac{D}{1 + D - i\theta_0} \right)^{1/2}, \quad c = 4\pi^2 B^2 \frac{1 - i\theta_0}{1 + D - i\theta_0}, \quad (\text{H-19})$$

to obtain

$$|c_0|^2 = |a_0|^2 \frac{D}{\sqrt{D_2}}, \quad |c|^2 = (2\pi B)^4 \frac{1 + \theta_0^2}{D_2},$$

$$c_r = 4\pi^2 B^2 \frac{D_1}{D_2}, \quad c_i = -4\pi^2 B^2 \frac{D\theta_0}{D_2}, \quad (\text{H-20})$$

where

$$D_1 = 1 + D + \theta_0^2, \quad D_2 = (1 + D)^2 + \theta_0^2. \quad (\text{H-21})$$

When substituted in (H-18), there follows, for the WDF of  $s$  in (H-15),

$$W_s(t, f) = 2E_0 \left( \frac{D}{D_1} \right)^{1/2} \exp \left[ -\frac{1}{D_1} \left\{ (1 + \theta_0^2) (2\pi B t)^2 + D_2 \left( \frac{f}{B} \right)^2 - 2D\theta_0 (2\pi B t) \left( \frac{f}{B} \right) \right\} \right]. \quad (\text{H-22})$$

As bandwidth  $B$  of filter  $H$  in (H-7) tends to infinity, then  $D \rightarrow \infty$ ,

$D_1 \rightarrow D$ ,  $D_2 \rightarrow D^2$ , and (H-22) yields

$$W_s(t, f) \rightarrow 2E_0 \exp \left[ - (1 + \theta_0^2) \frac{t^2}{\sigma_0^2} - (2\pi \sigma_0 f)^2 + 4\pi \theta_0 f t \right] \text{ as } B \rightarrow \infty. \quad (\text{H-23})$$

This agrees with (91) and (78). More generally, in order to keep the scale factor  $(D/D_1)^{1/2}$  in (H-22) near 1, we need

$$D > 1 + \theta_0^2, \quad \text{that is, } B > \frac{\sqrt{1 + \theta_0^2}}{2\pi\sigma_0}. \quad (\text{H-24})$$

according to (H-21) and (H-16). But this latter quantity is just the bandwidth of signal  $s_0$ ; see (H-5). Thus condition (H-24) yields the physically intuitive statement that the filter passband should be wider than the input signal bandwidth, in order not to decrease the peak value of the WDF of the filter output signal.

The area of the elliptical contour of the general WDF in (H-22), at the  $1/e$  relative level, is  $1/2$  in the  $t, f$  plane, regardless of the values of any of the parameters of the input signal and filter; this follows by the direct use of (D-1), (D-19), and (D-20). It is also consistent with the general fact that this is true for any signal of the form of (H-17), as may be seen by application of appendix D directly to (H-18), where  $c$  and  $c_0$  are arbitrary complex constants.

The peak height of the signal WDF in (H-22) is  $2E_0\sqrt{D/D_1}$ ; hence, the product of peak height and effective area is  $E_0\sqrt{D/D_1}$ , which is just the energy of  $s$ :

$$E = \int dt |s(t)|^2 = E_0\sqrt{\frac{D}{D_1}} = \iint dt df W_s(t, f). \quad (\text{H-25})$$

This follows directly from (H-15) or (H-17).



The tilt of the major axis of the elliptical contours of (H-22) is given by  $\beta$  radians in the  $(2\pi Bt, f/B)$  plane, where

$$\tan(2\beta) = \frac{\theta_0}{1 + D/2} \quad (\text{H-26})$$

according to (D-5) and (H-21).

#### MEAN SIGNAL OUTPUT

The mean signal output of the WDF processor in figure 7 is given by (171) as

$$\begin{aligned} a &= \int d\tau \exp(-i2\pi f\tau) R_V(t, \tau) R_S(t, \tau) = \\ &= \int d\tau \exp(-i2\pi f\tau) R_{\tilde{\zeta}}(t, \tau) = W_{\tilde{\zeta}}(t, f) \quad (\text{H-27}) \end{aligned}$$

where

$$\tilde{\zeta}(t) = v(t) s(t) = c_0 \exp(-\tilde{c} t^2/2) \quad (\text{H-28})$$

and

$$\tilde{c} = c + \frac{1}{L^2} \quad (\text{H-29})$$

according to (H-8) and (H-15)-(H-19). By analogy to (H-18), we have

$$\begin{aligned}
 a = W_{\xi}(t, f) &= 2\sqrt{\pi} \frac{|c_0|^2}{\sqrt{\tilde{c}_r}} \exp\left[-\frac{t^2 |\tilde{c}|^2 + 4\pi^2 f^2 + 4\pi f t \tilde{c}_i}{\tilde{c}_r}\right] = \\
 &= 2E_0 \left(\frac{DR}{H_1}\right)^{1/2} \exp\left[-\frac{1}{H_1} \{H_2 x^2 + D_2 y^2 - 2RD\theta_0 xy\}\right], \quad (H-30)
 \end{aligned}$$

where we defined

$$R = (2\pi BL)^2, \quad x = t/L, \quad y = 2\pi fL,$$

$$H_1 = D_2 + RD_1 = (1 + D)(1 + D + R) + (1 + R)\theta_0^2,$$

$$H_2 = D_2 + 2RD_1 + R^2(1 + \theta_0^2) = (1 + D + R)^2 + (1 + R)^2\theta_0^2, \quad (H-31)$$

and used

$$\tilde{c}_r = \frac{H_1}{L^2 D_2}, \quad \tilde{c}_i = -\frac{RD\theta_0}{L^2 D_2}, \quad |\tilde{c}|^2 = \frac{H_2}{L^4 D_2}. \quad (H-32)$$

The area of the concentration ellipse of  $W_{\xi}$  in (H-30) at the 1/e relative level is 1/2 in the  $t, f$  plane, regardless of the sizes of  $D$  and  $R$ ; so the signal WDF is not spread by the filtering and weighting operations in figure 7, at least for this example of (H-1) coupled with (H-7) and (H-8).

The peak height of WDF  $W_{\xi}$  is given by the leading factor in (H-30). Since the effective area of this WDF is 1/2, the product of peak height and effective area is  $E_0 \sqrt{DR/H_1}$ , which is just the energy of  $\xi$ :

$$\tilde{E} = \int dt |\xi(t)|^2 = E_0 \left( \frac{DR}{(1 + D)(1 + D + R) + (1 + R)\theta_0^2} \right)^{1/2}. \quad (H-33)$$

The parameters  $\theta_0, D, R$  are given in (H-16) and (H-31).

We now define

$$L_b = \frac{L}{\sqrt{1+R}} = \frac{L}{\sqrt{1+(2\pi BL)^2}}; \quad \frac{1}{L_b^2} = \frac{1}{L^2} + (2\pi B)^2. \quad (H-34)$$

Then (H-30) and (H-31) become

$$W_S(t, f) = 2E_0 \left( \frac{DR}{H_1} \right)^{1/2} \exp \left[ - \frac{1}{H_1} \left\{ \frac{H_2}{1+R} \left( \frac{t}{L_b} \right)^2 + D_2(1+R)(2\pi L_b f)^2 - 2RD\theta_0(2\pi L_b f) \left( \frac{t}{L_b} \right) \right\} \right]. \quad (H-35)$$

The major axis of the elliptical contours is at angle  $\tilde{\beta}$  radians in the  $(t/L_b, 2\pi L_b f)$  plane, where

$$\tan(2\tilde{\beta}) = \frac{\theta_0(1+R)}{1+R+D+RD/2}. \quad (H-36)$$

Given measurements or observations  $\tilde{\beta}$  and  $\sigma_0$ , this can be immediately solved for  $\theta_0$ , where it is presumed that  $B$  and  $L$  are known since they are under our control.

As alternative fundamental parameter is more useful than the above; we introduce

$$M = (L/\sigma_0)^2, \quad (H-37)$$

which is the square of the ratio of weighting time to input signal duration.

Then (H-31) yields

$$R = DM, \quad (H-38)$$

where  $D = (2\pi B\sigma_0)^2$  just as defined in (H-16). Eliminating  $R$  in favor of  $D$  and  $M$ , the peak height of  $W_{\zeta}$  in (H-30) becomes

$$\text{Peak} = 2E_0 \left( \frac{D^2 M}{(1+D)(1+D+DM) + (1+DM)\theta_0^2} \right)^{1/2} \quad (\text{H-39})$$

As checks on this quantity, observe that as  $D \rightarrow \infty$ , the factor of  $2E_0$  in (H-39) approaches  $(M/(M+1))^{1/2}$ ; in order to keep this latter quantity near 1, we need  $M > 1$ , that is,  $L > \sigma_0$ . This is consistent with physical reasoning on figure 7. Alternatively, as  $M \rightarrow \infty$ , the factor of  $2E_0$  in (H-39) approaches  $(D/(1+D+\theta_0^2))^{1/2}$ ; in order to keep this near 1, we need (H-24) to be observed, just as before.

More generally, in order to keep the signal factor in (H-39) near unity, we need to choose the combination of  $D$  and  $M$  large enough. For example, to keep the factor at value  $F$ , that is, maintain

$$\left( \frac{D^2 M}{(1+D)(1+D+DM) + (1+DM)\theta_0^2} \right)^{1/2} = F \quad (< 1), \quad (\text{H-40})$$

we need to choose  $L$  in (H-37) such that

$$M = \frac{F^2 [(1+D)^2 + \theta_0^2]}{D[D - F^2(1+D+\theta_0^2)]} \quad (\text{H-41})$$

However, this relationship is useful only for

$$D > \frac{F^2}{1-F^2} (1 + \theta_0^2) \quad (\text{H-42})$$

A representative sketch of (H-40) is displayed in figure H-1. Small values of parameters  $M$  or  $D$  are not realizable without the other parameter tending to infinity, in order to maintain the factor in (H-40) at value  $F$ . Three numerical examples, for  $\theta_0 = 0, 1, 5$  are given in figures H-2, H-3, and H-4, respectively. The larger  $F$  values can only be achieved through rather large  $D$  and/or  $M$  values.

There is, however, a minimum value of the product,  $MD$ , required to realize a specified value  $F$  for the factor in (H-40), when  $\theta_0$  is specified. In fact, we find from (H-41) that, for given  $F$  and  $\theta_0$ , the product  $MD$  is minimized by the choices

$$D_{\text{opt}} = \frac{1 + \theta_0^2}{1 - F^2} \left[ F^2 + \sqrt{\frac{1 + F^4 \theta_0^2}{1 + \theta_0^2}} \right]$$

$$M_{\text{opt}} = \frac{2F^2}{1 - F^4} \left[ 1 + \sqrt{\frac{1 + F^4 \theta_0^2}{1 + \theta_0^2}} \right]. \quad (\text{H-43})$$

The value  $M_{\text{opt}}$  is relatively insensitive to  $\theta_0$ ; in fact, it varies from  $4F^2/(1 - F^4)$  to  $2F^2(1 - F^2)$  as  $\theta_0$  varies from 0 to  $\infty$ , which is less than a 2:1 variation.

The corresponding minimum product is

$$(\text{MD})_{\text{min}} = \frac{2F^2}{(1 - F^2)^2} \left[ 1 + F^2 \theta_0^2 + \sqrt{(1 + \theta_0^2)(1 + F^4 \theta_0^2)} \right]. \quad (\text{H-44})$$

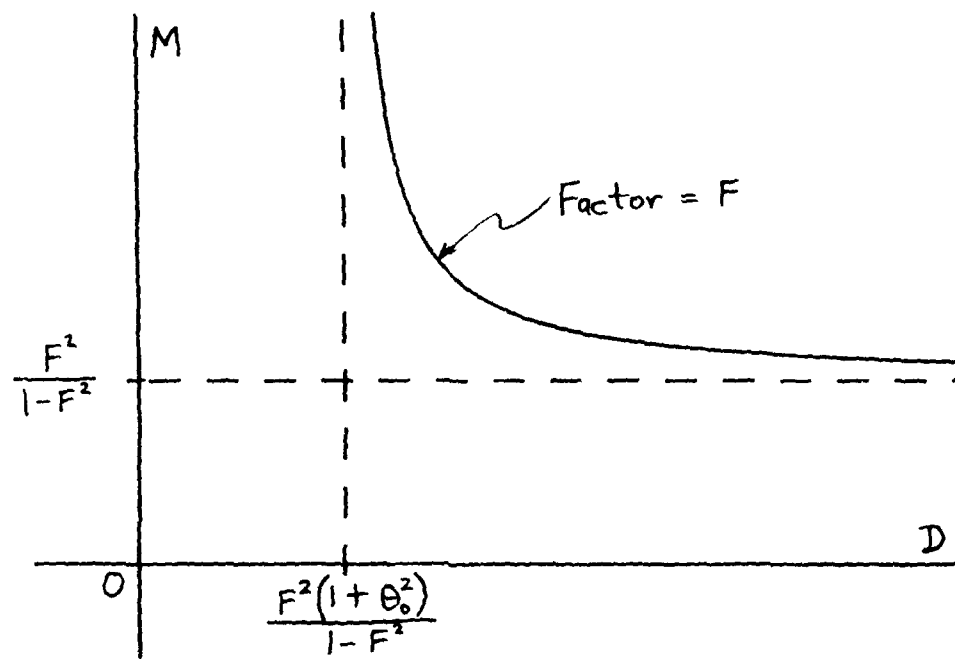


Figure H-1. Plot of (H-40) or (H-41) for Fixed  $\theta_0$ .

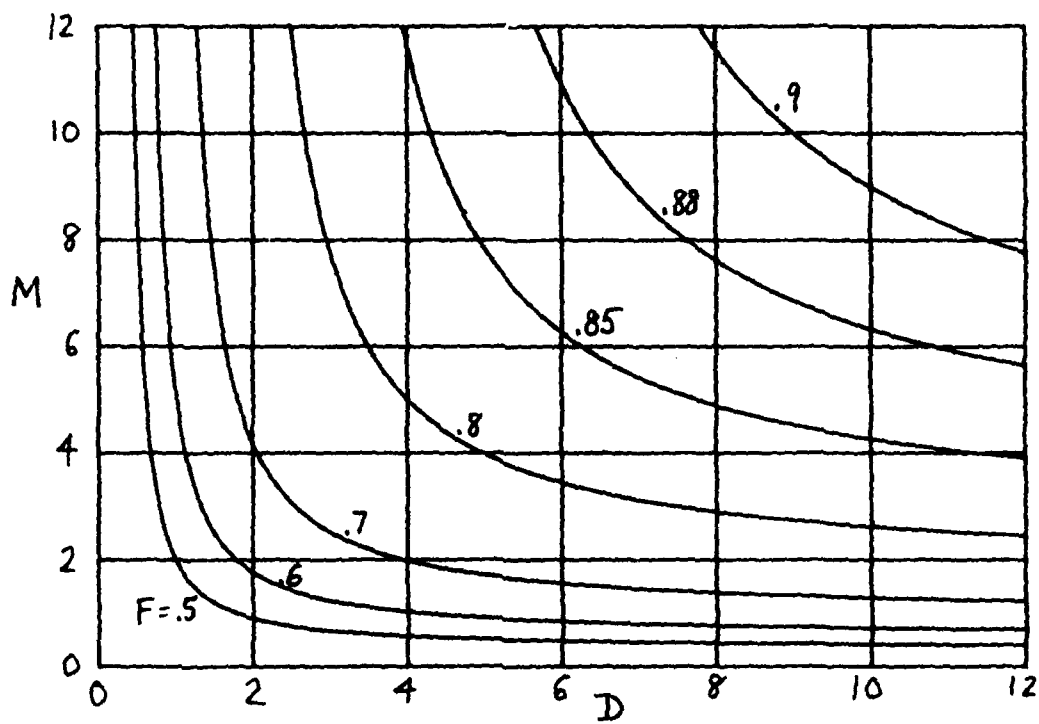


Figure H-2. Plot for  $\theta_0 = 0$

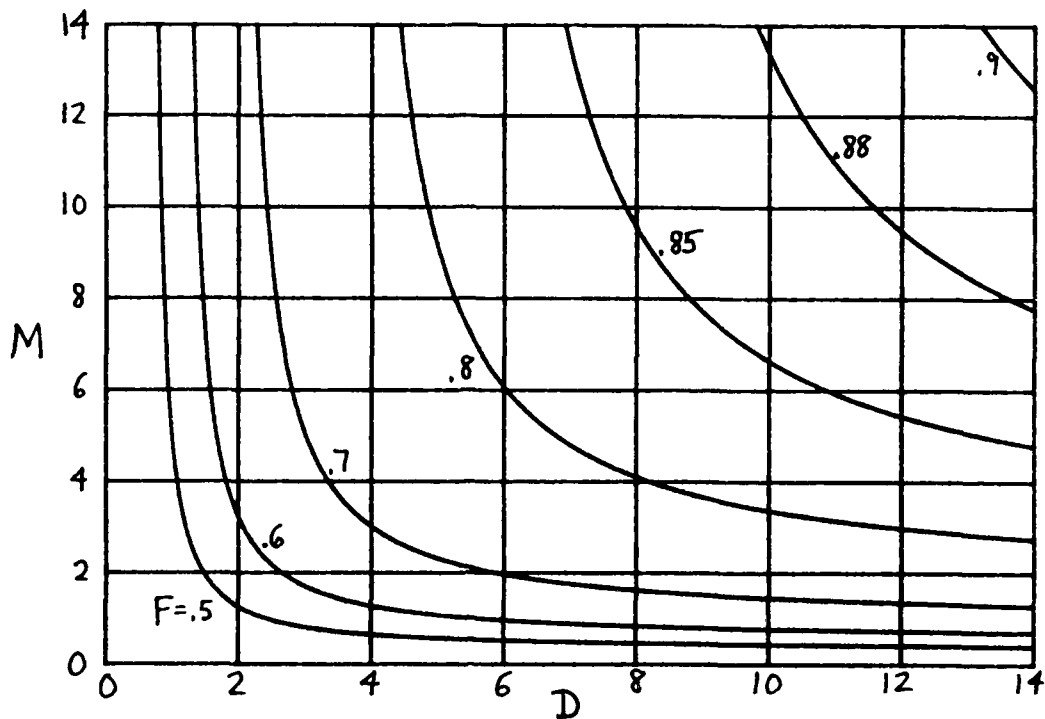


Figure H-3. Plot for  $\theta_0 = 1$

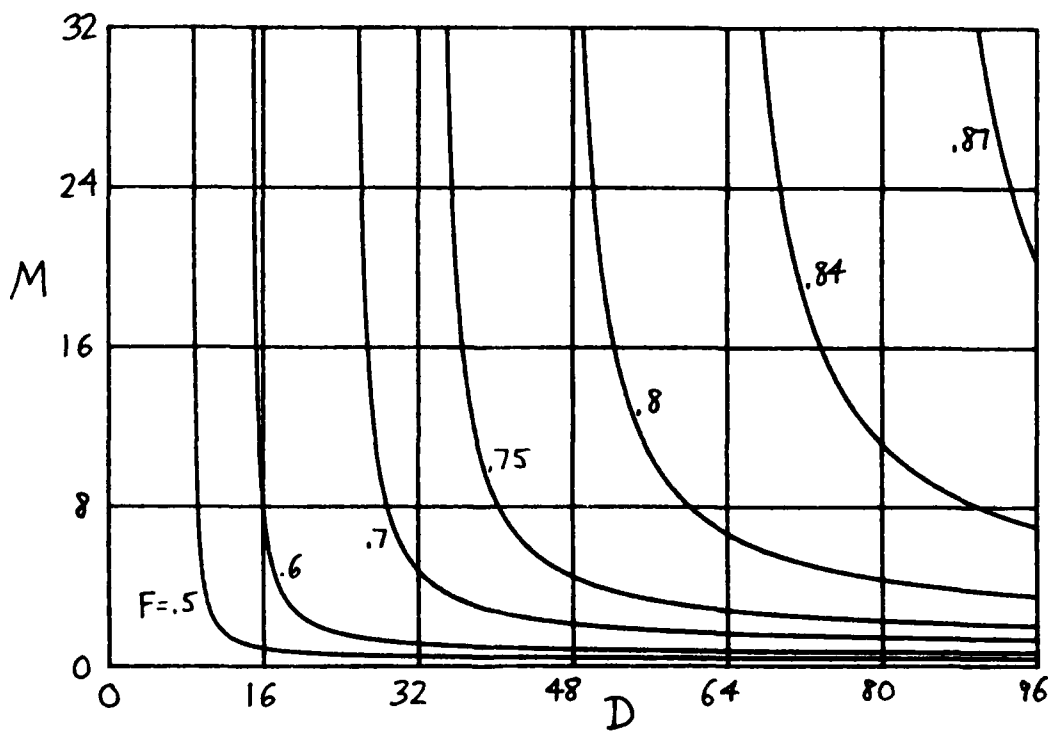


Figure H-4. Plot for  $\theta_0 = 5$

In particular,

$$(MD)_{\min} \sim \frac{4F^2}{(1-F^2)^2} (1 + F^2 \theta_0^2) + 1 \text{ as } \theta_0 \rightarrow \infty; \quad (H-45)$$

in fact, this is a good approximation except near  $\theta_0 = 0$ . Thus, large amounts of linear frequency modulation, or values of  $F$  near 1, require very large MD.

At the other extreme,

$$(MD)_{\min} = \frac{4F^2}{(1-F^2)^2} \text{ for } \theta_0 = 0. \quad (H-46)$$

For example, if  $F = 1/\sqrt{2}$ , this product is 8; thus relatively large values of the product are required, even at the low end where there is no linear frequency modulation. A plot of (H-44) is given in figure H-5, for various specified values of factor  $F$ .

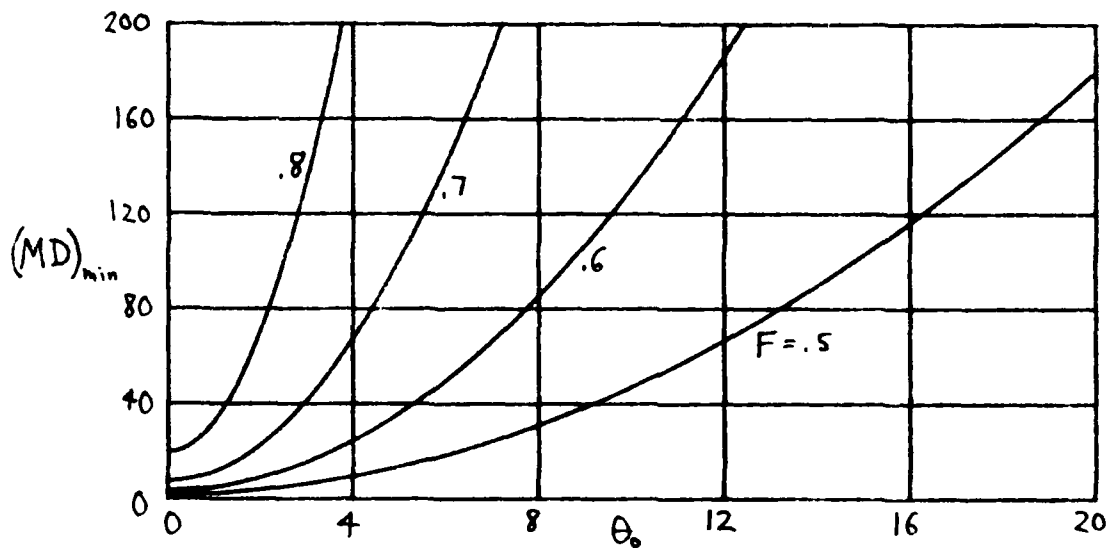


Figure H-5. Minimum MD Product



As a particular numerical example, for  $\theta_0 = 0$ ,  $F = 1/\sqrt{2}$ , we find

$$D_{\text{opt}} = 3, \quad M_{\text{opt}} = \frac{8}{3}, \quad (MD)_{\text{min}} = 8. \quad (\text{H-47})$$

So both  $D_{\text{opt}}$  and  $M_{\text{opt}}$  are somewhat larger than unity, even for  $F$  equal to  $1/\sqrt{2}$ . All these conclusions are drawn relative to the mean signal output alone; we now consider the noise output contributions.

#### MEAN NOISE OUTPUT

The mean noise output of the WDF processor in figure 7 is given by (172), (H-9), (H-13), and (H-31) as

$$\begin{aligned} \bar{b} &= W_V(t, f) \otimes G_n(f) = \\ &= N_d \left( \frac{R}{1+R} \right)^{1/2} \exp \left[ -\frac{t^2}{L^2} - \frac{f^2}{B^2} \frac{R}{1+R} \right]. \end{aligned} \quad (\text{H-48})$$

(As  $L \rightarrow \infty$ , that is, no weighting, then  $R \rightarrow \infty$ , and  $\bar{b} \rightarrow N_d \exp(-f^2/B^2) = G_n(f)$ , as expected.)

The noise factor in (H-48), namely

$$\left( \frac{R}{1+R} \right)^{1/2} = \left( \frac{DM}{1+DM} \right)^{1/2}, \quad (\text{H-49})$$

is virtually unity when the mean signal degradation is small, according to the results of figure H-5. Thus the ratio of peak signal-to-noise means is approximately  $2E_0/N_d$ , according to (H-30) and (H-48). These latter

quantities,  $E_0$  and  $N_d$ , are directly the input parameters to the WDF processor in figure 7; see (H-1) and (H-6).

#### VARIANCE OF $N \times N$ TERM

The variance of the  $N \times N$  term at the WDF processor output is given by the third line of (188) as

$$\begin{aligned}
 V_{NN} &= 2 W_V^2(t, f) \odot G_n^{(2)}(f) = \\
 &= N_d^2 \frac{R}{\sqrt{1+R}} \exp \left[ -\frac{2t^2}{L^2} - \frac{2f^2}{B^2} \frac{R}{1+R} \right]. \quad (H-50)
 \end{aligned}$$

Here, we also used (H-11) and (H-13). As  $L \rightarrow \infty$ , then  $M \rightarrow \infty$ ,  $R \rightarrow \infty$ , and  $V_{NN} \rightarrow \infty$ . Alternatively, as  $B \rightarrow \infty$ , then  $D \rightarrow \infty$ ,  $R \rightarrow \infty$ , and  $V_{NN} \rightarrow \infty$ .

These results for this particular example confirm the general observations in the sequel to (188).

The standard deviation of the  $N \times N$  term, namely  $\sqrt{V_{NN}}$ , is precisely equal to the noise mean output in (H-48) for all  $t, f$ , except for a constant factor  $(1+R)^{1/4} = (1+DM)^{1/4}$ . Also, the axes of the elliptical contours of (H-48) and (H-50) are parallel to the  $t$  and  $f$  axes and are independent of  $\theta_0$ , the amount of linear frequency modulation in the input signal.

## VARIANCE OF SxN TERM

The variance of the SxN terms at the WDF processor output is given by the last line of (188) or by double the results in (182). Upon substitution of (H-10), (H-12), and (H-15) in (182) and an extreme amount of manipulations, there follows variance

$$V_{SN} = 4E_0 N_d \frac{R\sqrt{D}}{\sqrt{H_3}} \exp[-\xi(t,f)] , \quad (H-51)$$

where

$$H_3 = (1 + D + R/2)(1 + D + R + DR/2) + (1 + R)(1 + R/2) \theta_0^2 \quad (H-52)$$

and  $\xi(t,f)$  is an elliptical function with minimum value at  $t = f = 0$ .

Namely,

$$\xi(t,f) = \frac{2t^2}{L^2} + c_r t^2 - \frac{\alpha^* \mu^2 + \alpha \mu^{*2} + 2\gamma |\mu|^2}{2(|\alpha|^2 - \gamma^2)} , \quad (H-53)$$

where

$$c = 4\pi^2 B^2 \frac{1 - i\theta_0}{1 + D - i\theta_0} ,$$

$$\alpha = \frac{1}{4} \left( c + \frac{2}{L^2} + 2\pi^2 B^2 \right) ,$$

$$\mu = - \left( \frac{c}{2} t + i2\pi f \right) ,$$

$$\gamma = \frac{1}{2} \pi^2 B^2 . \quad (H-54)$$

The quantity in the denominator of (H-53) can be simplified to

$$2(|\alpha|^2 - \gamma^2) = \frac{H_3}{2L^4 D_2} ; \quad (\text{H-55})$$

however,  $\xi(t,f)$  has not been reduced to its most compact form,

$$b_1 t^2 + b_2 f^2 + 2b_3 t f , \quad (\text{H-56})$$

due to the excessive amount of labor required to simplify and obtain  $b_1, b_2, b_3$ .

#### QUALITY MEASURE OF PERFORMANCE

We define a quality measure for the WDF processor output in figure 7 as

$$Q = \frac{\text{Difference of mean outputs}}{\text{Standard deviation of output}} = \frac{a}{(V_{SN} + V_{NN})^{1/2}} . \quad (\text{H-57})$$

The relevant quantities are given by (171) and (188) generally. For the specific example in this appendix, the quality measure, at peak signal location  $t = f = 0$ , is obtained by combining (H-30), (H-50), and (H-51):

$$Q = \left( \frac{E_o}{N_d} \right)^{1/2} \left( \frac{\frac{4E_o}{N_d} \frac{D\sqrt{1+R}}{H_1}}{1 + \frac{4E_o}{N_d} \sqrt{\frac{D(1+R)}{H_3}}} \right)^{1/2} . \quad (\text{H-58})$$

For convenience, we repeat the parameter definitions here:

$$\theta_0 = \alpha_0 \sigma_0^2, \quad D = (2\pi B \sigma_0)^2, \quad M = (L/\sigma_0)^2,$$

$$R = DM,$$

$$H_1 = (1 + D)(1 + D + R) + (1 + R)\theta_0^2,$$

$$H_3 = (1 + D + R/2)(1 + D + R + DR/2) + (1 + R)(1 + R/2)\theta_0^2. \quad (H-59)$$

It has already been observed in (H-24) and in the sequel to (H-39) that  $D > 1 + \theta_0^2$  and  $M > 1$  are desirable, in so far as the mean signal output is concerned. However, if filter bandwidth  $B$  ( $D$ ) is made too large, then too much noise is allowed through; alternatively, if weighting duration  $L$  ( $M$ ) is made too large, a noise degradation also results. Thus, it is expected that the quality ratio  $Q$  will peak for  $D$  in the neighborhood of  $1 + \theta_0^2$  and for  $M$  near 1.

It should be observed from (H-58) that even if input signal-to-noise measure  $E_0/N_d$  gets extremely large, the quality measure  $Q$  behaves according to  $\sqrt{E_0/N_d}$ , and not  $E_0/N_d$ . This is due to the saturation effects caused by the  $SxN$  term in the denominator of definition (H-57); it can also be seen directly from the quantitative result in (H-51), where variance  $V_{SN}$  is directly proportional to input signal energy  $E_0$  as well as the noise density level  $N_d$ .

The quality ratio  $Q$  in (H-58) is plotted versus  $M$  in figures H-6, H-7, H-8 for  $\theta_0 = 0, 1, 5$ , respectively. The input ratio  $E_0/N_d$  is kept at value 20 in all cases; the only other fundamental parameter,  $D$ , is varied over a range wide enough to encompass the maximum of  $Q$ . However, for ease of plotting the results, the values of  $D$  which are less than the critical value, which leads to the peak  $Q$ , are separated from those that are greater than the critical value. For example, in figure H-6,  $D = 1$  leads to the maximum value of  $Q$  that can be achieved for any value of  $M$ ; thus, the upper part of figure H-6 contains results for  $D \leq 1$ , while the lower part contains the remainder for  $D \geq 1$ . The corresponding critical values of  $D$  are 8 and 80 in figures H-7 and H-8, when  $\theta_0 = 1$  and 5, respectively.

One important observation that is made apparent by these figures is that near the maximum, the quality ratio  $Q$  is not too sensitive to  $M$  and  $D$ ; that is, the maximum is broad in the neighborhood of the best parameter pair  $M, D$ . It should also be observed that as  $\theta_0$  increases, the peak value of  $Q$  decreases, although the decrease is not very significant, at least over the range  $\theta_0 = 0, 1, 5$  used here. Finally, the values of the peaks in these figures are slightly less than  $\sqrt{E_0/N_d}$ , as anticipated above.

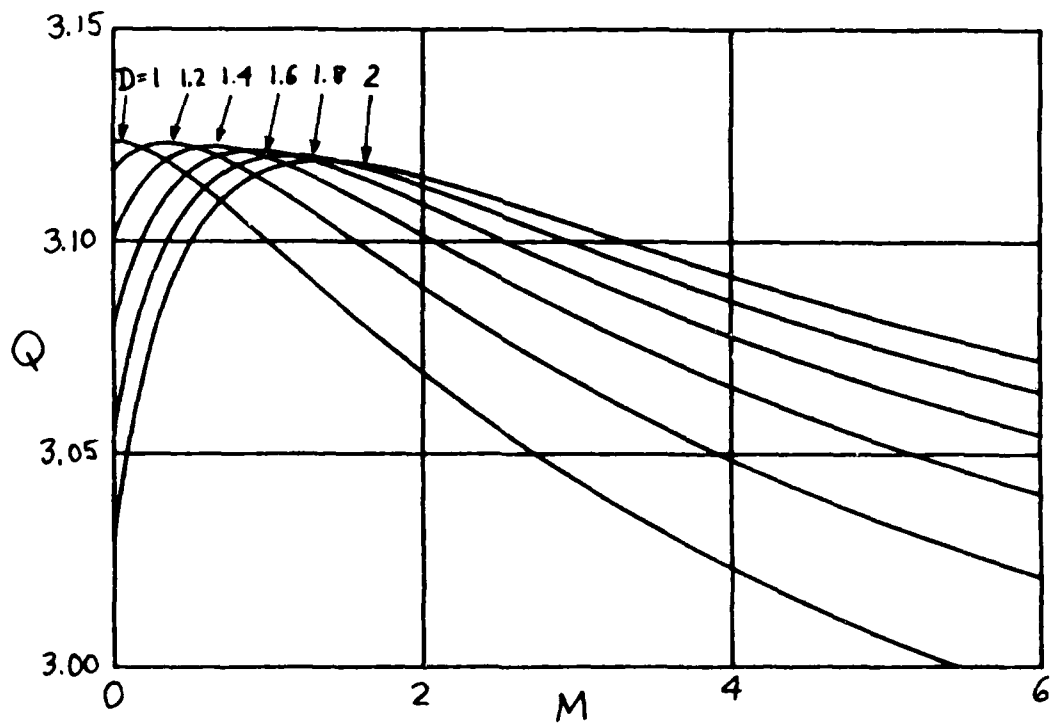
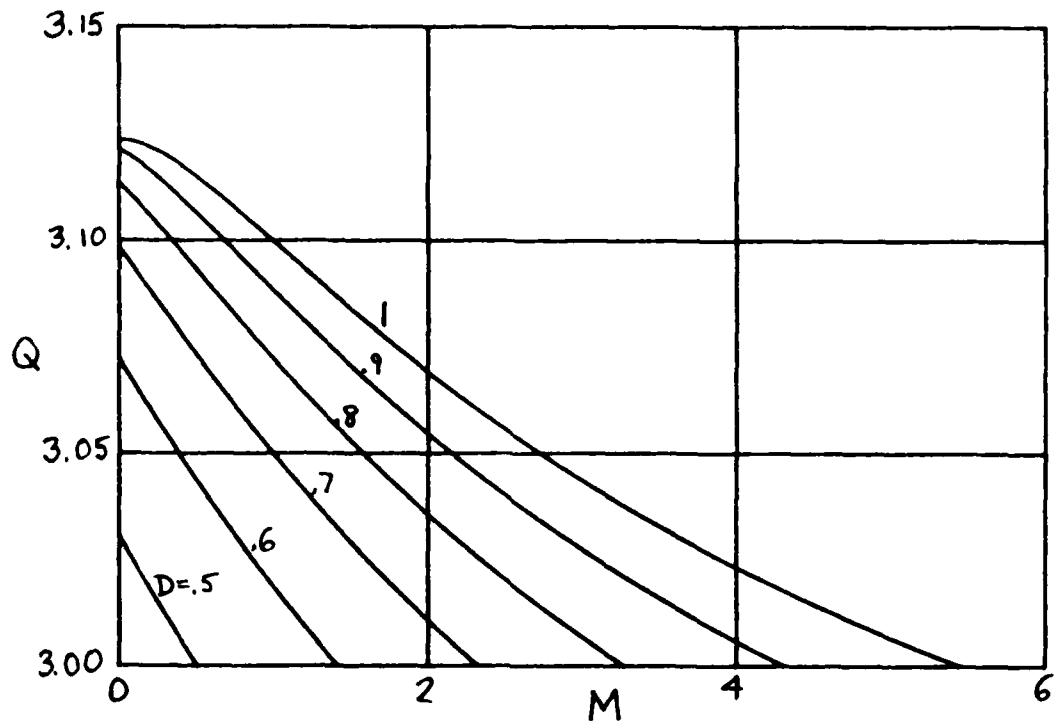


Figure H-6. Quality Ratio for  $\theta_0 = 0$ ,  $E_0/N_d = 20$

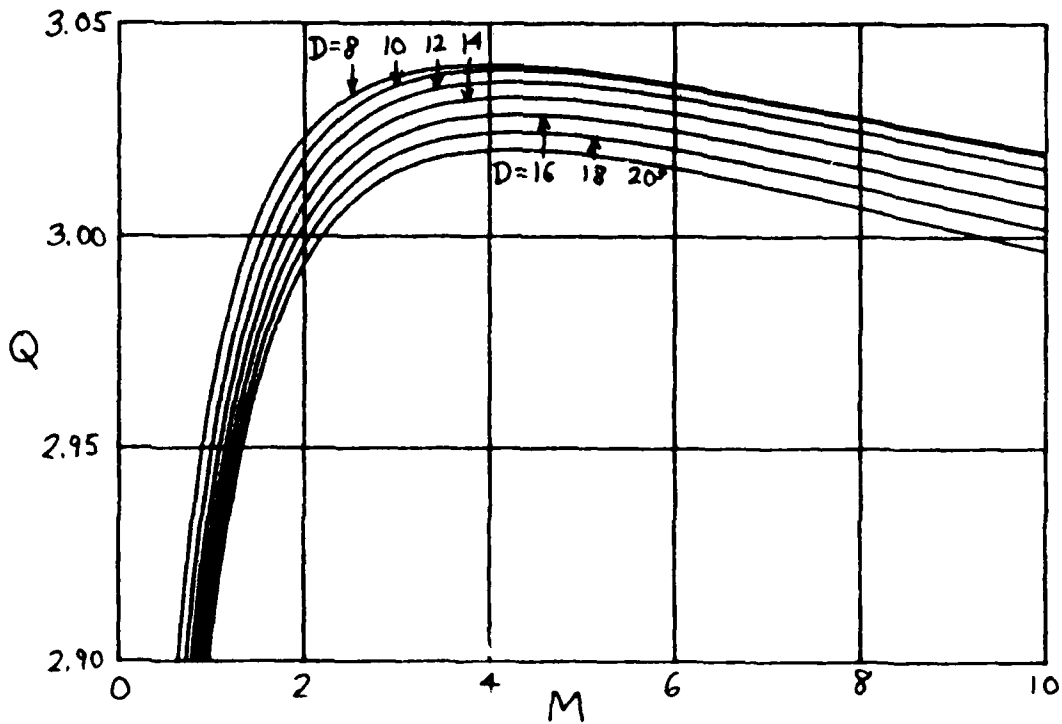
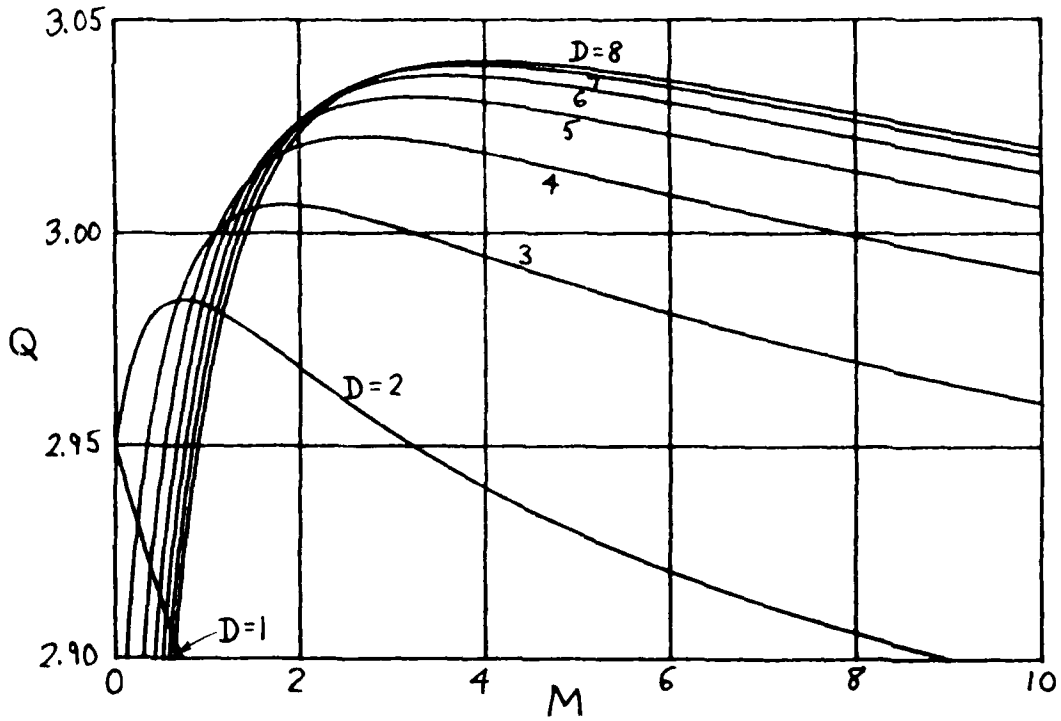


Figure H-7. Quality Ratio for  $\theta_0 = 1$ ,  $E_0/N_d = 20$



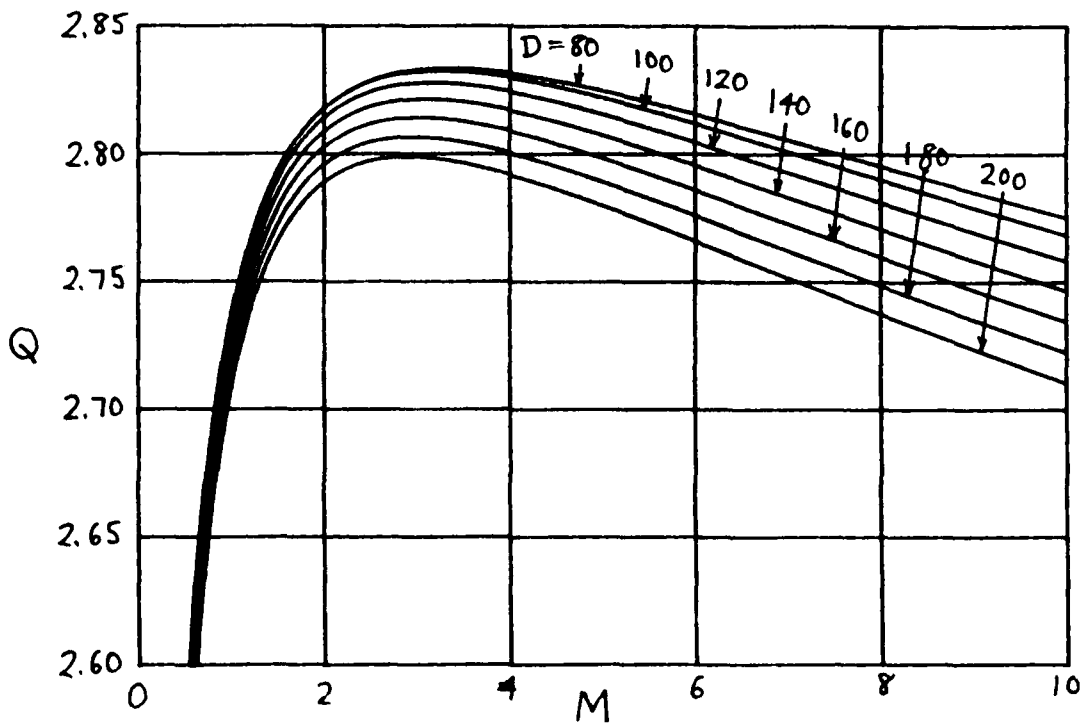
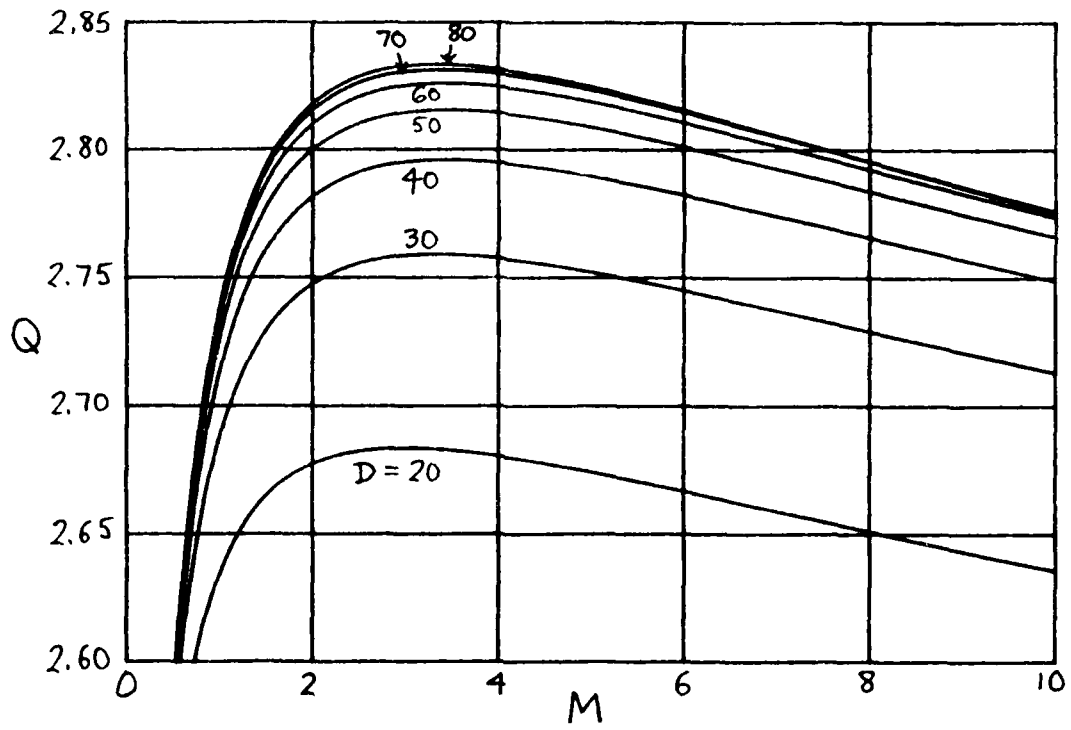


Figure H-8. Quality Ratio for  $\theta_0 = 5$ ,  $E_0/N_d = 20$

APPENDIX I. SMOOTHED WDF FOR  $s(t) = t \exp(-t^2/2)$ 

For the waveform

$$s(t) = t \exp(-t^2/2) \quad \text{for all } t, \quad (\text{I-1})$$

the WDF is

$$W_s(t, f) = 2\sqrt{\pi} \exp(-t^2 - 4\pi^2 f^2)(t^2 + 4\pi^2 f^2 - \frac{1}{2}) = 2\sqrt{\pi} \exp(-r^2)(r^2 - \frac{1}{2}), \quad (\text{I-2})$$

with energy

$$E = \int dt |s(t)|^2 = \sqrt{\pi} / 2. \quad (\text{I-3})$$

Contour plots of the WDF in (I-2) are concentric circles in the  $(t, 2\pi f)$  plane; in fact, (I-2) is a function only of  $r^2 = t^2 + (2\pi f)^2$ . The origin value of  $W_s$  is  $-2E = -\sqrt{\pi}$ , and the WDF is negative for  $r < 1/\sqrt{2}$ , while it is positive for  $r > 1/\sqrt{2}$ .

Let us smooth this WDF with the most compact WDF; namely, use the Gaussian weighting function in (G-23) with WDF (G-25) with  $\theta_c = 0$ ,  $\sigma_c = 1$ :

$$W_u(t, f) = 2 \exp(-t^2 - 4\pi^2 f^2) = 2 \exp(-r^2). \quad (\text{I-4})$$

The reason for these parameter choices of  $\theta_c$  and  $\sigma_c$  is that the contours of (I-4) are also circles in the  $(t, 2\pi f)$  plane and exactly match those of the waveform WDF in (I-2); this should lead to minimal spreading.

The result of smoothing (I-2) by (I-4) is

$$\begin{aligned} |S_U(t, f)|^2 &= W_S(t, f) \otimes W_U(t, f) = \\ &= \frac{1}{4} \sqrt{\pi} (t^2 + 4\pi^2 f^2) \exp\left(-\frac{1}{2}(t^2 + 4\pi^2 f^2)\right) = \frac{1}{4} \sqrt{\pi} r^2 \exp(-r^2/2), \end{aligned} \quad (I-5)$$

which has volume E as given by (I-3). Again, this is a function only of  $r^2$ , but it is never negative. This smoothed distribution is zero at  $r = 0$ , and peaks at  $r = \sqrt{2}$  with value .326. By contrast, the WDF in (I-2) is -1.77 at the origin, a large negative value. However, the waveform WDF in (I-2) does decay faster than the short-term spectral estimate in (I-5); this is an example of the tradeoffs that must be accepted when using short-term spectral estimation versus the WDF.

To lend credence to (I-5) as a better measure of the time-frequency content of  $s(t)$ , we observe that at  $t = 0$ , the center of gravity of (I-5) is

$$\bar{f}_0 = \frac{\int_{-\infty}^{\infty} df |S_U(0, f)|^2 f}{\int_0^{\infty} df |S_U(0, f)|^2} = \frac{1}{\pi} \sqrt{\frac{2}{\pi}}. \quad (I-6)$$

Then we expect that

$$A \sin(2\pi \bar{f}_0 t) \quad (I-7)$$

ought to be a good fit to  $s(t)$  of (I-1) for  $t$  near zero. In fact, plots of (I-1) and (I-7) for  $A = \exp(-.5)$  overlap for  $-1 < t < 1$ .

If we attempt this same procedure for WDF  $W_s$  in (I-2), the denominator is

$$\int_0^{\infty} df W_s(0, f) = 0, \quad (I-8)$$

giving rise to  $\bar{f}_0 = \infty$ , which is useless.

With respect to  $t = 1$  instead, we find center of gravity

$$\bar{f}_1 = \frac{\int_0^{\infty} df |S_u(1, f)|^2 f}{\int_0^{\infty} df |S_u(1, f)|^2} = \frac{1}{\pi} \sqrt{\frac{2}{\pi}} \frac{3}{4}. \quad (I-9)$$

Since  $s(t)$  in (I-1) peaks at  $t = 1$ , we expect that

$$A \cos(2\pi\bar{f}_1(t - 1)) \quad (I-10)$$

ought to be a good fit to  $s(t)$  for  $t$  near 1. In fact, plots of (I-1) and (I-10) for  $A = \exp(-.5)$  show very good agreement for  $.8 < t < 1.7$ .

Thus, smoothing of the WDF  $W_s$  in (I-2) by means of WDF  $W_u$  in (I-4), for this example, results in a very meaningful distribution function.

## APPENDIX J. DOUBLE CONVOLUTION OF TWO GAUSSIAN FUNCTIONS

By means of the double integral result

$$\begin{aligned} \iint dx dy \exp\left[-\frac{1}{2} \alpha x^2 - \frac{1}{2} \beta y^2 + \gamma xy + \mu x + \nu y\right] &= \\ &= \frac{2\pi}{(\alpha\beta - \gamma^2)^{1/2}} \exp\left[\frac{\beta\mu^2 + \alpha\nu^2 + 2\gamma\mu\nu}{2(\alpha\beta - \gamma^2)}\right] \end{aligned} \quad (J-1)$$

for  $\alpha_r > 0$ ,  $\beta_r > 0$ ,  $\alpha_r\beta_r > \gamma_r^2$ , it is readily shown that the double convolution of two general Gaussian functions is given by

$$\exp\left[-\frac{1}{2} ax^2 - \frac{1}{2} by^2 - \sqrt{ab} \rho xy\right] \otimes \exp\left[-\frac{1}{2} cx^2 - \frac{1}{2} dy^2 - \sqrt{cd} \lambda xy\right] = \quad (J-2)$$

$$= \frac{2\pi}{D^{1/2}} \exp\left[-\frac{N_1 x^2 + N_2 y^2 + 2N_3 xy}{2D}\right] \quad (J-3)$$

for  $a, b, c, d > 0$ ,  $|\rho| < 1$ ,  $|\lambda| < 1$ , where

$$D = ab(1 - \rho^2) + cd(1 - \lambda^2) + ad + bc - 2\sqrt{abcd} \rho \lambda$$

$$N_1 = ac[b(1 - \rho^2) + d(1 - \lambda^2)]$$

$$N_2 = bd[a(1 - \rho^2) + c(1 - \lambda^2)]$$

$$N_3 = \sqrt{abcd} [\sqrt{ab} \lambda(1 - \rho^2) + \sqrt{cd} \rho(1 - \lambda^2)] \quad (J-4)$$

Also, a useful auxiliary relation is

$$N_1 N_2 - N_3^2 = D abcd (1 - \rho^2)(1 - \lambda^2) . \quad (J-5)$$

Now let

$$\rho = \sin(\theta), \quad \text{where } -\frac{\pi}{2} < \theta < \frac{\pi}{2} ,$$

$$\lambda = \sin(\phi), \quad \text{where } -\frac{\pi}{2} < \phi < \frac{\pi}{2} . \quad (J-6)$$

Then the area of the contour ellipse at the  $1/e$  relative level of the first exp in (J-2) is

$$A_1 = \frac{2\pi}{\sqrt{ab} \cos(\theta)} \quad (J-7)$$

in the  $x,y$  plane, where we used (D-1), (D-19), and (D-20). Similarly, the area of the second exp in (J-2) is

$$A_2 = \frac{2\pi}{\sqrt{cd} \cos(\phi)} . \quad (J-8)$$

The sum of these two effective areas is

$$A_1 + A_2 = 2\pi \frac{\sqrt{ab} \cos(\theta) + \sqrt{cd} \cos(\phi)}{\sqrt{abcd} \cos(\theta) \cos(\phi)} . \quad (J-9)$$

On the other hand, the area of the contour ellipse at the  $1/e$  relative level of the smoothed exp in (J-3) is

$$A_3 = 2\pi \frac{\sqrt{D}}{\sqrt{abcd} \cos(\theta) \cos(\phi)} \quad (J-10)$$

in the  $x, y$  plane, where we can express  $D$  from (J-4) as

$$\begin{aligned} D &= ab \cos^2(\theta) + cd \cos^2(\phi) + ad + bc - 2\sqrt{abcd} \sin(\theta)\sin(\phi) = \\ &= [\sqrt{ab} \cos(\theta) + \sqrt{cd} \cos(\phi)]^2 + \left| \sqrt{ad} \exp(i\theta) - \sqrt{bc} \exp(i\phi) \right|^2 . \end{aligned} \quad (J-11)$$

Comparison of the square root of (J-11) with the numerator of (J-9) reveals that

$$A_3 \geq A_1 + A_2 , \quad (J-12)$$

with equality occurring if and only if

$$\sqrt{ad} = \sqrt{bc} \quad \text{and} \quad \theta = \phi . \quad (J-13)$$

That is, in order for  $A_3 = A_1 + A_2$ , we must have

$$\frac{d}{c} = \frac{b}{a} \quad \text{and} \quad \lambda = \rho . \quad (J-14)$$

Physically, this requirement states that the contour ellipses of the two exp terms in (J-2) must have the same ratio of major-to-minor axes and they must have the same tilt. If either condition is violated, then  $A_3 > A_1 + A_2$ , the exact amount depending on the second term in (J-11).

#### EFFICIENT CALCULATION OF GAUSSIAN FUNCTION

If the general two-dimensional Gaussian function in (J-2) is sampled on an equi-spaced grid, for purposes of convolution, it will be necessary to compute the quantity

$$Q_2(m, n) = \exp(-am^2 - bn^2 - cmn) \quad (J-15)$$

for integers  $-M \leq m \leq M$ ,  $-N \leq n \leq N$ . The following efficient procedure is based upon the general method given in [12].

We observe first that

$$Q_2(-m, -n) = Q_2(m, n) , \quad (J-16)$$

which cuts the effort by one-half. There also follows

$$Q_2(m, n) = Q_2(m, n - 1) Q_1(m, n) , \quad (J-17)$$

where

$$Q_1(m, n) = \exp[-b(2n - 1) - cm] = Q_1(m, n - 1) \exp(-2b) . \quad (J-18)$$

These recurrences can be started with

$$Q_1(m, 0) = \exp(b - cm) ,$$

$$Q_2(m, 0) = \exp(-am^2) = Q_2(-m, 0) . \quad (J-19)$$

Furthermore, these latter two quantities are available through the recurrence

$$\left. \begin{aligned} Q_1(m, 0) &= Q_1(m - 1, 0) \exp(-c) \\ Q_1(m - 1, 0) &= Q_1(m, 0) \exp(+c) \end{aligned} \right\} \text{for } m \geq 1 , \quad (J-20)$$



with

$$Q_1(0,0) = \exp(b) , \quad (J-21)$$

and the recurrence

$$\left. \begin{aligned} Q_2(m,0) &= Q_2(m-1,0) E(m) \\ E(m) &= E(m-1) \exp(-2a) \end{aligned} \right\} \text{for } m \geq 1 , \quad (J-22)$$

with

$$Q_2(0,0) = 1, \quad E(0) = \exp(a) . \quad (J-23)$$

The only case not covered by the above recurrences is for  $m = 0$ ; then

$$\left. \begin{aligned} Q_2(0,n) &= Q_2(0,n-1) F(n) \\ F(n) &= F(n-1) \exp(-2b) \end{aligned} \right\} \text{for } n \geq 1 , \quad (J-24)$$

with

$$F(0) = \exp(b) . \quad (J-25)$$

A program for the evaluation of (J-15) is given below. Only three exponentials, in lines 90-110, need to be evaluated. Also, the only storage required is for the final quantity  $Q_2(m,n)$  in lines 60-70. The auxiliary variables  $Q_1(m,n)$ ,  $E(m)$ ,  $F(n)$  introduced above need never be stored. The check on accuracy in lines 390-470 would be discarded, of course, in any

practical application; it is appended as a check on any typographical errors in entering the program into another computer.

```

10  A=.037          ! exp(-A m^2 - B n^2 - C m n)
20  B=.051          ! for -M<=m<=M, -N<=n<=N
30  C=.044
40  M=5
50  N=7
60  REDIM Q2(-M:M,-N:N)
70  DIM Q2(50,50)
80  DOUBLE M,N,Ms,Ns      ! INTEGERS
90  Ea=EXP(A)
100 Eb=EXP(B)
110 Ec=EXP(C)
120 Q2(0,0)=1.
130 E=Eb
140 E2b=Eb*Eb
150 FOR Ns=1 TO N
160 E=E/E2b
170 Q2(0,Ns)=Q2(0,Ns-1)*E
180 NEXT Ns
190 E=Ea
200 E2a=Ea*Ea
210 Q1po=Q1mo=Eb
220 FOR Ms=1 TO M
230 Q1p=Q1po=Q1po/Ec
240 Q1m=Q1mo=Q1mo*Ec
250 E=E/E2a
260 Q2(-Ms,0)=Q2(Ms,0)=Q2(Ms-1,0)*E
270 FOR Ns=1 TO N
280 Q1p=Q1p/E2b
290 Q1m=Q1m/E2b
300 Q2(Ms,Ns)=Q2(Ms,Ns-1)*Q1p
310 Q2(-Ms,Ns)=Q2(-Ms,Ns-1)*Q1m
320 NEXT Ns
330 NEXT Ms
340 FOR Ms=-M TO M
350 FOR Ns=1 TO N
360 Q2(-Ms,-Ns)=Q2(Ms,Ns)
370 NEXT Ns
380 NEXT Ms
390 Big=0.          ! MAXIMUM ERROR CHECK
400 FOR Ms=-M TO M
410 FOR Ns=-N TO N
420 E=EXP(-A*Ms*Ms-B*Ns*Ns-C*Ms*Ns)
430 Error=E-Q2(Ms,Ns)
440 Big=MAX(Big,ABS(Error))
450 NEXT Ns
460 NEXT Ms
470 PRINT Big
480 END

```

## REFERENCES

1. N. Yen, "Time and Frequency Representation of Acoustic Signals by Means of the Wigner Distribution Function: Implementation and Interpretation," Journal of Acoustical Society of America, vol. 81, no. 6, pp. 1841-1850, June 1987.
2. J. C. Andrieux et al, "Optimum Smoothing of the Wigner-Ville Distribution," IEEE Transactions on Acoustics, Speech, and Signal Processing, vol. ASSP-35, no. 6, pp. 764-768, June 1987.
3. Kai-Bor Yu and S. Cheng, "Signal Synthesis from Pseudo-Wigner Distribution and Applications," IEEE Transactions on Acoustics, Speech, and Signal Processing, vol. ASSP-35, no. 9, pp. 1289-1301, September 1987.
4. P. M. Woodward, Probability and Information Theory, With Applications to Radar, Pergamon Press, New York, NY, 1957.
5. A. H. Nuttall, Accurate Efficient Evaluation of Cumulative or Exceedance Probability Distributions Directly From Characteristic Functions, NUSC Technical Report 7023, Naval Underwater Systems Center, New London, CT, 1 October 1983.
6. D. Gabor, "Theory of Communication," Journal of Institute of Electrical Engineers, vol. 93, part III, pp. 429-457, 1946.
7. L. Cohen, "On a Fundamental Property of the Wigner Distribution Function," IEEE Transactions on Acoustics, Speech, and Signal Processing, vol. ASSP-35, no. 4, pp. 559-561, April 1987.

## REFERENCES (Cont'd)

8. L. Cohen and C. A. Pickover, "A Comparison of Joint Time-Frequency Distributions for Speech Signals," IEEE International Symposium on Circuits and Systems, pp. 42-45, August 1986.
9. L. Cohen and T. E. Posch, "Positive Time-Frequency Distribution Functions," IEEE Transactions on Acoustics, Speech, and Signal Processing, vol. ASSP-33, no. 1, pp. 31-38, February 1985.
10. L. Cohen and T. E. Posch, "Generalized Ambiguity Functions," IEEE International Conference on Acoustics, Speech, and Signal Processing, March 26-29, 1985.
11. N. D. Cartwright, "A Non-Negative Wigner-Type Distribution," Physics, vol. 83A, pp. 210-212, 1976.
12. A. H. Nuttall, Efficient Evaluation of Polynomials and Exponentials of Polynomials for Equi-Spaced Arguments, NUSC Technical Report 7995, Naval Underwater Systems Center, New London, CT, 1 April 1987. Also IEEE Transactions on Acoustics, Speech, and Signal Processing, vol. ASSP-35, no. 10, pp. 1486-1487, October 1987.
13. C. W. Helstrom, Statistical Theory of Signal Detection, Second Edition, Pergamon Press, New York, NY, 1968.
14. R. B. Blackman and J. W. Tukey, The Measurement of Power Spectra, Dover Publications, New York, NY, 1959.
15. A. H. Nuttall, A Shortcut in Calculus of Variations for Complex Functions, NUSC Technical Memorandum 2020-179-70, Naval Underwater Systems Center, New London, CT, 21 September 1970.

## INITIAL DISTRIBUTION LIST

Addressee	No. of Copies
ADMIRALTY RESEARCH ESTABLISHMENT, LONDON, ENGLAND (Dr. L. Lloyd)	1
APPLIED PHYSICS LAB, JOHN HOPKINS	2
APPLIED PHYSICS LAB, U. WASHINGTON (C. Eggen) Contract N00024-85-C-6264	1
APPLIED RESEARCH LAB, PENN STATE, (Dr. D. Ricker) Contract N00024-85-C-6041	2
APPLIED RESEARCH LAB, U. TEXAS (Dr. M. Frazer) Contract N00024-86-C-6134-4-2-3	2
A & T, STONINGTON, CT (H. Jarvis)	1
APPLIED SEISMIC GROUP, (R. Lacoss)	1
ASST SEC NAV	1
ASTRON RESEARCH & ENGR, SANTA MONICA, CA (Dr. A. Piersol)	1
AUSTRALIAN NATIONAL UNIV. CANBERRA, AUSTRALIA (Prof. B. Anderson)	1
BBN, Arlington, Va. (Dr. H. Cox)	1
BBN, Cambridge, MA (H. Gish)	1
BBN, New London, Ct. (Dr. P. Cable)	1
BELL COMMUNICATIONS RESEARCH, Morristown, NJ (J. Kaiser)	1
BENDAT, JULIUS DR., 833 Moraga Dr., LA, CA	1
DR. Norman Bleistein, Denver, CO 80222	1
CANBERRA COLLEGE OF ADV. EDUC, BELCONNEN, A.C.T. AUSTRALIA (P. Morgan)	1
COAST GUARD ACADEMY, New London, CT (Prof. J. Wolcin)	1
COAST GUARD R & D, Groton, CT (Library)	1
COGENT SYSTEMS, INC, (J. Costas)	1
CONCORDIA UNIVERSITY H-915-3, MONTREAL, QUEBEC CANADA (Prof. Jeffrey Krolik)	1
CNO (NOP24, NOP 224, NOP 353, NOP 951, NOP 981)	5
CNR-OCNR-00, 10, 11, 13, 10, ONT 23 & 231)	7
DTNSRDC, BETHESDA	1
DAVID W. TAYLOR RESEARCH CNTR, ANNAPOLIS, MD (P. Prendergast, Code 2744)	1
DARPA, ARLINGTON, VA (A. Ellinthorpe)	1
DALHOUSIE UNIV., HALIFAX, NOVA SCOTIA, CANADA (Dr. B. Ruddick)	1
DEFENCE RESEARCH ESTAB. ATLANTIC, DARTMOUTH, NOVA SCOTIA (Library)	1
DEFENCE RESEARCH ESTAB. PACIFIC, VICTORIA, CANADA (Dr. D. Thomson)	1
DEFENCE SCIENTIFIC ESTABLISHMENT, MINISTRY OF DEFENCE, AUCKLAND, N Z. (Dr. L. Hall)	1
DEFENSE SYSTEMS, INC, MC LEAN, VA (Dr. G. Sebestyen)	1
DIA	1
DTIC	1
DTNSRDC	1
DREXEL UNIV, (Prof. S. Kesler)	1
EDO CORP, College Point, NY (M. Blanchard)	1
NICRAD 87-NUSC-029 of 23 July 1987	1

## INITIAL DISTRIBUTION LIST

Addressee	No. of Copies
EG&G, Manassas, VA (Dr. J. Hughen and D. Frohman)	2
GENERAL ELECTRIC CO. PITTSFIELD, MA (Mr. R. Race)	1
GENERAL ELECTRIC CO, SYRACUSE, NY (Mr. J. L. Rogers)	1
GENERAL ELECTRIC CO, (D. Winfield) N00024-87-C-6087)	1
HAHN, WM, Apt. 701, 500 23rd St. NW, Wash, DC 20037	1
HARRIS SCIENTIFIC SERVICES, Dobbs Ferry, NY (B. Harris)	1
HUGHES AIRCRAFT, Fullerton, CA (S. Autrey)	1
HUGHES AIRCRAFT, Buena Park, CA (T. Posch)	1
IBM, Manassas, VA (G. Demuth)	1
INDIAN INSTITUTE OF SCIENCE, BANGALORE, INDIA (N. Srinivasa)	1
JOHNS HOPKINS UNIV, LAUREL, MD (J. C. Stapleton)	1
LINCOM CORP., NORTHBORO, MA 01532 (Dr. T. Schonhoff)	1
MAGNAVOX GOV & IND ELEC CO, Ft. Wayne, IN (R. Kenefic)	1
MARINE BIOLOGICAL LAB, Woods Hole, MA	1
MARINE PHYSICAL LABORATORY SCRIPPS	1
MARTIN MARIETTA BALTIMORE AEROSPACE, Baltimore, MD (S. Lawrence Marple)	1
MASS. INSTITUTE OF TECHNOLOGY (Prof. A. Baggaroer)	1
MBS SYSTEMS, NORWALK, CT (A. Winder)	1
MIDDLETON, DAVID, 127 E. 91st ST, NY, NY	1
NADC (5041, M. Mele)	1
NASC, NAIR-00,03	2
NATIONAL RADIO ASTRONOMY OBSERVATORY (F. Schwab)	1
NATO SACLANT ASW RESEARCH CENTRE, APO NY, NY 09019 (Library R. E. Sullivan and G. Tacconi)	3
NAVAIR (03, PMA 264)	2
NPS, MONTEREY, CA (C. W. Therrien)	1
NRL UND SOUND REF DET, ORLANDO, FL	1
NAVAL SEA SYSTEMS COMMAND-SEA-00	1
NAVAL SYSTEMS DIV., SIMRAD SUBSEA A/S, NORWAY (E. B. Lunde)	1
NAVSEA (63D, 63Y, 63X, PMS 411C, PMS 409, PMS 417, PMS 418)	7
NCEL	1
NCSC	1
NICHOLS RESEARCH CORP., Wakefield, MA (T. Marzetta)	1
NORDA (Dr. B. Adams)	1
NORTHEASTERN UNIV. (Prof. C. L. Nikias)	1
NORWEGIAN DEFENCE RESEARCH EST, NORWAY (Dr J. Glattetre)	1
NOSC, (C. Sturdevant; 73, J. Lockwood, F. Harris, 743, R. Smith; 62, R. Thuleen)	5
NRL, Washington, DC (Dr. J. Buccaro, Dr. E. Franchi, Dr. P. Abraham, Code 5132, A. A. Gerlach, W. Gabriel (Code 5370), and N. Yen (Code 5135)	6
NRL, Arlington, VA (N. L. Gerr, Code 1111)	1
NSWC	1
NSWC DET FT. LAUDERDALE	1
NSWC WHITE OAK LAB	1
NUSC DET FT. LAUDERDALE	1

## INITIAL DISTRIBUTION LIST

Addressee	No. of Copies
NUSC DET TUDOR HILL	1
NUSC DET WEST PALM BEACH (Dr. R. Kennedy Code 3802)	1
NWC	1
ORI CO, INC, New London, CT (G. Assard)	1
PENN STATE UNIV., State College, PA (F. Symons)	1
PROMETHEUS, INC, Sharon, MA (Dr. J. Byrnes)	1
PSI MARINE SCIENCES, New London, Ct. (Dr. R. Mellen)	1
PRICE, Dr. Robert, 80 Hill St., Lexington, Ma 02173	1
RAISBECK, Dr. Gordon, P.O. Box 4311, Portland, ME 04101	1
RAN RESEARCH LAB, DARLINGHURST, AUSTRALIA	1
RAYTHEON CO, Portsmouth, RI (J. Bartram, R. Connor) and S. S. Reese) NICRAD 87-NUSC 013	3
ROCKWELL INTERNATIONAL CORP, Anaheim, CA (L. Einstein and Dr. D. Elliott)	2
ROYAL MILITARY COLLEGE OF CANADA, (Prof. Y. Chan)	1
RUTGERS UNIV., Piscataway, NJ (Prof. S. Orfanidis)	1
RCA CORP, Moorestown, NJ (H. Upkowitz)	1
SAIC, Falls Church, VA (Dr. P. Mikhalevsky)	1
SAIC, New London, CT (Dr. F. Dinapoli)	1
SANDIA NATIONAL LABORATORY (J. Claasen)	1
SCRIPPS INSTITUTION OF OCEANOGRAPHY	1
SONAR & SURVEILLANCE GROUP, DARLINGHURST, AUSTRALIA	1
SOUTHEASTERN MASS. UNIV (Prof. C. H. Chen)	1
SPERRY CORP, GREAT NECK, NY	1
SPWAR-OO, PD 80, PMW 180	3
STATE UNIV. OF NY AT STONY BROOK (Prof. M. Barkat)	1
TEL-AVIV UNIV, TEL-AVIV, ISRAEL (Prof. E. Winstein)	1
TRACOR, INC, Austin, TX (Dr. T Leih and J. Wilkinson)	2
TRW FEDERAL SYSTEMS GROUP (R. Prager)	1
UNDERSEA ELECTRONICS PROGRAMS DEPT, SYRACUSE, NY (J. Rogers)	1
UNIV. OF ALBERTA, EDMONTON, ALBERTA, CANADA (K. Yeung)	1
UNIV OF CA, San Diego, CA (Prof. C. Helstrom)	1
UNIV. OF CT, Storrs, CT. (Library and Prof. C. Knapp)	2
UNIV OF FLA, GAINESVILLE, FL (D. Childers)	1
UNIV OF MICHIGAN, Cooley Lab, Ann Arbor, MI (Prof T. Birdsall)	1
UNIV. OF MINN, Minneapolis, Mn (Prof. M. Kaveh)	1
UNIV. OF NEWCASTLE, NEWCASTLE, NSW, CANADA (Prof. A. Cantoni)	1
UNIV. OF RI, Kingston, RI (Library, Prof. S. Kay, Prof. L. Scharf, and Prof. D. Tufts)	4
UNIV. OF SOUTHERN CA., LA. (Dr. A. Polydoros PHE 414)	1
UNIV. OF STRATHCLYDE, ROYAL COLLEGE, Glasgow, Scotland (Prof. T. Durrani)	1
UNIV. OF TECHNOLOGY, Loughborough, Leicestershire, England (Prof. J. Griffiths)	1
UNIV. OF WASHINGTON, Seattle (Prof. D. Lytle)	1
URICK, ROBERT, Silver Springs, MD	1
VAN ASSELT, HENRIK, USEA S.P.A., LA SPEZIA, ITALY	1
WERBNER, A., 60 Elm St., Medford, MA 02155	1

INITIAL DISTRIBUTION LIST

Addressee	No. of Copies
WESTINGHOUSE ELEC. CORP, WALTHAM, MA (D. Bennett)	1
WESTINGHOUSE ELEC. CORP, OCEANIC DIV, ANNAPOLIS, MD (Dr. H. L. Price and H. Newman N00024-87-C-6024)	2
WOODS HOLE OCEANOGRAPHIC INSTITUTION (Dr. R. Spindel and Dr. E. Weinstein)	2
YALE UNIV. (Library, Prof. P. Schultheiss and Prof. F. Tuteur)	2



ENDED

DATE

FILMED

8-88

DTIC